UC Riverside

UC Riverside Electronic Theses and Dissertations

Title

Mechanisms of Strigolactone Signal Transduction in Plants

Permalink

https://escholarship.org/uc/item/7kd365wn

Author

White, Alexandra Ray Foris

Publication Date

2024

Peer reviewed|Thesis/dissertation

eScholarship.org Powered by the California Digital Library
University of California

UNIVERSITY OF CALIFORNIA
RIVERSIDE

Mechanisms of Strigolactone Signal Transduction in Plants

A Dissertation submitted in partial satisfaction
of the requirements for the degree of

Doctor of Philosophy

in

Plant Biology

by

Alexandra White

September 2024

Dissertation Committee:
Dr. David Nelson, Chairperson
Dr. Julia Bailey-Serres
Dr. Jaimie Van Norman

Copyright by
Alexandra White
2024

The Dissertation of Alexandra White is approved:

Committee Chairperson

University of California, Riverside

Acknowledgements:

The text of chapter one of this dissertation in full is a reprint of the of the material as it appears in White, A. R. F., Mendez, J. A., Khosla, A., & Nelson, D. C. (2022). “Rapid analysis of strigolactone receptor activity in a *Nicotiana benthamiana dwarf14* mutant.” *Plant Direct*, 6(3), e389. David C. Nelson directed and conceptualized the experiments done in this chapter. Jose Mendez assisted with collection and analysis of phenotypic data for Figures 2 and 3. Aashima Khosla provided training and guidance on experiments preformed for Figures 4 and 5. We thank Dr. Gavin Flematti and Dr. Adrian Scaffidi (University of Western Australia) for supplying rac-GR24 and purified GR24 enantiomers. We thank James Eckhardt and Claudia Sepulveda for aiding at early stages of the project. We also thank Dr. David Tricoli and Bailey Van Bockern at the Plant Transformation Facility of the University of California, Davis for performing transformation of *N. benthamiana*. We gratefully acknowledge funding support from the US National Science Foundation (NSF) Research Traineeship (NRT) Program Grant DGE-1922642 “Plants3D” to AW, and NSF grants IOS-1740560 and IOS-1856741 to DCN.

The text of chapter two of this dissertation in full is a reprint of the material as it appears in the current revision of Alexandra R.F. White, Annalise Kane, Satoshi Ogawa, Ken Shirasu, David C. Nelson (2024) “An Atypical Subclade of KAI2d Proteins Attenuate Responses to Host-derived Strigolactones in a Hemiparasitic Plant, *Phtheirospermum japonicum*” *Plant Cell and Physiology*, in revision. David C. Nelson directed and conceptualized the experiments done in this chapter. Annalise Kane preformed the phylogenetic analyses presented in Figure 5. Satoshi Ogawa and Ken Shirasu provided genetic material used in Figures 1-4 and gave guidance during manuscript preparation.

I am eternally grateful for all of the support I have received during my graduate degree. I would first like to thank my mentor Dave Nelson. You have provided me invaluable guidance, taught me the importance of scientific integrity, and given me the space to grow as an independent scientist. Thank you for accepting my sassy personality and giving it back to me! I would like to thank my dissertation committee members Julia Bailey-Serres and Jaimie Van Norman for all of the advice and support you have both given me over the years. It has been a joy to be a part of such a collaborative and fun lab environment and that is due to the members of the Nelson lab both past and current. Thank you Aashima and Claudia for being my lab sisters and training me when I joined the lab. To Michael and Annalise for being my lab buddies. Specifically, Michael, I am so glad to have started and ended this program with a great friend. To my fantastic undergraduate researcher Xitlalli for all of your hard work. It has been a pleasure to work and grow friendships with all of you. I want to mention the undergraduate students from the dynamic genome course for your contribution to chapter two. I would also like to mention the members of the Nagel lab, Emily, Sam, Gaby, and Sabrina, it has been a delight to share a space with your lab.

I feel so lucky to be a part of a fantastic graduate community in the Botany Department at UCR. I am grateful to all of the friends I have made here, having you all in my life has eased the stress of graduate school. I want to thank my cohort pals, it has fun watching us all grow through these last six years. To all the friends who have attended bachelor night, special shout out to Brooke for introducing me to reality TV. To both Tyler and Emily for being my carpool buddies. To all of the rock-climbing buddies for providing a fun social activity for after work, and those that taught me how to climb outside. To every

friend who has dog sat Laszlo, you have been a huge help! Thank you to Liz and Emily for being my grad school mentors, my workout pals, and amazing friends.

Lastly, I want to thank my non-Riverside friends and my family. My parents have been an incredible support system for me throughout both my undergraduate and graduate journey. You have always encouraged my pursuit of knowledge and have been my biggest cheerleaders. I am grateful to my sisters for anchoring me during times of stress. You both have given my favorite job, being an auntie to your kids. I am also grateful to the support from my brothers-in-law. Throughout my PhD journey, my grandparents have been a source of immense support, with my grandma offering constant encouragement and the memory of Mamo and grandpa who have passed providing enduring inspiration. I want to thank my friends for giving me a space to have fun and always encouraging my goals. I also want to thank both of my southern California families, the Torres and Ceballos families, for welcoming me wholeheartedly in to their homes when I am not in Riverside. And finally, I want to thank my partner Marcelo and my emotional support dog Laszlo, I know I could not have achieved this degree without you. I am so grateful to Marcelo for keeping me fed these last few years and are always willing to walk the dog. You have been my rock these past six years not only always being there for me during the most stressful times but being a source of strength and constant encouragement.

Thank you to everyone who has supported me during my PhD. Your encouragement and belief in me have been crucial—I couldn't have done this alone, and I am deeply grateful for each of you.

Dedication:

Dedicated to Mamo and Grandpa for always encouraging me to be curious about the world.

ABSTRACT OF DISSERTATION:

Mechanisms of Strigolactone Signal Transduction in Plants

by

Alexandra White

Doctor of Philosophy, Graduate Program in Plant Biology
University of California, Riverside, September 2024
Dr. David Nelson, Chairperson

The strigolactone (SL) and karrikin (KAR) signaling pathways, two highly homologous pathways in plants, are not only essential in plant growth and development, symbiotic and parasitic interactions, and responses to environmental stresses, but also hold significant implications for the field of plant hormone biology. Understanding how these two complex pathways evolved to achieve specificity separate from one another while possibly maintaining a level of crosstalk has been a matter of great interest. The work in this dissertation, which aims to deepen knowledge of how receptors in each pathway interact with downstream protein partners.

While there have been numerous technological advancements for analyzing strigolactone receptors, the processes, such as stable transformations, can be laborious and time-consuming. In the first chapter, I present an innovative and alternate approach to evaluate the functionality of the strigolactone receptor, DWARF14 (D14), in a transient assay in *Nicotiana benthamiana*. This approach, using CRISPR-cas9 to knock out the two endogenous *N. benthamiana D14* genes, *D14a* and *D14b*, to analyze different strigolactone receptor functions in a transient system. The *Nbd14a,b* mutant displayed a typical *d14* phenotype, short and highly branched. Using this mutant background and a

ratiometric reporter system, I demonstrated how this system can evaluate D14 variants not previously investigated in a plant system.

Most research on strigolactone receptors has concentrated on ligand binding and perception. Nevertheless, interactions with downstream protein partners, specifically SUPPRESSOR OF MAX2 LIKE (SMXLs) proteins, play a crucial role in strigolactone signal transduction. My second chapter focuses on identifying and mapping the D14 amino acids necessary for SMXL interaction. I determine highly conserved amino acids in D14 and analyze if these residues convey interaction towards the SMXL7 protein partner by mutational analysis in both the transient system described in Chapter One and stable *Arabidopsis thaliana* lines. The data indicates that altering specific D14 residues affects SMXL interaction, but there is no clear interaction interface. Additionally, variant $D14^{D198A}$ showed a defective interaction with SMXL. However, the data suggests that the D198 residue is crucial for the protein's structure and stability.

Parasitic species in the Orobanchaceae family have evolved to sense host-derived SLs via the convergent evolution of karrikin receptors known as KAI2d proteins. In the last chapter, I used the transient *N. benthamiana* system to determine the functional roles of the seven KAI2d orthologs and the two SMAX1 orthologs found in the hemiparasite *Phtheirospermum japonicum*. The findings of this research, which discovered four PjKAI2d proteins are highly sensitive SL receptors, and two demonstrate inhibitory functions towards the sensitive receptors at low SL concentrations, hold great potential for further understanding and manipulation of plant-parasite interactions.

Table of Contents

Acknowledgments: ..... **iv**

Dedication: ..... **vii**

Abstract of the dissertation: ..... **viii**

List of Figures: ..... **xii**

List of Tables: ..... **xiii**

General introduction: **1**

References: 12

Chapter 1: Rapid analysis of strigolactone receptor activity in a *Nicotiana benthamiana dwarf14* mutant ***22***

Abstract: 22

Introduction: 21

Materials and methods: 28

Results: 33

Discussion: 38

References: 46

Figures: 55

Supplementary figures and legends: 60

Chapter 2: Identification of residues required for receptor-target interactions during strigolactone signaling **62**

Abstract: 62

Introduction: 63

Materials and methods: 74

Results and Discussion: 78

Conclusion: 88

References: 91

Figures: 100

Supplementary tables: 109

Chapter 3: An Atypical Subclade of KAI2d Proteins Attenuate Responses to Host-derived Strigolactones in a Hemiparasitic Plant, *Phtheirospermum japonicum* .. **117**

Abstract: 117
Introduction: 118
Materials and methods: 125
Results: 128
Discussion: 133
References: 137
Figures: 143
Supplemental figures and tables: 151
Conclusion and future directions: **155**
References: 158

List of Figures:

Chapter 1:

Figure 1.1 Mutation of two *D14* genes in *Nicotiana benthamiana* with CRISPR-Cas9 55
Figure 1.2 *Nbd14a,b* has more axillary bud outgrowth and reduced height.....56
Figure 1.3 *Nbd14a,b* has smaller leaves and petioles 57
Figure 1.4 AtSMXL7 degradation in *N. benthamiana* is *NbD14*-dependent.....58
Figure 1.5 AtSMXL7 degradation is altered when co-expressed with AtD14 variants. 60
Figure S1.1 $AtD14^{D167A}$ is less sensitive to *rac*-GR24 than wt AtD14. 60

Chapter 2:

Figure 2.1: Identifying amino acid residues to assess their role in SMXL7 interaction 100
Figure 2.2: Assessment of D14 variant ability to target SMXL7 for degradation 102
Figure 2.3: Reevaluation of interesting D14 variants in SMXL7 degradation assay 103
Figure 2.4: Majority of D14 variants rescue *Atd14* branching phenotype in T1 generation 105
Figure 2.5: The D198A mutation does not rescue the branching or height phenotype of *Atd14*.....106
Figure 2.6: Analysis of D14 variant stability and MAX2 induced degradation.....107
Figure 2.7: DynaMut predictions suggest stabilizing and destabilizing effects of mutations 108

Chapter 3:

Figure 3.1. Generation of a SL-insensitive *N. benthamiana* mutant.....143
Figure 3.2 Analysis of PjKAI2d activity 145
Figure 3.3 Attenuation of PjSMAX1.1 degradation by PjKAI2d2 and PjKAI2d3.2..146
Figure 3.4 Catalytic serine is required for PjKAI2d2 and PjKAI2d3.2 attenuation effects 147
Figure 3.5 Phylogenetic analysis of KAI2 proteins in parasitic plants.....148
Figure 3.6 PjKAI2d amino acid identities at the MAX2 interface 149
Figure 3.7 Model for strigolactone signaling attenuation during parasite chemotropism.....150

List of Tables:

Chapter 1:

Supplementary Table S1.1 Primers used in this study.....61

Chapter 2:

Table S2.1 Selected residues and values.....109

Table S2.2 Primer sequences 112

Chapter 3:

Table S3.1 Primer sequences 151

Table S3.2 *NbKAI2* coding sequences 152

General introduction:

The impact of rapid climate change caused by increased global warming on agriculture has been significant and devastating (Malhi et al., 2021). Climate change has led to dramatic temperature fluctuations, higher incidence of plant diseases and pathogens, extreme weather events, and poor nutrient availability in soil (Ebi et al., 2021; Garrett et al., 2021; Jansson & Hofmockel, 2020; Ristaino et al., 2021; Vose et al., 2021). The growing global population further exacerbates these challenges, making plant research crucial for human survival (Springmann et al., 2018; Wheeler & von Braun, 2013). As a result, current plant research is dedicated to enhancing plant resilience to environmental factors associated with climate change while maintaining high crop yields to support the increasing population (Rivero et al., 2022). With the advancement of genetic tools, researchers can now engineer crops with higher yields, more robust defense mechanisms, and a remarkable ability to withstand stress (Lew et al., 2020; Rivero et al., 2022; Shelake et al., 2022; Tian et al., 2021).

Understanding how plants respond and adapt to external stimuli and stress is crucial, as plants use a precise system of small-molecule signaling to coordinate their responses to environmental inputs. Ten characterized plant hormone signaling pathways are responsible for plant growth, development, immunity, defense, and stress response(Vanstraelen & Benková, 2012). For example, when plants experience drought, the signaling molecule abscisic acid (ABA) facilitates the rapid closure of stomata to prevent water from escaping(Hsu et al., 2021). When soil has low nutrient availability, plants over-accumulate strigolactones (SLs) to inhibit shoot and root branching to

conserve energy(Luo et al., 2021). While these signaling pathways have distinct responses, they are often entangled with one another to organize specific responses.

The diverse functions of strigolactones:

While SLs have long been recognized as significant in plant biology, their recent emergence as a crucial class of plant hormones(Gomez-Roldan et al., 2008; Umehara et al., 2008) has brought them to the forefront of research. Initially discovered as host-exuded potent germination stimulants of parasitic weeds in the Orobanchaceae family(Cook et al., 1966), SLs are now understood to be critical rhizospheric signals between plants and AM fungi, aiding in the formation of mutualistic relationships during low nutrient conditions(Akiyama et al., 2005; Akiyama & Hayashi, 2006). As carotenoid-derived phytohormones, SLs play crucial roles in plant growth and development, such as shoot and root architecture, leaf senescence, and secondary stem growth(Agusti et al., 2011; Gomez-Roldan et al., 2008; Kapulnik et al., 2011; Ruyter-Spira et al., 2011; Ueda & Kusaba, 2015; Umehara et al., 2008; Yamada et al., 2014). The diverse roles of SLs, both exogenously and endogenously for plants, have gained significant interest and research in the field of plant biology.

Since SLs were discovered, over 30 unique SLs have been identified(Guercio et al., 2023). There are two major groups within the SLs: canonical and non-canonical. Canonical SLs contain an ABC tricyclic lactone ring connected to a methyl-butenolide D ring via a 2'R configured enol-ether bridge(Butler, 1994; Yoneyama et al., 2018; Zwanenburg et al., 2009, 2016; Zwanenburg & Pospísil, 2013). SLs without the ABC ring structure are considered non-canonical but do have a moiety connected to the D ring(Charnikhova et al., 2017; Kim et al., 2014; Umehara et al., 2015; Xie et al., 2017,

2019). Canonical SLs are further divided into strigol-type or orbanchol-type based on the orientation of the C ring. While it remains unclear the exact function of each SL, some plant species can biosynthesize both canonical and non-canonical and/or strigol and orbanchol-type(Yoneyama et al., 2018)(Seto & Yamaguchi, 2014; Yoneyama & Brewer, 2021). In contrast, some plant species produce only one type: canonical versus non-canonical and/or orbanchol versus strigol-type(Yoneyama et al., 2018)(Seto & Yamaguchi, 2014; Yoneyama & Brewer, 2021). Interestingly, endogenous SL signaling components did not emerge until the gymnosperm lineage; however, genes involved in SL biosynthesis show functionality in the liverwort lineage(Kyozuka et al., 2022). The evolutionary history of SLs implies that SLs originally functioned as rhizospheric signals and were later adopted as plant hormones as plants evolved(Kyozuka et al., 2022). While the biosynthesis and production of SLs is a fascinating growing field in SL biology, this thesis focuses on the core components of SL signaling. Specifically, it is unclear how SL receptors interact with downstream protein partners, which is a critical step in SL signal transduction.

Ligand perception by D14 and KAI2:

Many genes involved in SL biosynthesis and SL signaling were discovered by analyzing mutants with an increased branching phenotype from different species, such as rice, pea, and petunia. The gene responsible for SL perception, *DWARF14 (D14)*, was first identified in rice tillering mutants produced through traditional breeding practices to increase yield(Arite et al., 2009; Ishikawa et al., 2005). In a seminal study, the SL signaling role of a D14 ortholog, known as DAD2, was determined in *Petunia*. This study revealed that highly branched *dad2* mutants exhibit insensitivity to SL-induced branching inhibition.

Furthermore, DAD2 can hydrolyze SLs into biologically inactive molecules.(Hamiaux et al., 2012). Numerous studies have examined D14 as the SL receptor in other species, including *Arabidopsis thaliana(de Saint Germain et al., 2016; Lauressergues et al., 2015; Waters et al., 2012; White et al., 2022)*. D14 is amongst the α/β hydrolase protein family, a globular family of proteins containing a characteristic α/β hydrolase fold. D14 often maintains ligand-specific hydrolytic activity via a highly conserved serine-histidine-aspartate catalytic triad(Bauer et al., 2020). D14 is not the only α/β hydrolase in plant hormone signaling as the receptor for gibberellin is also an α/β hydrolase, GID1(Griffiths et al., 2006; Nakajima et al., 2006; Ueguchi-Tanaka et al., 2005). GID1, however, does not contain a functional catalytic triad due to a histidine-to-valine switch where the histidine is essential for hydrolase activity and, therefore, only functions as a GA receptor(Ueguchi-Tanaka et al., 2005). In fact, unlike most hormone receptors, D14 displays hydrolytic activity towards SLs(Hamiaux et al., 2012; Nakamura et al., 2013; Zhao et al., 2013). Furthermore, when the serine or histidine residues comprising the catalytic triad are mutated, the protein is catalytically inactive and does not interact with downstream protein partners, rendering the protein completely non-functional(Hamiaux et al., 2012; Nakamura et al., 2013; Seto et al., 2019). Shockingly, when the aspartate residue in the catalytic triad is mutated, the enzymatic function is lost. Still, the signaling function is not, suggesting this mutation bypasses the role hydrolysis has in signaling(Seto et al., 2019).

Intriguingly, the SL signaling pathway is closely related and shares core components with the karrikin signaling pathway. Karrikins (KARs) are small butenolide compounds found in smoke from burnt plant material(Chiwocha et al., 2009). Many plant species use these compounds as germination stimulants in post-fire habitats(Merritt et al., 2009; Nelson et al., 2012). KAR-induced germination responses rely on KAI2 signaling.

However, a growing body of evidence suggests an endogenous role for this pathway that does not require karrikins(Waters et al., 2012).

D14 is closely related to the karrikin receptor, KARRIKIN INSENSITIVE2 (KAI2)(Bythell-Douglas et al., 2017; Machin et al., 2020; Waters et al., 2012). Furthermore, the core karrikin signaling components, including KAI2, are conserved across land plants, and KAI2 is the ancestral lineage from which the D14 lineage emerged through a gene duplication event and neofunctionalization before the gymnosperm lineage(Bythell-Douglas et al., 2017; Machin et al., 2020).

Biochemically, KAI2 weakly interacts with karrikin molecules and has a stronger affinity for non-natural SL stereoisomers, suggesting KAI2 requires an endogenous ligand that is more similar to SLs than KARs(Bürger et al., 2019; Flematti et al., 2016; Guo et al., 2013; Kagiyama et al., 2013; Waters, Scaffidi, Moulin, et al., 2015; J. Yao et al., 2018, 2021). KARs do not induce KAI2 interactions with downstream protein partners where non-natural SL stereoisomers do(Khosla, Morffy, et al., 2020; L. Wang et al., 2020; Xu et al., 2018). This biochemical and molecular evidence, along with the conservation of the KAI2 lineage, suggests there is an endogenous KAI2 ligand (KL) that KAR molecules mimic(Bonhomme & Guillory, 2022; Conn & Nelson, 2015; Flematti et al., 2013; Guercio et al., 2022; Machin et al., 2020; Stirling et al., 2024).

Like D14, KAI2 also has the conserved serine-histidine-aspartate catalytic triad required for function(Khosla, Morffy, et al., 2020; Khosla, Rodriguez-Furlan, et al., 2020; Waters, Scaffidi, Flematti, et al., 2015). The KAR signaling pathway is involved in many essential plant processes, such as germination, hypocotyl elongation, and drought tolerance(W. Li et al., 2017, 2020; Nelson et al., 2010; Stanga et al., 2016; Waters et al., 2012). Because of the elusive nature of discovering KL, ligand perception, ligand

preferences, and hydrolytic activity are under-studied for KAI2 proteins compared to D14. One exception to this would be the divergent clade of KAI2 receptors (KAI2d) found in parasitic weeds in the Orobanchaceae family(Conn et al., 2015). This clade has undergone a rapid expansion and, through convergent evolution, specifically in the ligand binding pocket, can perceive host-derived SLs and utilize them as germination stimulants(Conn et al., 2015; Pang et al., 2020; Toh et al., 2015; Tsuchiya et al., 2018; Y. Wang et al., 2021).

The significance of protein partners in SL and KAR signaling:

While ligand perception by D14 is the initial step in turning on the SL response, protein partner interactions initiate the signaling cascade. One such interaction is with the F-box protein MORE AXILLARY GROWTH 2 (MAX2). MAX2 was discovered in *Arabidopsis* mutant populations, having defects in leaf senescence, photomorphogenesis, and increased branching(Shen et al., 2007; Woo et al., 2001). Genetic analysis revealed that MAX2 is a core component in SL and KAR signaling(Hamiaux et al., 2012; Nelson et al., 2011; Soundappan et al., 2015; Stirnberg et al., 2007). The involvement of MAX2 in these signaling pathways is not shocking, as many other plant hormones, such as auxin, gibberellin, abscisic acid, and jasmonic acid, require other F-box proteins for signal transduction(Abd-Hamid et al., 2020; Yu et al., 2007). In fact, before the discovery of D14, it was thought MAX2 was the SL receptor as F-box proteins are receptors for the auxin and JA signaling pathways(Abd-Hamid et al., 2020; Blázquez et al., 2020; Yu et al., 2007). F-box proteins participate in the Skp1-Cullin-F-box (SCF) E3 ubiquitin ligase complex. They are responsible for protein partner recognition in which the protein partner is tagged

with ubiquitin by the complex and subsequently degraded by the 26S-proteasome(Abd-Hamid et al., 2020; Blázquez et al., 2020; Stirnberg et al., 2007; Yu et al., 2007).

A significant step forward in the SL field came when a crystal structure of D14 was in complex with rice MAX2 (known as D3 in rice)(R. Yao et al., 2016). D14 displayed a significant conformational change in this structure compared to the apo structure and provided a clear interaction surface between the two proteins(R. Yao et al., 2016; Zhao et al., 2013). This structure has since been deemed the likely active and closed conformation of D14(R. Yao et al., 2016). Recent work focusing on MAX2/D3 has determined that the C-terminal helix (CTH) has multiple conformations that affect SL hydrolysis and recruitment of downstream targets for degradation(Tal et al., 2022).

D14 is also targeted for degradation in an SL and MAX2-dependent manner as a form of feedback regulation(Chevalier et al., 2014). However, a recent study found that while MAX2 is primarily responsible for D14 degradation, D14 also undergoes MAX2-independent degradation(Martín-Fontecha et al., 2024). Similarly, KAI2 undergoes degradation following KAR treatment via an unknown MAX2-independent mechanism(Waters, Scaffidi, Flematti, et al., 2015).

The proteolytic targets of the SL-D14-MAX2 complex belong to the SUPPRESSOR OF MAX2 1-LIKE (SMAX1/SMXL) family of proteins(Jiang et al., 2013; Kerr et al., 2021; Soundappan et al., 2015; Stanga et al., 2013; L. Wang et al., 2015; Zhou et al., 2013, 2016). The primary function of ligand-activated D14 and KAI2 proteins is to target SMXL proteins for degradation. These SMXL proteins serve as critical regulators of growth and development, and SLs or KL/KARs can suppress their activity. In *Arabidopsis*, eight proteins make up this family, and SMXL6/7/8, all homologs of D53 in rice, are responsible for SL-induced responses(Liang et al., 2016; Soundappan et al., 2015; L. Wang et al.,

2015). Similarly, two of the paralogs, SMAX1 and SMXL2, are the targets of the KAI2 signaling pathway(Khosla, Morffy, et al., 2020; Soundappan et al., 2015; Stanga et al., 2013, 2016; Villaécija-Aguilar et al., 2019; L. Wang et al., 2020; Zheng et al., 2021).

Similar to the evolution of the receptor lineage for these two signaling pathways, SMAX1/SMXL2 type SMXLs form the more ancestral lineage compared to SL-related SMXLs, emerging at the base of spermatophytes. The diversification of the SL-related SMXLs did not occur until angiosperms(Moturu et al., 2018; Walker et al., 2019). Notably, while gymnosperms contain D14 and KAI2 orthologs, they lack an ortholog of SMXL7/D53-type SMXLs(Bythell-Douglas et al., 2017; Moturu et al., 2018; Walker et al., 2019). A recent study analyzing *Ginkgo biloba* and *Sciadopitys verticillata* KAI2 and D14 signaling found *GbSMAX1* is induced by both types of SL enantiomers and is expressed in both leaf and axillary bud tissue, suggesting activation of both the KAI2 and D14 signaling pathways(Kodama et al., 2023). Because there is no apparent SL-related SMXL ortholog in gymnosperms, KAI2 and D14 may target the SMAX1 ortholog and achieve specificity by differential expression patterns(Kodama et al., 2023).

There is evidence of crosstalk between the two pathways in angiosperms that D14 can target SMAX1 and SMXL2 for degradation in some physiological conditions(Q. Li et al., 2022; L. Wang et al., 2020). This promiscuity of D14 might only be observed under high SL treatments, protoplast systems, or under osmotic stress(Q. Li et al., 2022; L. Wang et al., 2020).

SMXL proteins are substantial in size, comprising of multiple domains that serve distinct functions. For example, SMAX1/SMXL2 and SMXL6/7/8 contain an RGKT motif required for SCFMAX2-dependent polyubiquitination(Jiang et al., 2013; Khosla, Morffy, et al., 2020; Soundappan et al., 2015; L. Wang et al., 2015, 2020; Zheng et al., 2021; Zhou

et al., 2013). Interestingly, the other SMXLs in this family, SMXL3/4/5 proteins, do not contain an RGKT motif(Wallner et al., 2017). Therefore these proteins do not undergo MAX2-mediated degradation(Temmerman et al., 2022). This family of proteins includes an ETHYLENE-RESPONSE FACTOR Amphiphilic Repression (EAR) motif that is responsible for protein interactions with TOPLESS (TPL)/TPL-Related (TPR), transcriptional corepressors(Jiang et al., 2013; Khosla, Morffy, et al., 2020; Plant et al., 2021; Soundappan et al., 2015; L. Wang et al., 2015, 2020; Zheng et al., 2021; Zhou et al., 2013). Transcriptional co-repression is a standard mode for regulation in other hormone signaling pathways such as brassinosteroids, auxin, jasmonic acid, and GA(Plant et al., 2021). Therefore, through interactions with transcriptional corepressors, these proteins regulate each signaling pathway, and their degradation releases that repression, turning on the transcriptional response for each pathway.

Typically, the F-box protein in hormone signaling pathways is responsible for downstream target recognition of the SCF complex. However, this is likely not true in SL and KAR signaling(Blázquez et al., 2020). Still, it remains unclear if MAX2 can differentiate between SMAX1/SMXL2 proteins and SMXL6/7/8 type proteins. Because there is no crystal structure of all three proteins in a complex, the site for the SMXL interface on MAX2 has yet to be determined. MAX2 proteins across land plants are highly conserved, so it is plausible that the interface is the same, possibly requiring the same residues. The D14-MAX2 interaction surface is a highly conserved region between D14 and KAI2 proteins, suggesting MAX2 cannot differentiate between the two receptors(Bythell-Douglas et al., 2017). Finally, while the precise steps necessary for complex formation remain unclear, there is evidence of SL-dependent interactions between D14-MAX2 and D14-SMXL7 in planta. Conversely, such interactions have not been observed between MAX2-SMXL7,

suggesting the necessity of D14 for the D14-SMXL7 interaction(Liang et al., 2016). Therefore, this specificity is likely due to SMAX1/SMXL2 and SMXL6/7/8 recognition by KAI2 or D14, respectively(Khosla, Morffy, et al., 2020; Soundappan et al., 2015; L. Wang et al., 2015, 2020; Zhou et al., 2013).

How the KAI2 and D14 signaling pathways evolved to be distinct from one another has yet to be determined, and I propose this occurs through protein-partner interactions. This dissertation explores and enhances our understanding of how specific receptors interact with their SMXL protein partners and how this interaction leads to their breakdown. Specifically, it focuses on receptors involved in the SL and KAI2 signaling pathways and amino acid residues on the receptors required for SMXL interaction.

In the first chapter, I characterize a double mutant knockout line for two *D14* homologs in *Nicotiana benthamiana.* Our lab's previous work led to the development of a ratiometric reporter system, a practical tool for transiently expressing target proteins in *N. benthamiana* to monitor protein degradation(Khosla, Rodriguez-Furlan, et al., 2020). This system's transcript contains the coding sequence of the target protein fused to a fluorescent protein (the reporter), a self-cleaving peptide, F2A, and a second fluorescent protein (the reference)(Khosla, Rodriguez-Furlan, et al., 2020). By measuring the reporter: reference ratio under different conditions or treatments, we can detect target protein degradation. In the specific context of the *Nbd14a,b* mutant background, the AtSMXL7 reporter remains stable under SL treatment and degrades when co-expressed with another plasmid containing D14(White et al., 2022). Using this system, I developed a practical tool for analyzing how different D14 variants affect SMXL stability without interference from endogenous *Nb*D14(White et al., 2022).

In chapter two, I sought to establish the amino acids on the AtD14 surface responsible for facilitating the interaction with SMXL proteins. I determined 67 highly conserved surface exposed residues through an amino acid conservation analysis. With the help of Freshman undergraduates in the UC Riverside Dynamic Genome course (BIOL20), each residue of interest was mutated to alanine using site-directed mutagenesis. I employed the transient system from Chapter One to test each variant's ability to target AtSMXL7 for degradation. The variants with interesting responses were stably transformed into the *Atd14* mutant background and assessed for rescuing the branching phenotype of *Atd14*. Lastly, I tested the stability and degradation of the variants.

In the final chapter, I aimed to evaluate which of the seven KAI2d receptors in the hemiparasitic weed *Pthiosperum japonicum* target PjSMAX1 for degradation using the transient degradation system with PjSMAX1 as the target protein. From this work, I found four receptors highly sensitive to SLs regarding PjSMAX1 co-expression and degradation. The three other receptors were unable to target PjSMAX1 for degradation. Interestingly, when one of these non-responsive receptors was co-transformed with a responsive receptor, I discovered an inhibition in PjSMAX1 degradation under low SL treatment.

In brief, my work has produced a new tool for analyzing D14 variants and SL-related SMXL stability, identified amino acid residues on D14 important for SMXL interaction, and provided a novel understanding of parasitic SL receptors.

References:

Abd-Hamid, N.-A., Ahmad-Fauzi, M.-I., Zainal, Z., & Ismail, I. (2020). Diverse and dynamic roles of F-box proteins in plant biology. Planta, 251(3), 68.

Agusti, J., Herold, S., Schwarz, M., Sanchez, P., Ljung, K., Dun, E. A., Brewer, P. B., Beveridge, C. A., Sieberer, T., Sehr, E. M., & Greb, T. (2011). Strigolactone signaling is required for auxin-dependent stimulation of secondary growth in plants. Proceedings of the National Academy of Sciences of the United States of America, 108(50), 20242–20247.

Akiyama, K., & Hayashi, H. (2006). Strigolactones: chemical signals for fungal symbionts and parasitic weeds in plant roots. Annals of Botany, 97(6), 925–931.

Akiyama, K., Matsuzaki, K.-I., & Hayashi, H. (2005). Plant sesquiterpenes induce hyphal branching in arbuscular mycorrhizal fungi. Nature, 435(7043), 824–827.

Arite, T., Umehara, M., Ishikawa, S., Hanada, A., Maekawa, M., Yamaguchi, S., & Kyozuka, J. (2009). d14, a strigolactone-insensitive mutant of rice, shows an accelerated outgrowth of tillers. Plant & Cell Physiology, 50(8), 1416–1424.

Bauer, T. L., Buchholz, P. C. F., & Pleiss, J. (2020). The modular structure of α/β-hydrolases. The FEBS Journal, 287(5), 1035–1053.

Blázquez, M. A., Nelson, D. C., & Weijers, D. (2020). Evolution of Plant Hormone Response Pathways. Annual Review of Plant Biology, 71, 327–353.

Bonhomme, S., & Guillory, A. (2022). Synthesis and signalling of strigolactone and KAI2-ligand signals in bryophytes. Journal of Experimental Botany, 73(13), 4487–4495.

Bürger, M., Mashiguchi, K., Lee, H. J., Nakano, M., Takemoto, K., Seto, Y., Yamaguchi, S., & Chory, J. (2019). Structural Basis of Karrikin and Non-natural Strigolactone Perception in Physcomitrella patens. Cell Reports, 26(4), 855–865.e5.

Butler, L. G. (1994). Chemical Communication Between the Parasitic Weed <italic>Striga</italic> and Its Crop Host. In Allelopathy (Vol. 582, pp. 158–168). American Chemical Society.

Bythell-Douglas, R., Rothfels, C. J., Stevenson, D. W. D., Graham, S. W., Wong, G. K.-S., Nelson, D. C., & Bennett, T. (2017). Evolution of strigolactone receptors by gradual neo-functionalization of KAI2 paralogues. BMC Biology, 15(1), 52.

Charnikhova, T. V., Gaus, K., Lumbroso, A., Sanders, M., Vincken, J.-P., De Mesmaeker, A., Ruyter-Spira, C. P., Screpanti, C., & Bouwmeester, H. J. (2017). Zealactones. Novel natural strigolactones from maize. Phytochemistry, 137, 123–131.

Chevalier, F., Nieminen, K., Sánchez-Ferrero, J. C., Rodríguez, M. L., Chagoyen, M., Hardtke, C. S., & Cubas, P. (2014). Strigolactone promotes degradation of DWARF14, an α/β hydrolase essential for strigolactone signaling in Arabidopsis. The Plant Cell, 26(3), 1134–1150.

Chiwocha, S. D. S., Dixon, K. W., Flematti, G. R., Ghisalberti, E. L., Merritt, D. J., Nelson, D. C., Riseborough, J.-A. M., Smith, S. M., & Stevens, J. C. (2009). Karrikins: A new family of plant growth regulators in smoke. Plant Science: An International Journal of Experimental Plant Biology, 177(4), 252–256.

Conn, C. E., Bythell-Douglas, R., Neumann, D., Yoshida, S., Whittington, B., Westwood, J. H., Shirasu, K., Bond, C. S., Dyer, K. A., & Nelson, D. C. (2015). PLANT EVOLUTION. Convergent evolution of strigolactone perception enabled host detection in parasitic plants. Science, 349(6247), 540–543.

Conn, C. E., & Nelson, D. C. (2015). Evidence that KARRIKIN-INSENSITIVE2 (KAI2) Receptors may Perceive an Unknown Signal that is not Karrikin or Strigolactone. Frontiers in Plant Science, 6, 1219.

Cook, C. E., Whichard, L. P., Turner, B., Wall, M. E., & Egley, G. H. (1966). Germination of Witchweed (Striga lutea Lour.): Isolation and Properties of a Potent Stimulant. Science, 154(3753), 1189–1190.

de Saint Germain, A., Clavé, G., Badet-Denisot, M.-A., Pillot, J.-P., Cornu, D., Le Caer, J.-P., Burger, M., Pelissier, F., Retailleau, P., Turnbull, C., Bonhomme, S., Chory, J., Rameau, C., & Boyer, F.-D. (2016). An histidine covalent receptor and butenolide complex mediates strigolactone perception. Nature Chemical Biology, 12(10), 787–794.

Ebi, K. L., Vanos, J., Baldwin, J. W., Bell, J. E., Hondula, D. M., Errett, N. A., Hayes, K., Reid, C. E., Saha, S., Spector, J., & Berry, P. (2021). Extreme Weather and Climate Change: Population Health and Health System Implications. Annual Review of Public Health, 42, 293–315.

Flematti, G. R., Scaffidi, A., Waters, M. T., & Smith, S. M. (2016). Stereospecificity in strigolactone biosynthesis and perception. Planta, 243(6), 1361–1373.

Flematti, G. R., Waters, M. T., Scaffidi, A., Merritt, D. J., Ghisalberti, E. L., Dixon, K. W., & Smith, S. M. (2013). Karrikin and cyanohydrin smoke signals provide clues to new endogenous plant signaling compounds. Molecular Plant, 6(1), 29–37.

Garrett, K. A., Nita, M., De Wolf, E. D., Esker, P. D., Gomez-Montano, L., & Sparks, A. H. (2021). Chapter 24 - Plant pathogens as indicators of climate change. In T. M. Letcher (Ed.), Climate Change (Third Edition) (pp. 499–513). Elsevier.

Gomez-Roldan, V., Fermas, S., Brewer, P. B., Puech-Pagès, V., Dun, E. A., Pillot, J.-P., Letisse, F., Matusova, R., Danoun, S., Portais, J.-C., Bouwmeester, H., Bécard, G., Beveridge, C. A., Rameau, C., & Rochange, S. F. (2008). Strigolactone inhibition of shoot branching. Nature, 455(7210), 189–194.

Griffiths, J., Murase, K., Rieu, I., Zentella, R., Zhang, Z.-L., Powers, S. J., Gong, F., Phillips, A. L., Hedden, P., Sun, T.-P., & Thomas, S. G. (2006). Genetic characterization and functional analysis of the GID1 gibberellin receptors in Arabidopsis. The Plant Cell, 18(12), 3399–3414.

Guercio, A. M., Palayam, M., & Shabek, N. (2023). Strigolactones: diversity, perception, and hydrolysis. Phytochemistry Reviews, 22(2), 339–359.

Guercio, A. M., Torabi, S., Cornu, D., Dalmais, M., Bendahmane, A., Le Signor, C., Pillot, J.-P., Le Bris, P., Boyer, F.-D., Rameau, C., Gutjahr, C., de Saint Germain, A., & Shabek, N. (2022). Structural and functional analyses explain Pea KAI2 receptor diversity and reveal stereoselective catalysis during signal perception. Communications Biology, 5(1), 126.

Guo, Y., Zheng, Z., La Clair, J. J., Chory, J., & Noel, J. P. (2013). Smoke-derived karrikin perception by the α/β-hydrolase KAI2 from Arabidopsis. Proceedings of the National Academy of Sciences of the United States of America, 110(20), 8284–8289.

Hamiaux, C., Drummond, R. S. M., Janssen, B. J., Ledger, S. E., Cooney, J. M., Newcomb, R. D., & Snowden, K. C. (2012). DAD2 is an α/β hydrolase likely to be involved in the perception of the plant branching hormone, strigolactone. Current Biology: CB, 22(21), 2032–2036.

Hsu, P.-K., Dubeaux, G., Takahashi, Y., & Schroeder, J. I. (2021). Signaling mechanisms in abscisic acid-mediated stomatal closure. The Plant Journal: For Cell and Molecular Biology, 105(2), 307–321.

Ishikawa, S., Maekawa, M., Arite, T., Onishi, K., Takamure, I., & Kyozuka, J. (2005). Suppression of tiller bud activity in tillering dwarf mutants of rice. Plant & Cell Physiology, 46(1), 79–86.
Jansson, J. K., & Hofmockel, K. S. (2020). Soil microbiomes and climate change. Nature Reviews. Microbiology, 18(1), 35–46.

Jiang, L., Liu, X., Xiong, G., Liu, H., Chen, F., Wang, L., Meng, X., Liu, G., Yu, H., Yuan, Y., Yi, W., Zhao, L., Ma, H., He, Y., Wu, Z., Melcher, K., Qian, Q., Xu, H. E., Wang, Y., & Li, J. (2013). DWARF 53 acts as a repressor of strigolactone signalling in rice. Nature, 504(7480), 401–405.

Kagiyama, M., Hirano, Y., Mori, T., Kim, S.-Y., Kyozuka, J., Seto, Y., Yamaguchi, S., & Hakoshima, T. (2013). Structures of D14 and D14L in the strigolactone and karrikin signaling pathways. Genes to Cells: Devoted to Molecular & Cellular Mechanisms, 18(2), 147–160.

Kapulnik, Y., Delaux, P.-M., Resnick, N., Mayzlish-Gati, E., Wininger, S., Bhattacharya, C., Séjalon-Delmas, N., Combier, J.-P., Bécard, G., Belausov, E., Beeckman, T., Dor, E., Hershenhorn, J., & Koltai, H. (2011). Strigolactones affect lateral root formation and root-hair elongation in Arabidopsis. Planta, 233(1), 209–216.

Kerr, S. C., Patil, S. B., de Saint Germain, A., Pillot, J.-P., Saffar, J., Ligerot, Y., Aubert, G., Citerne, S., Bellec, Y., Dun, E. A., Beveridge, C. A., & Rameau, C. (2021). Integration of the

SMXL/D53 strigolactone signalling repressors in the model of shoot branching regulation in Pisum sativum. The Plant Journal: For Cell and Molecular Biology, 107(6), 1756–1770.

Khosla, A., Morffy, N., Li, Q., Faure, L., Chang, S. H., Yao, J., Zheng, J., Cai, M. L., Stanga, J., Flematti, G. R., Waters, M. T., & Nelson, D. C. (2020). Structure–Function Analysis of SMAX1 Reveals Domains That Mediate Its Karrikin-Induced Proteolysis and Interaction with the Receptor KAI2. The Plant Cell, 32(8), 2639–2659.

Khosla, A., Rodriguez-Furlan, C., Kapoor, S., Van Norman, J. M., & Nelson, D. C. (2020). A series of dual-reporter vectors for ratiometric analysis of protein abundance in plants. Plant Direct, 4(6), e00231.

Kim, H. I., Kisugi, T., Khetkam, P., Xie, X., Yoneyama, K., Uchida, K., Yokota, T., Nomura, T., McErlean, C. S. P., & Yoneyama, K. (2014). Avenaol, a germination stimulant for root parasitic plants from Avena strigosa. Phytochemistry, 103, 85–88.

Kodama, K., Xie, X., & Kyozuka, J. (2023). The D14 and KAI2 Orthologs of Gymnosperms Sense Strigolactones and KL Mimics, Respectively, and the Signals Are Transduced to Control Downstream Genes. Plant & Cell Physiology. https://doi.org/10.1093/pcp/pcad072

Kyozuka, J., Nomura, T., & Shimamura, M. (2022). Origins and evolution of the dual functions of strigolactones as rhizosphere signaling molecules and plant hormones. Current Opinion in Plant Biology, 65, 102154.

Lauressergues, D., André, O., Peng, J., Wen, J., Chen, R., Ratet, P., Tadege, M., Mysore, K. S., & Rochange, S. F. (2015). Strigolactones contribute to shoot elongation and to the formation of leaf margin serrations in Medicago truncatula R108. Journal of Experimental Botany, 66(5), 1237–1244.

Lew, T. T. S., Sarojam, R., Jang, I.-C., Park, B. S., Naqvi, N. I., Wong, M. H., Singh, G. P., Ram, R. J., Shoseyov, O., Saito, K., Chua, N.-H., & Strano, M. S. (2020). Species-independent analytical tools for next-generation agriculture. Nature Plants, 6(12), 1408–1417.

Liang, Y., Ward, S., Li, P., Bennett, T., & Leyser, O. (2016). SMAX1-LIKE7 Signals from the Nucleus to Regulate Shoot Development in Arabidopsis via Partially EAR Motif-Independent Mechanisms. The Plant Cell, 28(7), 1581–1601.

Li, Q., Martín-Fontecha, E. S., Khosla, A., White, A. R. F., Chang, S., Cubas, P., & Nelson, D. C. (2022). The strigolactone receptor D14 targets SMAX1 for degradation in response to GR24 treatment and osmotic stress. Plant Communications, 3(2), 100303.

Li, W., Nguyen, K. H., Chu, H. D., Van Ha, C., Watanabe, Y., Osakabe, Y., Leyva-González, M. A., Sato, M., Toyooka, K., Voges, L., Tanaka, M., Mostofa, M. G., Seki, M., Seo, M., Yamaguchi, S., Nelson, D. C., Tian, C., Herrera-Estrella, L., & Tran, L.-S. P. (2017). The karrikin receptor KAI2 promotes drought resistance in Arabidopsis thaliana. PLoS Genetics, 13(11), e1007076.

Li, W., Nguyen, K. H., Chu, H. D., Watanabe, Y., Osakabe, Y., Sato, M., Toyooka, K., Seo, M., Tian, L., Tian, C., Yamaguchi, S., Tanaka, M., Seki, M., & Tran, L.-S. P. (2020). Comparative functional analyses of DWARF14 and KARRIKIN INSENSITIVE 2 in drought adaptation of Arabidopsis thaliana. The Plant Journal: For Cell and Molecular Biology, 103(1), 111–127.

Luo, Z., Janssen, B. J., & Snowden, K. C. (2021). The molecular and genetic regulation of shoot branching. Plant Physiology, 187(3), 1033–1044.

Machin, D. C., Hamon-Josse, M., & Bennett, T. (2020). Fellowship of the rings: a saga of strigolactones and other small signals. The New Phytologist, 225(2), 621–636.

Malhi, G. S., Kaur, M., & Kaushik, P. (2021). Impact of Climate Change on Agriculture and Its Mitigation Strategies: A Review. Sustainability: Science Practice and Policy, 13(3), 1318.

Martín-Fontecha, E. S., Cardinale, F., Bürger, M., Prandi, C., & Cubas, P. (2024). Novel Mechanisms of Strigolactone-Induced DWARF14 Degradation in Arabidopsis thaliana. In bioRxiv (p. 2024.01.10.574527). https://doi.org/10.1101/2024.01.10.574527

Merritt, D. J., Dixon, K. W., Flematti, G. R., & Ghisalberti, E. L. (2009). Karrikinolide - A phytoreactive compound derived from smoke with applications in horticulture, ecological restoration and agriculture. Acta Horticulturae, 813, 155–170.

Moturu, T. R., Thula, S., Singh, R. K., Nodzyński, T., Vařeková, R. S., Friml, J., & Simon, S. (2018). Molecular evolution and diversification of the SMXL gene family. Journal of Experimental Botany, 69(9), 2367–2378.

Nakajima, M., Shimada, A., Takashi, Y., Kim, Y.-C., Park, S.-H., Ueguchi-Tanaka, M., Suzuki, H., Katoh, E., Iuchi, S., Kobayashi, M., Maeda, T., Matsuoka, M., & Yamaguchi, I. (2006). Identification and characterization of Arabidopsis gibberellin receptors. The Plant Journal: For Cell and Molecular Biology, 46(5), 880–889.

Nakamura, H., Xue, Y.-L., Miyakawa, T., Hou, F., Qin, H.-M., Fukui, K., Shi, X., Ito, E., Ito, S., Park, S.-H., Miyauchi, Y., Asano, A., Totsuka, N., Ueda, T., Tanokura, M., & Asami, T. (2013). Molecular mechanism of strigolactone perception by DWARF14. Nature Communications, 4, 2613.

Nelson, D. C., Flematti, G. R., Ghisalberti, E. L., Dixon, K. W., & Smith, S. M. (2012). Regulation of seed germination and seedling growth by chemical signals from burning vegetation. Annual Review of Plant Biology, 63, 107–130.

Nelson, D. C., Flematti, G. R., Riseborough, J.-A., Ghisalberti, E. L., Dixon, K. W., & Smith, S. M. (2010). Karrikins enhance light responses during germination and seedling development in Arabidopsis thaliana. Proceedings of the National Academy of Sciences of the United States of America, 107(15), 7095–7100.

Nelson, D. C., Scaffidi, A., Dun, E. A., Waters, M. T., Flematti, G. R., Dixon, K. W., Beveridge, C. A., Ghisalberti, E. L., & Smith, S. M. (2011). F-box protein MAX2 has dual roles in karrikin and strigolactone signaling in Arabidopsis thaliana. Proceedings of the National Academy of Sciences of the United States of America, 108(21), 8897–8902.

Pang, Z., Zhang, X., Ma, F., Liu, J., Zhang, H., Wang, J., Wen, X., & Xi, Z. (2020). Comparative Studies of Potential Binding Pocket Residues Reveal the Molecular Basis of ShHTL Receptors in the Perception of GR24 in Striga. Journal of Agricultural and Food Chemistry, 68(45), 12729–12737.
Plant, A. R., Larrieu, A., & Causier, B. (2021). Repressor for hire! The vital roles of TOPLESS-mediated transcriptional repression in plants. The New Phytologist, 231(3), 963–973.

Ristaino, J. B., Anderson, P. K., Bebber, D. P., Brauman, K. A., Cunniffe, N. J., Fedoroff, N. V., Finegold, C., Garrett, K. A., Gilligan, C. A., Jones, C. M., Martin, M. D., MacDonald, G. K., Neenan, P., Records, A., Schmale, D. G., Tateosian, L., & Wei, Q. (2021). The persistent threat of emerging plant disease pandemics to global food security. Proceedings of the National Academy of Sciences of the United States of America, 118(23). https://doi.org/10.1073/pnas.2022239118

Rivero, R. M., Mittler, R., Blumwald, E., & Zandalinas, S. I. (2022). Developing climate-resilient crops: improving plant tolerance to stress combination. The Plant Journal: For Cell and Molecular Biology, 109(2), 373–389.

Ruyter-Spira, C., Kohlen, W., Charnikhova, T., van Zeijl, A., van Bezouwen, L., de Ruijter, N., Cardoso, C., Lopez-Raez, J. A., Matusova, R., Bours, R., Verstappen, F., & Bouwmeester, H. (2011). Physiological effects of the synthetic strigolactone analog GR24 on root system architecture in Arabidopsis: another belowground role for strigolactones? Plant Physiology, 155(2), 721–734.

Seto, Y., & Yamaguchi, S. (2014). Strigolactone biosynthesis and perception. Current Opinion in Plant Biology, 21, 1–6.

Seto, Y., Yasui, R., Kameoka, H., Tamiru, M., Cao, M., Terauchi, R., Sakurada, A., Hirano, R., Kisugi, T., Hanada, A., Umehara, M., Seo, E., Akiyama, K., Burke, J., Takeda-Kamiya, N., Li, W., Hirano, Y., Hakoshima, T., Mashiguchi, K., … Yamaguchi, S. (2019). Strigolactone perception and deactivation by a hydrolase receptor DWARF14. Nature Communications, 10(1), 191.

Shelake, R. M., Kadam, U. S., Kumar, R., Pramanik, D., Singh, A. K., & Kim, J.-Y. (2022). Engineering drought and salinity tolerance traits in crops through CRISPR-mediated genome editing: Targets, tools, challenges, and perspectives. Plant Communications, 3(6), 100417.

Shen, H., Luong, P., & Huq, E. (2007). The F-box protein MAX2 functions as a positive regulator of photomorphogenesis in Arabidopsis. Plant Physiology, 145(4), 1471–1483.

Soundappan, I., Bennett, T., Morffy, N., Liang, Y., Stanga, J. P., Abbas, A., Leyser, O., & Nelson, D. C. (2015). SMAX1-LIKE/D53 Family Members Enable Distinct MAX2-Dependent Responses to Strigolactones and Karrikins in Arabidopsis. The Plant Cell, 27(11), 3143–3159.

Springmann, M., Clark, M., Mason-D'Croz, D., Wiebe, K., Bodirsky, B. L., Lassaletta, L., de Vries, W., Vermeulen, S. J., Herrero, M., Carlson, K. M., Jonell, M., Troell, M., DeClerck, F., Gordon, L. J., Zurayk, R., Scarborough, P., Rayner, M., Loken, B., Fanzo, J., … Willett, W. (2018). Options for keeping the food system within environmental limits. Nature, 562(7728), 519–525.

Stanga, J. P., Morffy, N., & Nelson, D. C. (2016). Functional redundancy in the control of seedling growth by the karrikin signaling pathway. Planta, 243(6), 1397–1406.

Stanga, J. P., Smith, S. M., Briggs, W. R., & Nelson, D. C. (2013). SUPPRESSOR OF MORE AXILLARY GROWTH2 1 controls seed germination and seedling development in Arabidopsis. Plant Physiology, 163(1), 318–330.

Stirling, S. A., Guercio, A. M., Patrick, R. M., Huang, X.-Q., Bergman, M. E., Dwivedi, V., Kortbeek, R. W. J., Liu, Y.-K., Sun, F., Tao, W. A., Li, Y., Boachon, B., Shabek, N., & Dudareva, N. (2024). Volatile communication in plants relies on a KAI2-mediated signaling pathway. Science, 383(6689), 1318–1325.

Stirnberg, P., Furner, I. J., & Ottoline Leyser, H. M. (2007). MAX2 participates in an SCF complex which acts locally at the node to suppress shoot branching. The Plant Journal: For Cell and Molecular Biology, 50(1), 80–94.
Tal, L., Palayam, M., Ron, M., Young, A., Britt, A., & Shabek, N. (2022). A conformational switch in the SCF-D3/MAX2 ubiquitin ligase facilitates strigolactone signalling. Nature Plants, 8(5), 561–573.

Temmerman, A., Guillory, A., Bonhomme, S., Goormachtig, S., & Struk, S. (2022). Masks Start to Drop: Suppressor of MAX2 1-Like Proteins Reveal Their Many Faces. Frontiers in Plant Science, 13, 887232.

Tian, Z., Wang, J.-W., Li, J., & Han, B. (2021). Designing future crops: challenges and strategies for sustainable agriculture. The Plant Journal: For Cell and Molecular Biology, 105(5), 1165–1178.

Toh, S., Holbrook-Smith, D., Stogios, P. J., Onopriyenko, O., Lumba, S., Tsuchiya, Y., Savchenko, A., & McCourt, P. (2015). Structure-function analysis identifies highly sensitive strigolactone receptors in Striga. Science, 350(6257), 203–207.

Tsuchiya, Y., Yoshimura, M., & Hagihara, S. (2018). The dynamics of strigolactone perception in Striga hermonthica: a working hypothesis. Journal of Experimental Botany, 69(9), 2281–2290.

Ueda, H., & Kusaba, M. (2015). Strigolactone Regulates Leaf Senescence in Concert with Ethylene in Arabidopsis. Plant Physiology, 169(1), 138–147.

Ueguchi-Tanaka, M., Ashikari, M., Nakajima, M., Itoh, H., Katoh, E., Kobayashi, M., Chow, T.-Y., Hsing, Y.-I. C., Kitano, H., Yamaguchi, I., & Matsuoka, M. (2005). GIBBERELLIN INSENSITIVE DWARF1 encodes a soluble receptor for gibberellin. Nature, 437(7059), 693–698.

Umehara, M., Cao, M., Akiyama, K., Akatsu, T., Seto, Y., Hanada, A., Li, W., Takeda-Kamiya, N., Morimoto, Y., & Yamaguchi, S. (2015). Structural Requirements of Strigolactones for Shoot Branching Inhibition in Rice and Arabidopsis. In Plant and Cell Physiology (Vol. 56, Issue 6, pp. 1059–1072). https://doi.org/10.1093/pcp/pcv028

Umehara, M., Hanada, A., Yoshida, S., Akiyama, K., Arite, T., Takeda-Kamiya, N., Magome, H., Kamiya, Y., Shirasu, K., Yoneyama, K., Kyozuka, J., & Yamaguchi, S. (2008). Inhibition of shoot branching by new terpenoid plant hormones. Nature, 455(7210), 195–200.

Vanstraelen, M., & Benková, E. (2012). Hormonal interactions in the regulation of plant development. Annual Review of Cell and Developmental Biology, 28, 463–487.

Villaécija-Aguilar, J. A., Hamon-Josse, M., Carbonnel, S., Kretschmar, A., Schmid, C., Dawid, C., Bennett, T., & Gutjahr, C. (2019). SMAX1/SMXL2 regulate root and root hair development downstream of KAI2-mediated signalling in Arabidopsis. PLoS Genetics, 15(8), e1008327.

Vose, R. S., Huang, B., Yin, X., Arndt, D., Easterling, D. R., Lawrimore, J. H., Menne, M. J., Sanchez-Lugo, A., & Zhang, H. M. (2021). Implementing full spatial coverage in NOAA's global temperature analysis. Geophysical Research Letters, 48(4). https://doi.org/10.1029/2020gl090873

Walker, C. H., Siu-Ting, K., Taylor, A., O'Connell, M. J., & Bennett, T. (2019). Strigolactone synthesis is ancestral in land plants, but canonical strigolactone signalling is a flowering plant innovation. BMC Biology, 17(1), 70.

Wallner, E.-S., López-Salmerón, V., Belevich, I., Poschet, G., Jung, I., Grünwald, K., Sevilem, I., Jokitalo, E., Hell, R., Helariutta, Y., Agustí, J., Lebovka, I., & Greb, T. (2017). Strigolactone- and Karrikin-Independent SMXL Proteins Are Central Regulators of Phloem Formation. In Current Biology (Vol. 27, Issue 8, pp. 1241–1247). https://doi.org/10.1016/j.cub.2017.03.014

Wang, L., Wang, B., Jiang, L., Liu, X., Li, X., Lu, Z., Meng, X., Wang, Y., Smith, S. M., & Li, J. (2015). Strigolactone Signaling in Arabidopsis Regulates Shoot Development by Targeting D53-Like SMXL Repressor Proteins for Ubiquitination and Degradation. The Plant Cell, 27(11), 3128–3142.
Wang, L., Xu, Q., Yu, H., Ma, H., Li, X., Yang, J., Chu, J., Xie, Q., Wang, Y., Smith, S. M., Li, J., Xiong, G., & Wang, B. (2020). Strigolactone and Karrikin Signaling Pathways Elicit Ubiquitination and Proteolysis of SMXL2 to Regulate Hypocotyl Elongation in Arabidopsis. The Plant Cell, 32(7), 2251–2270.

Wang, Y., Yao, R., Du, X., Guo, L., Chen, L., Xie, D., & Smith, S. M. (2021). Molecular basis for high ligand sensitivity and selectivity of strigolactone receptors in Striga. Plant Physiology, 185(4), 1411–1428.

Waters, M. T., Nelson, D. C., Scaffidi, A., Flematti, G. R., Sun, Y. K., Dixon, K. W., & Smith, S. M. (2012). Specialisation within the DWARF14 protein family confers distinct responses to karrikins and strigolactones in Arabidopsis. Development , 139(7), 1285–1295.

Waters, M. T., Scaffidi, A., Flematti, G., & Smith, S. M. (2015). Substrate-Induced Degradation of the α/β-Fold Hydrolase KARRIKIN INSENSITIVE2 Requires a Functional Catalytic Triad but Is Independent of MAX2. Molecular Plant, 8(5), 814–817.

Waters, M. T., Scaffidi, A., Moulin, S. L. Y., Sun, Y. K., Flematti, G. R., & Smith, S. M. (2015). A Selaginella moellendorffii Ortholog of KARRIKIN INSENSITIVE2 Functions in Arabidopsis Development but Cannot Mediate Responses to Karrikins or Strigolactones. The Plant Cell, 27(7), 1925–1944.

Wheeler, T., & von Braun, J. (2013). Climate change impacts on global food security. Science, 341(6145), 508–513.

White, A. R. F., Mendez, J. A., Khosla, A., & Nelson, D. C. (2022). Rapid analysis of strigolactone receptor activity in a Nicotiana benthamiana dwarf14 mutant. Plant Direct, 6(3), e389.

Woo, H. R., Chung, K. M., Park, J. H., Oh, S. A., Ahn, T., Hong, S. H., Jang, S. K., & Nam, H. G. (2001). ORE9, an F-box protein that regulates leaf senescence in Arabidopsis. The Plant Cell, 13(8), 1779–1790.

Xie, X., Kisugi, T., Yoneyama, K., Nomura, T., Akiyama, K., Uchida, K., Yokota, T., McErlean, C. S. P., & Yoneyama, K. (2017). Methyl zealactonoate, a novel germination stimulant for root parasitic weeds produced by maize. Journal of Pesticide Science, 42(2), 58–61.

Xie, X., Mori, N., Yoneyama, K., Nomura, T., Uchida, K., Yoneyama, K., & Akiyama, K. (2019). Lotuslactone, a non-canonical strigolactone from Lotus japonicus. Phytochemistry, 157, 200–205.

Xu, Y., Miyakawa, T., Nosaki, S., Nakamura, A., Lyu, Y., Nakamura, H., Ohto, U., Ishida, H., Shimizu, T., Asami, T., & Tanokura, M. (2018). Structural analysis of HTL and D14 proteins reveals the basis for ligand selectivity in Striga. Nature Communications, 9(1), 3947.

Yamada, Y., Furusawa, S., Nagasaka, S., Shimomura, K., Yamaguchi, S., & Umehara, M. (2014). Strigolactone signaling regulates rice leaf senescence in response to a phosphate deficiency. Planta, 240(2), 399–408.

Yao, J., Mashiguchi, K., Scaffidi, A., Akatsu, T., Melville, K. T., Morita, R., Morimoto, Y., Smith, S. M., Seto, Y., Flematti, G. R., Yamaguchi, S., & Waters, M. T. (2018). An allelic series at the KARRIKIN INSENSITIVE 2 locus of Arabidopsis thaliana decouples ligand hydrolysis and receptor degradation from downstream signalling. The Plant Journal: For Cell and Molecular Biology, 96(1), 75–89.

Yao, J., Scaffidi, A., Meng, Y., Melville, K. T., Komatsu, A., Khosla, A., Nelson, D. C., Kyozuka, J., Flematti, G. R., & Waters, M. T. (2021). Desmethyl butenolides are optimal ligands for karrikin receptor proteins. The New Phytologist. https://doi.org/10.1111/nph.17224

Yao, R., Ming, Z., Yan, L., Li, S., Wang, F., Ma, S., Yu, C., Yang, M., Chen, L., Chen, L., Li, Y., Yan, C., Miao, D., Sun, Z., Yan, J., Sun, Y., Wang, L., Chu, J., Fan, S., … Xie, D. (2016). DWARF14 is a non-canonical hormone receptor for strigolactone. Nature, 536(7617), 469–473.
Yoneyama, K., & Brewer, P. B. (2021). Strigolactones, how are they synthesized to regulate plant growth and development? Current Opinion in Plant Biology, 63, 102072.

Yoneyama, K., Xie, X., Yoneyama, K., Kisugi, T., Nomura, T., Nakatani, Y., Akiyama, K., & McErlean, C. S. P. (2018). Which are the major players, canonical or non-canonical strigolactones? Journal of Experimental Botany, 69(9), 2231–2239.

Yu, H., Wu, J., Xu, N., & Peng, M. (2007). Roles of F-box proteins in plant hormone responses. Acta Biochimica et Biophysica Sinica, 39(12), 915–922.

Zhao, L.-H., Zhou, X. E., Wu, Z.-S., Yi, W., Xu, Y., Li, S., Xu, T.-H., Liu, Y., Chen, R.-Z., Kovach, A., Kang, Y., Hou, L., He, Y., Xie, C., Song, W., Zhong, D., Xu, Y., Wang, Y., Li, J., … Xu, H. E. (2013). Crystal structures of two phytohormone signal-transducing α/β hydrolases: karrikin-signaling KAI2 and strigolactone-signaling DWARF14. Cell Research, 23(3), 436–439.

Zheng, X., Yang, X., Chen, Z., Xie, W., Yue, X., Zhu, H., Chen, S., & Sun, X. (2021). Arabidopsis SMAX1 overaccumulation suppresses rosette shoot branching and promotes leaf and petiole elongation. Biochemical and Biophysical Research Communications, 553, 44–50.

Zhou, F., Lin, Q., Zhu, L., Ren, Y., Zhou, K., Shabek, N., Wu, F., Mao, H., Dong, W., Gan, L., Ma, W., Gao, H., Chen, J., Yang, C., Wang, D., Tan, J., Zhang, X., Guo, X., Wang, J., … Wan, J. (2013). D14-SCF(D3)-dependent degradation of D53 regulates strigolactone signalling. Nature, 504(7480), 406–410.

Zhou, F., Lin, Q., Zhu, L., Ren, Y., Zhou, K., Shabek, N., Wu, F., Mao, H., Dong, W., Gan, L., Ma, W., Gao, H., Chen, J., Yang, C., Wang, D., Tan, J., Zhang, X., Guo, X., Wang, J., … Wan, J. (2016). Corrigendum: D14-SCF(D3)-dependent degradation of D53 regulates strigolactone signalling. Nature, 532(7599), 402.

Zwanenburg, B., Mwakaboko, A. S., Reizelman, A., Anilkumar, G., & Sethumadhavan, D. (2009). Structure and function of natural and synthetic signalling molecules in parasitic weed germination. Pest Management Science, 65(5), 478–491.

Zwanenburg, B., & Pospísil, T. (2013). Structure and activity of strigolactones: new plant hormones with a rich future. Molecular Plant, 6(1), 38–62.

Zwanenburg, B., Pospíšil, T., & Ćavar Zeljković, S. (2016). Strigolactones: new plant hormones in action. Planta, 243(6), 1311–1326.

Chapter 1: Rapid analysis of strigolactone receptor activity in a *Nicotiana benthamiana dwarf14* mutant

Abstract:

DWARF14 (D14) is an α/ β-hydrolase and receptor for the plant hormone strigolactone (SL) in angiosperms. Upon SL perception, D14 works with MORE AXIL- LARY GROWTH2 (MAX2) to trigger polyubiquitination and degradation of DWARF53(D53)-type proteins in the SUPPRESSOR OF MAX2 1-LIKE (SMXL) family. We used CRISPR-Cas9 to generate knockout alleles of the two homoeologous D14 genes in the *Nicotiana benthamiana* genome. The *Nbd14a,b* double mutant had sev- eral phenotypes that are consistent with the loss of SL perception in other plants, including increased axillary bud outgrowth, reduced height, shortened petioles, and smaller leaves. A ratiometric fluorescent reporter system was used to monitor degra- dation of SMXL7 from *Arabidopsis thaliana* (AtSMXL7) after transient expression in *N. benthamiana* and treatment with the strigolactone analog GR24. AtSMXL7 was degraded after treatment with $GR24^{5DS}$, which has the stereochemical configuration of natural SLs, as well as its enantiomer $GR24^{ent\text{-}5DS}$.In *Nbd14a,b* leaves, AtSMXL7 abundance was unaffected by *rac*-GR24 or either GR24 stereoisomer. Transient coexpression of AtD14 with the AtSMXL7 reporter in *Nbd14a,b* restored the degra- dation response to *rac*-GR24, but required an active catalytic triad. We used this platform to evaluate the ability of several *AtD14* mutants that had not been charac- terized in plants to target AtSMXL7 for degradation.

Introduction:

Strigolactones (SLs) are a family of plant hormones derived from β-carotene that have diverse functions in plants (Bouwmeester et al., 2021; Machin et al., 2020; Waters et al., 2017). SLs regulate axillary bud outgrowth (tillering), stem elongation, auxin transport, root elongation, leaf shape, leaf angle, leaf senescence, cambial growth, susceptibility to pathogenic microbes and root-knot nematodes, stomatal closure responses, and drought tolerance (Agusti et al., 2011; Bu et al., 2014; Gomez-Roldan et al., 2008; Kalliola et al., 2020; Kapulnik et al., 2011; Lahari et al., 2019; Lauressergues et al., 2015; Li et al., 2017, 2020; Marzec et al., 2016; Nasir et al., 2019; Ruyter-Spira et al., 2011; Scaffidi et al., 2013; Shindo et al., 2020; Shinohara et al., 2013; Soundappan et al., 2015; Ueda & Kusaba, 2015; Umehara et al., 2008; Van Ha et al., 2014; Yamada et al., 2014). SLs are also exuded by roots into the rhizosphere, especially under nutrient-poor conditions. There, SLs stimulate hyphal branching and metabolic activity of arbuscular mycorrhizal (AM) fungi, promoting beneficial symbiotic interactions with the host plant (Akiyama et al., 2005; Besserer et al., 2006, 2008; Kobae et al., 2018; Kretzschmar et al., 2012).

SL perception in flowering plants is mediated by the α/β hydrolase DWARF14 (D14)/DECREASED APICAL DOMINANCE (DAD2)/RAMOSUS3 (RMS3) (Arite et al., 2009; de Saint Germain et al., 2016; Hamiaux et al., 2012; Waters et al., 2012). Upon activation by SL, D14 associates with the F-box protein MORE AXILLARY GROWTH2 (MAX2)/DWARF3(D3), which acts as an adapter component of an SCF (Skp1–Cullin–F-box) E3 ubiquitin ligase complex. Activated D14 also associates with a subset of proteins in the SUPPRESSOR OF MAX2 1-LIKE (SMXL) family that are known as DWARF53 (D53) in rice and petunia, and SMXL6, SMXL7, and SMXL8 in *Arabidopsis thaliana*. This

leads to the polyubiquitination of D53-type SMXLs by SCF^{MAX2} and their degradation by the 26S proteasome (Jiang et al., 2013; Lee et al., 2020; Shabek et al., 2018; Soundappan et al., 2015; Wang, Wang, et al., 2015; Yao et al., 2016; Zhou et al., 2013).

A very similar signaling mechanism is used by karrikins (KARs), a class of plant growth regulators found in smoke. KAR signaling requires SCF^{MAX2} and an ancient paralog of D14 known as KARRIKIN INSENSITIVE2 (KAI2)/HYPOSENSITIVE TO LIGHT (HTL) (Nelson et al., 2011; Sun & Ni, 2011; Waters et al., 2012). In addition to mediating responses to KARs, KAI2 is hypothesized to perceive an unidentified, endogenous KAI2 ligand (KL) (Conn & Nelson, 2016; Sun et al., 2016). Upon activation, KAI2-SCF^{MAX2} targets SMAX1 and its close paralog SMXL2 for degradation (Khosla, Morffy, et al., 2020; Stanga et al., 2013; Stanga et al., 2016; Wang et al., 2020; Zheng et al., 2020). This pathway regulates seed germination, hypocotyl/mesocotyl elongation, seedling responses to light, leaf shape, cuticle development, drought tolerance, root skewing, root hair density and elongation, and the capacity for AM symbiosis (Bunsick et al., 2020; Carbonnel et al., 2020; Choi et al., 2020; Gutjahr et al., 2015; Li et al., 2017, 2020; Nelson et al., 2009, 2010; Shen et al., 2007; Soundappan et al., 2015; Stanga et al., 2013, 2016; Sun & Ni, 2011; Swarbreck et al., 2019; Villaécija-Aguilar et al., 2019; Zheng et al., 2020). In *A. thaliana*, SMAX1 and SMXL2 also associate with D14 and are targeted for degradation when a SL analog is applied, indicating some crosstalk between the SL and KAR signaling pathways may occur (Li et al., 2022; Wang et al., 2020).

D14 has highly conserved roles in angiosperms. This has been demonstrated through analysis of *d14* mutants in petunia (*Petunia hybrida*), rice (*Orzya sativa*), *A. thaliana*, canola (*Brassica napus*), pea (*Pisum sativum*), barley (*Hordeum vulgare*), hexaploid wheat (*Triticum aestivum*), barrel medic (*Medicago truncatula*), and *Lotus*

japonicus, as well as RNAi knockdown of *D14* in soybean (*Glycine max*) hairy roots (Ahmad et al., 2020; Arite et al., 2009; Carbonnel et al., 2020; de Saint Germain et al., 2016; Hamiaux et al., 2012; Lauressergues et al., 2015; Liu et al., 2021; Marzec et al., 2016; Stanic et al., 2021; Waters et al., 2012). *D14* orthologs from cotton (*Gossypium hirsutum*), poplar (*Populus trichocarpa*), and chrysanthemum (*Dendranthema grandiflorum*) have also been studied indirectly through cross-species complementation of an *Arabidopsis d14* (*Atd14*) mutant (Wang et al., 2019; Wen et al., 2015; Zheng et al., 2016). This approach enables *in vivo* analysis of gene function for species that have fewer genetic resources available or are less tractable to genetic studies than the major model plant systems (e.g., species lacking insertion/TILLING mutant collections and effective transformation methods). For example, this method has been used to identify SL receptors in root parasitic plants that arose from neofunctionalization of *KAI2/HTL* paralogs (Conn et al., 2015; de Saint Germain et al., 2021; Toh et al., 2015).

The utility of the cross-species complementation approach is limited by the compatibility of the transgene product of interest with its noncognate cellular environment. For example, some *MAX2* and *KAI2/HTL* transgenes from petunia; the bryophytes *Selaginella moellendorffii*, *Marchantia polymorpha*, and *Physcomitrium* (formerly *Physcomitrella*) *patens*; and the parasitic plant *Striga hermonthica* are nonfunctional or only partially functional in *Arabidopsis* (Conn et al., 2015; Drummond et al., 2011; Liu et al., 2014; Toh et al., 2015). This does not necessarily mean that these genes have reduced function in their native context; instead, the proteins they encode may not be able to interact well with *Arabidopsis* orthologs of their signaling partners (Khosla & Nelson, 2016). For example, at least two *S. hermonthica* KAI2/HTL proteins that are inactive in *Arabidopsis* can bind SL sensitively in vitro but cannot interact with *Arabidopsis* MAX2

(AtMAX2), or for that matter ShMAX2 (Wang et al., 2021). Conversely, *S. hermonthica* HTL7 (ShHTL7) causes *Arabidopsis* seed to germinate in the presence of picomolar SL. This response is several orders of magnitude lower than that conferred by ShHTL proteins with similar SL affinities in vitro and is likely due to the unusually high affinity of ShHTL7 for AtMAX2 (Toh et al., 2015; Tsuchiya et al., 2015; Uraguchi et al., 2018; Wang et al., 2021). Another disadvantage of the cross-species complementation approach to investigate gene function is that it typically takes several generations to obtain homozygous transgenic lines that are suitable to study. Therefore, methods to evaluate plant gene function ex situ that are fast and also allow the cointroduction of compatible transgene partners are desirable.

We previously developed a ratiometric reporter system (pRATIO) that can monitor changes in the relative abundance of a transiently expressed target protein compared with a reference protein (Khosla, Rodriguez Furlan, et al., 2020). In this Gateway-compatible system, a gene of interest (target) is translationally fused to a fluorescent or bioluminescent reporter. The target is cotranscribed with a reference gene that also encodes a fluorescent or bioluminescent reporter (Khosla, Rodriguez Furlan, et al., 2020). A modified “self-cleaving” 2A peptide derived from foot-and-mouth disease virus is encoded between the two genes, causing the target and reference proteins to be separated during translation. This approach enables multicistronic, stoichiometric expression in eukaryotes (Luke et al., 2010).

The pRATIO system has been applied successfully in *Nicotiana benthamiana*, a native Australian species that is closely related to tobacco (*Nicotiana tabacum*), to investigate degradation of Arabidopsis SMAX1, SMXL7, and KAI2 (Bally et al., 2018; Khosla, Morffy, et al., 2020; Khosla, Rodriguez Furlan, et al., 2020). When transiently

expressed in *N. benthamiana* leaves, the *Arabidopsis* SMXL7 (AtSMXL7) ratiometric reporter is degraded after treatment with *rac*-GR24, a racemic mixture of the synthetic SL analog $GR24^{5DS}$ and its enantiomer, $GR24^{ent\text{-}5DS}$. In contrast, KAR_1 or KAR_2 treatments, which are expected to activate KAI2, do not affect AtSMXL7 stability (Khosla, Morffy, et al., 2020). This is consistent with prior studies that show degradation of rice D53 and *Arabidopsis* SMXL6, SMXL7, and SMXL8 in response to GR24, but not KAR_1 treatments (Jiang et al., 2013; Wang, Wang, et al., 2015; Zhou et al., 2013). It also indicates that a receptor(s) in *N. benthamiana* is able to target AtSMXL7 for degradation in response to one or both components of *rac*-GR24.

GR24-induced degradation of D53-type SMXLs is dependent on D14 in rice and Arabidopsis (Jiang et al., 2013; Samodelov et al., 2016; Wang, Wang, et al., 2015; Zhou et al., 2013). Genetic and evolutionary evidence also support the idea that AtSMXL7 is targeted by AtD14 and not AtKAI2 (Machin et al., 2020; Soundappan et al., 2015; Waters et al., 2015). Therefore, the AtSMXL7 degradation response is likely mediated by one or both of the two nearly identical *D14* homoeologs found in the *N. benthamiana* genome. However, the possibility has been raised that there can be crosstalk between KAI2 and SMXL6, SMXL7, and SMXL8 in the regulation of Arabidopsis root skewing (Swarbreck et al., 2019). The *N. benthamiana* genome contains four *KAI2* paralogs that are likely to encode functional proteins. Also, KAI2 proteins are not limited to KAR perception. *Arabidopsis* KAI2 is activated by $GR24^{ent\text{-}5DS}$, whereas in parasitic plants, some evolutionarily “divergent” KAI2 (KAI2d) proteins are able to perceive $GR24^{5DS}$ and natural SLs (Conn et al., 2015; de Saint Germain et al., 2021; Nelson, 2021; Toh et al., 2015; Tsuchiya et al., 2015). Therefore, it is not clear whether any NbKAI2 proteins might contribute to *rac*-GR24-induced degradation of AtSMXL7 in *N. benthamiana*. We

reasoned that transient coexpression in *N. benthamiana* could provide a way to rapidly evaluate the ability of D14 variants to target a SMXL7 ratiometric reporter for degradation. This could enable medium-throughput screens for mutations that affect D14 signaling activity or its protein–protein interactions with SMXL7. Pairs of D14-SMXL7 proteins from other species could also be evaluated as long as compatibility with *N. benthamiana* MAX2 is maintained. For this approach to be most effective, however, the endogenous SL receptors in *N. benthamiana* would need to be removed. Therefore, we used CRISPR-Cas9 to knock out *N. benthamiana D14a* and *D14b*. We evaluate the combined roles of these genes in *N. benthamiana* shoot development. We also demonstrate that this mutant background can be used to analyze the capacity of *Arabidopsis* D14 variants to degrade AtSMXL7.

Materials and methods:

Genes

NbD14a is found on Sol Genomics Network (SGN) scaffold Niben101Scf02153 (*N. benthamiana* Genome v1.0.1; (Bombarely et al., 2012)) and on *Nicotiana benthamiana* Sequencing Consortium (NbSC) scaffold NbLab330C11 (*N.benthamiana* v3.3; (Naim et al., 2012)). *NbD14b* is found on SGN scaffold Niben101Scf06949 and on NbSC scaffold NbLab330C03. *AtD14* (AT3G03990) and *AtSMXL7* (AT2G29970) have been previously described (Waters et al., 2012; Stanga et al., 2013).

Construction of CRISPR-Cas9 constructs

20-nt guide sequences were selected from the CRISPR-P 2.0 database for the *Nicotiana benthamiana* genome (v0.4.4) to simultaneously target NbS00019774g0007 and NbS00024870g0006 with no mismatches (Bombarely et al., 2012; Liu et al., 2017). The next most likely off-target sites (based on off-score) for each guide selected had at least three mismatches and were located in intergenic or intron regions. The two guide sequences were cloned into the pHEE401E vector according to the simplified protocol for two gRNA expression cassettes for dicots (Wang et al., 2015b). Briefly, high-fidelity PCR amplification of a pCBC-DT1T2 template (containing a U6-26 terminator and U6-29 promoter) with overlapping primers was performed to add on a guide sequence and BsaI restriction site at each end. Primer sequences for NbD14-DT1-BsF, NbD14-DT1-F0, NbD14-DT2-R0, and NbD14-DT2-BsR are described in Supplementary Table 1. After purification of the extended PCR fragment, GoldenGate cloning with BsaI and pHEE401E was performed. Electrocompetent *E. coli* (strain DH5a) was transformed with the reaction product and selected on solid Luria Broth (LB) medium supplemented with 50 mg/L kanamycin. Colony PCR was performed with U6-26p-F and U6-29p-R. Plasmids were purified from colonies positive for a successful vector insertion (726 bp product) and both guide sequences were verified by Sanger sequencing with U6-26p-F and U6-29p-F. *Agrobacterium tumefaciens* (strain GV3101) was transformed with the pHEE401E-NbD14 construct and selected on solid LB medium supplemented with 50 mg/L kanamycin, 25 mg/L gentamicin, and 25 mg/L rifampicin.

Stable transformation of *Nicotiana benthamiana*

Transformation of *N. benthamiana* with the pHEE401E-NbD14 construct was performed by the Plant Transformation Facility at University of California, Davis. Newly expanded

leaves from *in vitro*-grown *Nicotiana benthamiana* plantlets were removed and cut into 1 cm^2 pieces while suspended in a solution of *Agrobacterium tumefaciens* adjusted to an OD_{600} of 0.1-0.2. Leaf pieces were transferred abaxial side down onto co-cultivation medium consisting of Murashige and Skoog minimal organics with 8% (w/v) agar medium (MSO) supplemented with 30 g/L sucrose, 2.0 mg/L 6-benzylaminopurine (BAP) and 200 µM acetosyringone, pH 5.6-5.8, and incubated 2 d at 23°C in the dark. After 2 d, leaf pieces were transferred to shoot induction medium consisting of MSO medium supplemented with 30 g/L sucrose, 2.0 mg/L BAP, 400 mg/L carbenicillin, 250 mg/L cefotaxime, 25 mg/L hygromycin and incubated for 10 d at 26 C under a 16 h light (intensity 30 µM m^2 s^{-1}):8 h dark photoperiod. After 10 d, tissue was subcultured every 21 d onto the same medium formulation until buds developed. Developing buds were then transferred to elongation medium consisting of MSO medium supplemented with 30 g/L sucrose, 0.1 mg/L BAP, 400 mg/L carbenicillin, 250 mg/L cefotaxime, and 25 mg/L hygromycin and the tissue was subcultured every 21 d until shoots developed. After shoots reached 3-4 cm in height, they were harvested and transferred to rooting medium consisting of 0.5x MSO medium supplemented with 15 g/L sucrose, 0.2 mg/L indole-3-butyric acid (IBA), 400 mg/L carbenicillin, 250 mg/L cefotaxime, and 25 mg/L hygromycin for 14 d.

Plant growth conditions

Plants used in growth, branching, and leaf morphology assays were grown on soil in a greenhouse in Riverside, CA from beginning of October 2019 through to mid December 2019. Plants were watered regularly every other day. Plants used in images for Figure 2A and SMXL7 degradation assays were grown on soil in a growth room under long day conditions (16 h white light at intensity 120 µM m^2 s^{-1}/8 h dark) at 22°C.

Genotyping

DNA was extracted from young leaf tissue using the DNAzol protocol (Molecular Research Center, Inc) and analyzed by PCR with Taq DNA polymerase (New England Biolabs). *NbD14a* was amplified with NbD14a,b-F and NbD14a-3'UTR-R primers with the following thermal cycling conditions: 95°C for 3 min; 40 cycles of 95°C for 30 s, 59°C for 30 s, 68°C for 2 min; 68°C for 5 min. NbD14a,b-F and NbD14a-R were used for Sanger sequencing of purified PCR products. The first exon of *NbD14b* was amplified with NbD14a,b-F and NbD14b-Intron-R, and the second exon was amplified with NbD14b-Intron-F and NbD14b-R with the following thermal cycling conditions: 95°C for 3 min; 35 cycles of 95℃ for 30 s, 52°C for 30 s, 68℃ for 1 min; 68°C for 5 min. NbD14a,b-F, NbD14b-Intron-R, NbD14b-Intron-F, and NbD14b-R were used for Sanger sequencing of purified PCR products. The absence of the pHEE401E T-DNA was validated using pHEE401EhygB-F and pHEE401EhygB-R primers for the hygromycin resistance gene with the following thermal cycling conditions: 95°C for 3 min; 40 cycles of 95°C for 30 s, 57°C for 30 s, 68°C for 45 s; 68°C for 5 min.

Plant growth, shoot branching, and leaf morphology assays

One-week old seedlings were transplanted and grown for 51 d in the greenhouse. From the base of each plant and in developmental order, each branch at the base of the node was cut off and measured from the cutoff point to the meristematic zone and the leaf was photographed. Each plant was measured from the soil level to the shoot apical meristem. Excised leaves were photographed and petiole length, leaf blade length, and leaf blade

width were measured using ImageJ (NIH). Graphs and statistical analysis were performed in Prism (GraphPad).

SMXL7 degradation assays

$GR24^{5DS}$, $GR24^{ent\text{-}5DS}$, and *rac*-GR24 were synthesized and purified by Dr. Adrian Scaffidi and Dr. Gavin Flematti (University of Western Australia). The ratiometric reporter for AtSMXL7, pRATIO3212-SMXL7, is previously described (Khosla et al., 2020a). pRATIO3212-SMXL7 was transformed into an *Agrobacterium tumefaciens* strain GV3101 that also carries a plasmid expressing p19, a suppressor of gene-silencing. AtD14 variants were synthesized (Twist Bioscience), cloned into an ampicillin-resistant pDONR220 entry vector, sequence-verified, and cloned into the plant transformation vector pGWB415 (Nakagawa et al., 2007) using Gateway BP and LR cloning enzymes (Invitrogen). pGWB415-D14 vectors were transformed into *A. tumefaciens* strain GV3101. Transient transformation of *Nicotiana benthamiana* and measurement of mScarlet-I and Venus was performed as described previously in a detailed protocol (Khosla and Nelson, 2020), with the following modifications for the cell densities of *A. tumefaciens* cultures resuspended in infiltration media prior to injection in *N. benthamiana* leaves: Figure 4A, final OD_{600}=0.6; Figure 4B, final OD_{600}=1.2, with a 1:1 composition of pRATIO/p19:pGWB415 strains; Figure 5, final OD_{600}=0.9, with an 8:1 composition of pRATIO/p19:pGWB415 strains. Graphs and statistical analysis were performed in Prism (GraphPad).

Results:

Knockout of two *D14* genes in *N. benthamiana* with CRISPR-Cas9

N. benthamiana is an allotetraploid that carries two *D14* homoeologs in its genome (Figure 1a). The coding sequences of *NbD14a* and *NbD14b* are 97% identical at the nucleotide level, resulting in only three amino acid differences (Ala/Thr84, Leu/Ile119, and Ala/Thr257) between the 267-aa proteins. We selected a pair of Cas9-compatible gRNAs that would simultaneously target both *NbD14* genes in each of their two exons (Figure 1). These gRNAs were cloned into an egg cell-specific promoter-controlled CRISPR-Cas9 vector that was originally developed for use in *A. thaliana* (Wang, Xing, et al., 2015). This construct was stably introduced into wild-type (wt) *N. benthamiana* through *Agrobacterium tumefaciens*-mediated transformation. We identified a homozygous *Nbd14a Nbd14b* double mutant (hereafter, *Nbd14a,b*) in the T0 generation and subsequently isolated a line free of the CRISPR-Cas9 transgene. The *Nbd14a-1* allele is composed of two mutations: The first is a 14 bp deletion in exon 1 that results in a frameshift after Arg109 and premature truncation of the protein, and the second is a 1-bp deletion in exon 2 (Figure 1b). The *Nbd14b-1* allele is a 1-bp deletion at the same position in exon 2, which causes a frameshift after Cys209 (Figure 1b). This results in loss of the Asp217 and His246 residues of the catalytic triad in addition to many other amino acids. Both Asp217 and His246 are required for SL hydrolysis by *Arabidopsis* D14 in vitro, and the catalytic histidine residue is necessary for D14 activity in planta (Seto et al., 2019). Therefore, both *d14* alleles are expected to cause a complete loss-of-function.

N. benthamiana d14a,b has increased shoot branching and altered leaf shape

Loss-of-function mutations in D14 cause increased branching/tillering and semi-dwarf stature in rice, barley, *Arabidopsis*, canola, petunia, pea, *M. truncatula*, and *L.*

japonicus (Arite et al., 2009; Arumingtyas et al., 1992; Carbonnel et al., 2020; de Saint Germain et al., 2016; Hamiaux et al., 2012; Lauressergues et al., 2015; Marzec et al., 2016; Napoli & Ruehle, 1996; Stanic et al., 2021; Waters et al., 2012). To determine whether D14 has a similar role in *N. benthamiana*, we examined the shoot architecture of 5-week-old plants grown under greenhouse conditions. To our complete lack of surprise, *Nbd14a,b* plants had a more compact, "bushy" shoot architecture compared with wt (Figure 2a). *Nbd14a,b* plants had more axillary branches than wt (Figure 2b). We measured outgrowth of the first nine axillary buds of each plant and found that the three most basal axillary shoots were significantly longer in *Nbd14a,b* than wt (Figure 2a,c). At the younger, apical nodes, bud outgrowth was reduced, and there was no significant difference in the lengths of *Nbd14a,b* and wt axillary shoots. Consistent with the semi-dwarf phenotype of *d14* mutants in other angiosperms, we also observed that the height of *Nbd14a,b* plants was reduced significantly compared with wt (Figure 2a,d).

The petioles of *Arabidopsis d14* leaves have substantially reduced length compared with wt. In addition, the length and width of *d14* leaves are reduced, resulting in a smaller and more rounded blade shape overall (Scaffidi et al., 2013; Soundappan et al., 2015; Waters et al., 2012). In *M. truncatula*, *d14* leaflets have increased "solidity" due to increased but shallower serrations at the leaflet margin (Lauressergues et al., 2015). These observations led us to examine leaf morphology in *Nbd14a,b*. We measured the petiole length, blade length, and blade width of the subtending leaf for each of the first nine axillary buds (Figure 3). The petioles of the first five *Nbd14a,b* leaves were significantly shorter than wt (Figure 3a). Blade length and width were also reduced significantly for most of the five oldest *Nbd14a,b* leaves (Figure 3b,c). The most apical leaves of *Nbd14a,b* and wt had similar dimensions, at least at this age. Together, these

data indicate that loss of *NbD14a* and *NbD14b* alters the shoot architecture and leaf morphology of *N. benthamiana* similarly to *d14* mutants in other angiosperms.

GR24-stimulated degradation of AtSMXL7 in *N. benthamiana* requires *NbD14a,b*

We previously used a ratiometric reporter system (pRATIO3212) to show that AtSMXL7 expressed in wt *N. benthamiana* leaves is degraded after treatment with *rac*-GR24, but not KAR_1 or KAR_2 (Figure 4a; Khosla, Morffy, et al., 2020). To determine whether it is the $GR24^{5DS}$ or $GR24^{ent\text{-}5DS}$ component of *rac*-GR24 that triggers AtSMXL7 degradation, we tested the effects of optically pure compounds. Both 10-µM $GR24^{5DS}$ and $GR24^{ent\text{-}5DS}$ caused a statistically significant reduction in the ratio of fluorescence signals from the AtSMXL7-mScarlet-I target relative to the reference protein, Venus (Figure 4b). However, $GR24^{5DS}$ caused a stronger decline of the SMXL7 reporter than $GR24^{ent\text{-}5DS}$, at least within the 16-h treatment period ($p = .012$, Student's two-tailed t test). We investigated whether GR24-induced degradation of AtSMXL7 in *N. benthamiana* is D14-dependent, or if other proteins such as KAI2 might also contribute. AtSMXL7-mScarlet-I abundance was not affected by treatment with *rac*-GR24 or either of the purified GR24 stereoisomers in *Nbd14a,b* leaves (Figure 4b). This strongly suggests that AtSMXL7 degradation after GR24 treatment in *N. benthamiana* is only caused by NbD14 proteins. This result further implies that NbD14 proteins are more responsive to $GR24^{5DS}$, which shares a stereochemical configuration with naturally occurring SLs, than to $GR24^{ent\text{-}5DS}$. Arabidopsis D14 shows a similar preference for $GR24^{5DS}$ (Flematti et al., 2016; Samodelov et al., 2016; Scaffidi et al., 2014).

We next tested whether cotransformation of AtD14 could restore *rac*-GR24-induced degradation of the AtSMXL7 reporter to the *Nbd14a,b* mutant. As negative

controls, we compared the effects of an empty vector (pGWB415) and an AtD14^{S97A} mutant on AtSMXL7 degradation. Like many other α/β-hydrolases, D14 has a highly conserved Ser-His-Asp catalytic triad that is necessary for its enzymatic activity. AtD14^{S97A} does not hydrolyze SL and is non-functional in plants (Abe et al., 2014; Hamiaux et al., 2012; Seto et al., 2019). Treatment with 10-μM *rac*-GR24 caused a statistically significant decrease in the AtSMXL7 target-to-reference ratio when 35S:AtD14 was cotransformed, but had no effect on samples co- transformed with empty vector or 35S:AtD14^{S97A} (Figure 4c). This demonstrated that transient expression of AtD14 could rescue SL signaling in *Nbd14a,b*. It also raised the possibility that this approach could be used to evaluate the ability of different D14 variants to trigger SMXL7 degradation.

A rapid assay for the induction of AtSMXL7 degradation by AtD14 mutants

A recent study identified several amino acid substitutions that affect yeast two-hybrid interactions of *Petunia x hybrida* DAD2 (PhDAD2, a D14 ortholog) with PhMAX2A and/or the SMXL7 ortholog PhD53A (Lee et al., 2020). An F135A substitution enhanced PhDAD2 interactions with PhD53A in the absence of *rac*-GR24 but did not affect interactions with PhMAX2A. By contrast, N242I enhanced PhDAD2 interactions with PhMAX2A, but not PhD53A, in the absence of *rac*-GR24. When these substitutions were combined, the PhDAD2 mutant protein showed enhanced interactions with both PhD53A and PhMAX2A that were not further stimulated by *rac*-GR24. A third sub- stitution, D166A, disrupted PhDAD2 interactions with PhMAX2A but not PhD53A (Lee et al., 2020). Based on these results, PhDAD2^{F135A} and PhDAD2^{N242I} might be expected to have hypersensitive responses to SL, whereas PhDAD2^{D166A} may be insensitive to SL. Because these PhDAD2 variants were not tested in plants, however, it is possible that some of the

altered interactions are specific to yeast two-hybrid and do not translate to effects on SL signaling activity.

We reasoned that the *Nbd14a,b* mutant could provide a fast assay of D14 signaling activity that complements approaches such as yeast two-hybrid. We synthesized amino acid substitutions in AtD14 that were equivalent to those previously characterized in PhDAD2: F136A, K243I, F136A/K243I, and D167A. We then tested the ability of these AtD14 variants to trigger degradation of an AtSMXL7 ratiometric reporter after 2-, 10-, 50-, and 250-nM rac-GR24 treatments when coexpressed in *Nbd14a,b* leaves. AtD14^{F136A} showed a similar response to rac-GR24 as wt AtD14 (Figure 5a). AtD14^{K243I} caused stronger degradation of the SMXL7 reporter than wt AtD14 at 10 nM and higher concentrations of *rac*-GR24 (Figure 5b). The AtD14$^{F136A/K243I}$ double mutant showed a similarly enhanced response to *rac*-GR24 as AtD14^{K243I} (Figure 5c). It is notable that AtD14$^{F136A/K243I}$ responded positively to *rac*-GR24, which was not expected from the yeast two-hybrid assay of the equivalent DAD2 mutant (Lee et al., 2020). AtD14^{D167A} did not trigger AtSMXL7 degradation as effectively as wt AtD14 (Figure 5d). In the presence of 1-μM *rac*-GR24, the relative fluorescence of AtSMXL7 reporter was reduced 16% by AtD14^{D167A} compared with 43% by wt AtD14 (Figure S1). Because DAD2^{D166A} appeared to have lost the *rac*-GR24-induced yeast two-hybrid interaction with PhMAX2A, the observation of any *rac*-GR24 response by AtD14^{D167A} was also unex- pected (Lee et al., 2020). These results support the potential for the *Nbd14a,b* mutant to serve as a platform for first-pass screens of D14 variants in plants. This system may reveal changes to SL signaling activity that are not apparent in nonplant assays.

Discussion:

Here, we have shown that D14 proteins in *N. benthamiana* have similar functions in plant development and SL signaling as in other angiosperms. We did not investigate whether *NbD14a* and *NbD14b* have different roles in development or SL signaling. As these homoeologs are only distinguished at the protein level by three conservative amino acid substitutions, we anticipate that any differences in function would be due to unique expression patterns rather than protein activity. However, distinguishing their expression patterns would be challenging due to the very high nucleotide-level similarity (97% identity) of *NbD14a* and *NbD14b* coding sequences.

The *Nbd14a,b* double mutant shows increased axillary bud outgrowth, reduced stature, and altered leaf morphology (Figures 2 and 3). The increase in axillary branch number in *Nbd14a,b* plants is primarily due to stronger outgrowth of buds at the most basal nodes (Figure 2c). This pattern of basitonic development, in which basal bra- nches show more vigorous outgrowth than the apical branches, is also found in the SL-insensitive or SL-deficient *decreased apical dominance* (*dad*) mutants of *P. hybrida*, a related solanaceous species (Drummond et al., 2009; Hamiaux et al., 2012; Napoli & Ruehle, 1996; Snowden et al., 2005). Some *Nbd14a,b* leaves show decreased petiole length, leaf blade length, and leaf blade width (Figure 3). As with axillary bud outgrowth, these phenotypes are more pronounced in the smaller, older leaves found at basal nodes. By contrast, apical leaves of *Nbd14a,b* are similar to wt.

The similar developmental phenotypes of *Nbd14a,b* and SL- insensitive mutants in other species implies that SL signaling is disrupted in this mutant. Indeed, we observed that *Nbd14a,b* has lost the ability to target an AtSMXL7 reporter for degradation in response to exogenous SL analogs (Figure 4). This strongly suggests that AtSMXL7

degradation is D14-dependent and does not involve NbKAI2 protein(s). Importantly, the SL response of *Nbd14a,b*, as indicated by AtSMXL7 reporter degradation, could be rescued through transient expression of wt AtD14.

These results are consistent with the central role of D14 in SL signaling and developmental control that has been well-established in other plants. The novel value of the *Nbd14a,b* mutant lies, however, in the utility of *N. benthamiana* as a medium for analyses of transiently expressed plant proteins. *N. benthamiana* is commonly used for transient expression experiments due to the simplicity of transformation and the robust transgene expression that can be achieved within a few days (Bally et al., 2018). We proposed that *Nbd14a,b* could provide a useful genetic background to perform preliminary analyses of the SL signaling activity of D14 variants. This may enable explorations of how D14 mutations affect ligand specificity or how D14 interactions with specific SMXL protein targets are achieved.

To test this idea, we examined the ability of several mutant forms of D14 to activate SMXL7 degradation. The AtD14^{S97A} mutant showed no response to *rac*-GR24, consistent with previous work that demonstrated this mutation abolishes SL hydrolysis and signaling (Figure 4c; Hamiaux et al., 2012; Abe et al., 2014; Seto et al., 2019). AtD14^{D167A} had reduced SL signaling activity, presumably due to reduced interaction with MAX2 (Figure 5d). In contrast to the observation of abolished yeast two-hybrid interactions between DAD2^{D166A} and PhMAX2a, our data suggest that AtD14^{D167A} has not completely lost the ability to work with MAX2 (Lee et al., 2020). Based on yeast two-hybrid experiments with DAD2 mutants, AtD14^{F136A} and AtD14^{K243I} were expected to have enhanced or constitutive interactions with SMXL7 and MAX2, respectively (Lee et al., 2020). These mutations might be expected to cause hypersensitive SL responses by priming or enhancing SCF^{MAX2}-

D14-SMXL7 complex formation. We observed mildly enhanced responses to *rac*-GR24 from AtD14^{K243I} and AtD14$^{F136A/K243I}$, but AtD14^{F136A} appeared to have normal responses (Figure 5a–c). This might imply that interaction between SCF^{MAX2} and D14 is more of a limiting factor for formation of the SL signaling complex than interaction between D14 and SMXL7. Interestingly, the exquisitely sensitive, picomolar response to SL conferred by ShHTL7 is due to enhanced affinity for MAX2 rather than SL itself (Wang et al., 2021). Altogether, this assay enables a complementary analysis of D14 variants that reveals details of how they perform in plants, which may differ somewhat from in vitro or nonplant methods.

Assays that evaluate the activity of SL receptors can be useful tools to investigate the contributions of specific amino acids to SL rec- ognition or signaling, or to screen for chemicals that affect SL signaling. To compare our approach and its utility with other alternatives, we discuss below the three major types of assays for SL receptors: (1) those that evaluate a SL receptor alone, (2) those that test protein–protein interactions between a SL receptor and MAX2 and/or its targets, and (3) those that report degradation of the SL receptor or its SMXL target protein(s), which are direct results of SL signaling.

In vitro assays for SL binding and hydrolysis by D14

A range of biochemical techniques have been used to evaluate the ability of D14 or KAI2 proteins to bind, hydrolyze, and be activated by SL. Isothermal calorimetry (ITC) and surface plasmon resonance are effective ways to measure the in vitro affinity (i.e., Kd) of SL receptors for SL. These techniques have been used to study D14, several KAI2-like proteins in Physcomitrella patens, and a set of 60 mutants of ShHTL7 (Bürger et al., 2019; Kagiyama et al., 2013; Pang et al., 2020). Yoshimulactone green (YLG) competition

assays are another popular method to assess the affinity of a SL receptor for different ligands. In these in vitro assays, the SL analog YLG is hydrolyzed by the receptor, releasing a fluorescent byproduct. Compounds are tested for their ability to competitively interfere with YLG hydrolysis, producing a half-maximal inhibitory concentration (IC_{50}) value that generally corre- sponds with the receptor's affinity for the compound (Tsuchiya et al., 2015). The YLG competition assay was used to identify a D14 inhibitor from a chemical library of 800 compounds, as well as to test a set of binding pocket mutants of ShHTL7 (Uraguchi et al., 2018; Yoshimura et al., 2018). Hydrolysis of SL results in attachment of the methylbutenolide group from SL onto the catalytic His residue of the receptor (de Saint Germain et al., 2016; Yao et al., 2016). Formation of this "covalently linked intermediate molecule" (CLIM) can be tracked with liquid chromatography-mass spectrometry and serves as another readout of a SL receptor's activity on a SL or SL analog. However, substrate-binding and hydrolysis rates may correlate poorly with the receptor's signaling activity (Uraguchi et al., 2018). Differential scanning fluorimetry (DSF) or nano DSF have often been used to monitor shifts in the melting temperature or intrinsic fluorescence of SL receptors that are induced by potential ligands in vitro (Bürger et al., 2019; Hamiaux et al., 2012, 2018; Seto et al., 2019; Waters et al., 2015). These changes may indicate conformational changes in the SL receptor that correspond with its activation for downstream signal transduction.

In vitro assays for SL binding or activation of the SL receptor require purification of the protein of interest, which does not seem to pose a significant roadblock. A bigger issue is that these assays do not report how SL perception by the receptor affects downstream signal- ing events or incorporate the effects of in vivo factors (e.g., protein partners) on the receptor's ligand-binding, hydrolysis, or signaling activities. For example, the presence of

MAX2 is known to slow SL hydrolysis by D14 in vitro, and the affinity of D14 for D53/SMXL7 is enhanced by the presence of MAX2 (Shabek et al., 2018; Yao et al., 2016). This is also a potential weakness of in silico approaches such as molecular docking, pharmacophore modeling, and molecular dynamics simulations that model interactions between SL receptors in isolation and potential ligands (Bürger & Chory, 2020; Fukui et al., 2017; Lee et al., 2020; Mashita et al., 2016).

An in vivo assay for SL binding

A recent study has provided an exciting new approach to measure SL binding in vivo as well as in vitro. These SL biosensors incorporate a circularly permuted GFP (cpGFP) protein into an external loop joining alpha-helices 6 and 7 of DAD2 or ShHTL7 (Chesterfield et al., 2020). SL induces conformational shifts in DAD2 or ShHTL7 that also affect the conformation of cpGFP, reducing its fluorescence. A second fluo- rescent protein fused to the biosensor enables ratiometric measure- ments of fluorescence that bypass problems with varying biosensor abundance. In tobacco protoplasts, the DAD2-based biosensor can detect *rac*-GR24 concentrations as low as 100 nM (Chesterfield et al., 2020). Because this system is sensitive to even single amino acid shifts in the placement of the cpGFP and must be fine-tuned for each SL receptor, it may be better suited for screening for agonist or antagonist molecules of the receptor than evaluating the effects of receptor mutations. Also, while this system is able to provide valuable information on binding and detection of SLs by two SL receptors in vitro or in vivo, it does not address how perception affects downstream signaling.

Assays for SL-induced protein–protein interactions

Other SL receptor assays have focused on protein–protein interac-tions that are induced by SL perception. One advantage of these approaches is that they can identify factors beyond ligand-binding and hydrolysis that affect SL signaling. In vitro pulldowns, coimmunoprecipitation from plant tissue, size-exclusion chromatography, and AlphaScreen are proven ways to assess interactions between SL receptors, MAX2/D3, and SMXL proteins (Jiang et al., 2013; Shabek et al., 2018; Wang et al., 2020, 2021; Yao et al., 2016, 2017; Zhao et al., 2015; Zhou et al., 2013). Generally, these are low-throughput assays that can be quite challenging to perform due to difficulties in obtaining sufficient amounts of stable, soluble MAX2, and SMXL proteins. Yeast two-hybrid or three-hybrid assays that test interactions between SL receptors, MAX2, and/or SMXL proteins are better suited for testing the effects of SL receptor mutations or screening chemical libraries and have been successfully used for these purposes (Hamiaux et al., 2012; Lee et al., 2020; Nakamura et al., 2019; Seto et al., 2019; Toh et al., 2014; Wang et al., 2021). However, yeast-based interaction assays may produce false-positive results, at least for some KAI2 proteins (Wang et al., 2021; Yao et al., 2018).

Assays for SL-induced proteolysis

The method we have described in this paper falls within a third class of assays that measure SL-induced degradation of SL signaling components. These assays are relatively fast and highly specific readouts of SL signaling activity, whereas other downstream effects such as shoot branching, parasitic seed germination, or transcriptional responses may be affected by factors in addition to SLs. D14 is degraded after SL treatment in Arabidopsis and rice (Chevalier et al., 2014; Hu et al., 2017). An Arabidopsis line expressing a D14 fusion to luciferase has been developed as an in vivo

assay for the ability of various SLs and SL analogs to induce D14 degradation (Sanchez et al., 2018). Most similar to our system are the ratiometric SL signaling sensors StrigoQuant and Strigo-D2 (Samodelov et al., 2016; Song et al., 2022). StrigoQuant expresses Renilla luciferase and a SMXL6 fusion to firefly luciferase in a single transcript. These two reporters are separated during translation due to an intervening 2A peptide. StrigoQuant has been deployed in *Arabidopsis* protoplasts, where it can report SMXL6 degradation induced by *rac*-GR24 or SLs at concentrations as low as 10 pM. Although achieving efficient protoplast isolation and transformation can be challenging, StrigoQuant offers the distinct advantage of being able to perform experiments with the many SL pathway mutants available for *Arabidopsis*. Coexpression of rice D14 with Strigoquant is able to restore SL-induced SMXL6-degradation responses to the *Arabidopsis d14* mutant, demonstrating that it is feasible to test SL receptor variants with this system (Samodelov et al., 2016). Strigo-D2 coexpresses from separate *35S* promoters a SMXL6 C-terminal domain (SMXL6-D2) fused to the yellow fluorescent protein mVenus and a nuclear-localized mCherry reference protein (Song et al., 2022). Overexpression of SMXL6-D2-mVenus has less negative impact on Arabidopsis growth and produces higher signal intensities than full-length SMXL6-mVenus. The Strigo-D2 system provides a rapid (within 20 min) and sensitive readout of SL response in transgenic Arabidopsis plants. Responses to applied 5-deoxystrigol concentrations as low as 5 nM can be detected, and a range of responsiveness can be observed in different plant tissues (Song et al., 2022). Putatively, the activity of D14 variants could be evaluated in the *d14* Strigo-D2 background through the generation of stable transgenic lines, although this may be time-consuming.

Limitations of assays for SL-induced proteolysis in *N. benthamiana*

We propose to use the *Nbd14a,b*-pRATIO system we have established here as a complement to the techniques described above, but it has its own limitations. The success of this approach requires that heterologous proteins are compatible with endogenous *N. benthamiana* SL signaling components. For example, if NbMAX2 is not able to interact effectively with either the transiently coexpressed D14 or SMXL7 ratiometric reporter, the assays will fail. In cases where NbMAX2 is not compatible, it may be possible to co-express a MAX2 clone derived from the species of interest. Another constraint to this approach is the presence of endogenous SLs that may activate some transiently expressed SL receptors prior to the application of an agonist. Receptors with high sensitivity to SL may still be identified by causing low SMXL7 reporter abundance pretreatment. However, adding a mutation that blocks SL biosynthesis to the *Nbd14a,b* line would be a useful way to eliminate background activation of D14 transgenes. Finally, it should be noted that our system is not suitable for studying the SL receptors in parasitic plants that mediate host perception. These SL receptors are neofunctionalized paralogs of KAI2 that target SMAX1 for degradation (Nelson, 2021). Thus, the endogenous KAI2 proteins that remain present in *Nbd14a,b* may confuse evaluations of SMAX1 reporter degradation by parasite SL receptors.

References:

Abe, S. et al. (2014). Carlactone is converted to carlactonoic acid by MAX1 in Arabidopsis and its methyl ester can directly interact with AtD14 in vitro. Proc. Natl. Acad. Sci. U. S. A. 111: 18084–18089.

Agusti, J., Herold, S., Schwarz, M., Sanchez, P., Ljung, K., Dun, E.A., Brewer, P.B., Beveridge, C.A., Sieberer, T., Sehr, E.M., and Greb, T. (2011). Strigolactone signaling is required for auxin-dependent stimulation of secondary growth in plants. Proc. Natl. Acad. Sci. U. S. A. 108: 20242–20247.

Ahmad, M.Z., Rehman, N.U., Yu, S., Zhou, Y., Haq, B.U., Wang, J., Li, P., Zeng, Z., and Zhao, J. (2020). GmMAX2-D14 and -KAI interaction-mediated SL and KAR signaling play essential roles in soybean root nodulation. Plant J. 101: 334–351.

Akiyama, K., Matsuzaki, K.-I., and Hayashi, H. (2005). Plant sesquiterpenes induce hyphal branching in arbuscular mycorrhizal fungi. Nature 435: 824–827.

Arite, T., Umehara, M., Ishikawa, S., Hanada, A., Maekawa, M., Yamaguchi, S., and Kyozuka, J. (2009). d14, a Strigolactone-Insensitive Mutant of Rice, Shows an Accelerated Outgrowth of Tillers. Plant and Cell Physiology 50: 1416–1424.

Arumingtyas, E.L., Floyd, R.S., Gregory, M.J., and Mufert, I.C. (1992). Branching in Pisum: inheritance and allelism tests with 17 ramosus mutants. Pisum Genetics 24: 17–31.

Bally, J., Jung, H., Mortimer, C., Naim, F., Philips, J.G., Hellens, R., Bombarely, A., Goodin, M.M., and Waterhouse, P.M. (2018). The Rise and Rise of Nicotiana benthamiana: A Plant for All Reasons. Annu. Rev. Phytopathol. 56: 405–426.

Besserer, A., Bécard, G., Jauneau, A., Roux, C., and Séjalon-Delmas, N. (2008). GR24, a synthetic analog of strigolactones, stimulates the mitosis and growth of the arbuscular mycorrhizal fungus Gigaspora rosea by boosting its energy metabolism. Plant Physiol. 148: 402–413.

Besserer, A., Puech-Pagès, V., Kiefer, P., Gomez-Roldan, V., Jauneau, A., Roy, S., Portais, J.-C., Roux, C., Bécard, G., and Séjalon-Delmas, N. (2006). Strigolactones stimulate arbuscular mycorrhizal fungi by activating mitochondria. PLoS Biol. 4: e226.

Bombarely, A., Rosli, H.G., Vrebalov, J., Moffett, P., Mueller, L.A., and Martin, G.B. (2012). A draft genome sequence of Nicotiana benthamiana to enhance molecular plant-microbe biology research. Mol. Plant. Microbe. Interact. 25: 1523–1530.

Bouwmeester, H., Li, C., Thiombiano, B., Rahimi, M., and Dong, L. (2021). Adaptation of the parasitic plant lifecycle: germination is controlled by essential host signaling molecules. Plant Physiol. 185: 1292–1308.

Bunsick, M., Toh, S., Wong, C., Xu, Z., Ly, G., McErlean, C.S.P., Pescetto, G., Nemrish, K.E., Sung, P., Li, J.D., Scholes, J.D., and Lumba, S. (2020). SMAX1-dependent seed germination bypasses GA signalling in Arabidopsis and Striga. Nat Plants 6: 646–652.

Bu, Q., Lv, T., Shen, H., Luong, P., Wang, J., Wang, Z., Huang, Z., Xiao, L., Engineer, C., Kim, T.H., Schroeder, J.I., and Huq, E. (2014). Regulation of drought tolerance by the F-box protein MAX2 in Arabidopsis. Plant Physiol. 164: 424–439.

Bürger, M. and Chory, J. (2020). In-silico analysis of the strigolactone ligand-receptor system. Plant Direct 4: e00263.

Bürger, M., Mashiguchi, K., Lee, H.J., Nakano, M., Takemoto, K., Seto, Y., Yamaguchi, S., and Chory, J. (2019). Structural Basis of Karrikin and Non-natural Strigolactone Perception in Physcomitrella patens. Cell Rep. 26: 855–865.e5.

Carbonnel, S., Das, D., Varshney, K., Kolodziej, M.C., Villaécija-Aguilar, J.A., and Gutjahr, C. (2020). The karrikin signaling regulator SMAX1 controls Lotus japonicus root and root hair development by suppressing ethylene biosynthesis. Proc. Natl. Acad. Sci. U. S. A. 117: 21757–21765.

Carbonnel, S., Torabi, S., Griesmann, M., Bleek, E., and Tang, Y. (2019). Duplicated KAI2 receptors with divergent ligand-binding specificities control distinct developmental traits in Lotus japonicus. bioRxiv.

Chesterfield, R.J., Whitfield, J.H., Pouvreau, B., Cao, D., Alexandrov, K., Beveridge, C.A., and Vickers, C.E. (2020). Rational Design of Novel Fluorescent Enzyme Biosensors for Direct Detection of Strigolactones. ACS Synth. Biol. 9: 2107–2118.

Chevalier, F., Nieminen, K., Sánchez-Ferrero, J.C., Rodríguez, M.L., Chagoyen, M., Hardtke, C.S., and Cubas, P. (2014). Strigolactone promotes degradation of DWARF14, an α/β hydrolase essential for strigolactone signaling in Arabidopsis. Plant Cell 26: 1134–1150.

Choi, J. et al. (2020). The negative regulator SMAX1 controls mycorrhizal symbiosis and strigolactone biosynthesis in rice. Nat. Commun. 11: 2114.

Conn, C.E., Bythell-Douglas, R., Neumann, D., Yoshida, S., Whittington, B., Westwood, J.H., Shirasu, K., Bond, C.S., Dyer, K.A., and Nelson, D.C. (2015). PLANT EVOLUTION. Convergent evolution of strigolactone perception enabled host detection in parasitic plants. Science 349: 540–543.

Conn, C.E. and Nelson, D.C. (2015). Evidence that KARRIKIN-INSENSITIVE2 (KAI2) Receptors may Perceive an Unknown Signal that is not Karrikin or Strigolactone. Front. Plant Sci. 6: 1219.

Drummond, R.S.M., Martínez-Sánchez, N.M., Janssen, B.J., Templeton, K.R., Simons, J.L., Quinn, B.D., Karunairetnam, S., and Snowden, K.C. (2009). Petunia hybrida CAROTENOID CLEAVAGE DIOXYGENASE7 is involved in the production of negative and positive branching signals in petunia. Plant Physiol. 151: 1867–1877.

Drummond, R.S.M., Sheehan, H., Simons, J.L., Martínez-Sánchez, N.M., Turner, R.M., Putterill, J., and Snowden, K.C. (2011). The Expression of Petunia Strigolactone Pathway Genes is Altered as Part of the Endogenous Developmental Program. Front. Plant Sci. 2: 115.

Flematti, G.R., Scaffidi, A., Waters, M.T., and Smith, S.M. (2016). Stereospecificity in strigolactone biosynthesis and perception. Planta 243: 1361–1373.

Fukui, K., Yamagami, D., Ito, S., and Asami, T. (2017). A Taylor-Made Design of Phenoxyfuranone-Type Strigolactone Mimic. Front. Plant Sci. 8: 936.

Gomez-Roldan, V. et al. (2008). Strigolactone inhibition of shoot branching. Nature 455: 189–194.

Gutjahr, C. et al. (2015). Rice perception of symbiotic arbuscular mycorrhizal fungi requires the karrikin receptor complex. Science 350: 1521–1524.

Hamiaux, C., Drummond, R.S.M., Janssen, B.J., Ledger, S.E., Cooney, J.M., Newcomb, R.D., and Snowden, K.C. (2012). DAD2 is an α/β hydrolase likely to be involved in the perception of the plant branching hormone, strigolactone. Curr. Biol. 22: 2032–2036.

Hamiaux, C., Drummond, R.S.M., Luo, Z., Lee, H.W., Sharma, P., Janssen, B.J., Perry, N.B., Denny, W.A., and Snowden, K.C. (2018). Inhibition of strigolactone receptors by N-phenylanthranilic acid derivatives: Structural and functional insights. J. Biol. Chem. 293: 6530–6543.

Hu, Q. et al. (2017). DWARF14, A Receptor Covalently Linked with the Active Form of Strigolactones, Undergoes Strigolactone-Dependent Degradation in Rice. Front. Plant Sci. 8: 1935.

Jiang, L. et al. (2013). DWARF 53 acts as a repressor of strigolactone signalling in rice. Nature 504: 401–405.

Kagiyama, M., Hirano, Y., Mori, T., Kim, S.-Y., Kyozuka, J., Seto, Y., Yamaguchi, S., and Hakoshima, T. (2013). Structures of D14 and D14L in the strigolactone and karrikin signaling pathways. Genes Cells 18: 147–160.

Kalliola, M., Jakobson, L., Davidsson, P., Pennanen, V., Waszczak, C., Yarmolinsky, D., Zamora, O., Palva, E.T., Kariola, T., Kollist, H., and Brosché, M. (2020). Differential role of MAX2 and strigolactones in pathogen, ozone, and stomatal responses. Plant Direct 4: e00206.

Kapulnik, Y. et al. (2011). Strigolactones affect lateral root formation and root-hair elongation in Arabidopsis. Planta 233: 209–216.

Khosla, A., Morffy, N., Li, Q., Faure, L., Chang, S.H., Yao, J., Zheng, J., Cai, M.L., Stanga, J.P., Flematti, G.R., Waters, M., and Nelson, D.C. (2020a). Structure-Function Analysis of SMAX1 Reveals Domains that Mediate its Karrikin-Induced Proteolysis and Interaction with the Receptor KAI2. The Plant Cell: tpc.00752.2019.

Khosla, A. and Nelson, D.C. (2020). Ratiometric Measurement of Protein Abundance after Transient Expression of a Transgene in Nicotiana benthamiana. Bio Protoc 10: e3747.

Khosla, A. and Nelson, D.C. (2016). Strigolactones, super hormones in the fight against Striga. Curr. Opin. Plant Biol. 33: 57–63.

Khosla, A., Rodriguez-Furlan, C., Kapoor, S., Van Norman, J.M., and Nelson, D.C. (2020b). A series of dual-reporter vectors for ratiometric analysis of protein abundance in plants. Plant Direct 4.

Kobae, Y., Kameoka, H., Sugimura, Y., Saito, K., Ohtomo, R., Fujiwara, T., and Kyozuka, J. (2018). Strigolactone Biosynthesis Genes of Rice are Required for the Punctual Entry of Arbuscular Mycorrhizal Fungi into the Roots. Plant Cell Physiol. 59: 544–553.

Kretzschmar, T., Kohlen, W., Sasse, J., Borghi, L., Schlegel, M., Bachelier, J.B., Reinhardt, D., Bours, R., Bouwmeester, H.J., and Martinoia, E. (2012). A petunia ABC protein controls strigolactone-dependent symbiotic signalling and branching. Nature 483: 341–344.

Lahari, Z., Ullah, C., Kyndt, T., Gershenzon, J., and Gheysen, G. (2019). Strigolactones enhance root-knot nematode (Meloidogyne graminicola) infection in rice by antagonizing the jasmonate pathway. New Phytol. 224: 454–465.

Lauressergues, D., André, O., Peng, J., Wen, J., Chen, R., Ratet, P., Tadege, M., Mysore, K.S., and Rochange, S.F. (2015). Strigolactones contribute to shoot elongation and to the formation of leaf margin serrations in Medicago truncatula R108. J. Exp. Bot. 66: 1237–1244.

Lee, H.W., Sharma, P., Janssen, B.J., Drummond, R.S.M., Luo, Z., Hamiaux, C., Collier, T., Allison, J.R., Newcomb, R.D., and Snowden, K.C. (2020). Flexibility of the petunia strigolactone receptor DAD2 promotes its interaction with signaling partners. J. Biol. Chem. 295: 4181–4193.

Liu, H., Ding, Y., Zhou, Y., Jin, W., Xie, K., and Chen, L.-L. (2017). CRISPR-P 2.0: An Improved CRISPR-Cas9 Tool for Genome Editing in Plants. Mol. Plant 10: 530–532.

Liu, Q. et al. (2014). Striga hermonthica MAX2 restores branching but not the Very Low Fluence Response in the Arabidopsis thaliana max2 mutant. New Phytol. 202: 531–541.

Liu, R., Hou, J., Li, H., Xu, P., Zhang, Z., and Zhang, X. (2021). Association of TaD14-4D, a Gene Involved in Strigolactone Signaling, with Yield Contributing Traits in Wheat. Int. J. Mol. Sci. 22.

Li, W. et al. (2020). Comparative functional analyses of DWARF14 and KARRIKIN INSENSITIVE 2 in drought adaptation of Arabidopsis thaliana. Plant J. 103: 111–127.

Li, W. et al. (2017). The karrikin receptor KAI2 promotes drought resistance in Arabidopsis thaliana. PLoS Genet. 13: e1007076.

Luke, G., Escuin, H., De Felipe, P., and Ryan, M. (2010). 2A to the fore - research, technology and applications. Biotechnol. Genet. Eng. Rev. 26: 223–260.

Machin, D.C., Hamon-Josse, M., and Bennett, T. (2020). Fellowship of the rings: a saga of strigolactones and other small signals. New Phytol. 225: 621–636.

Marzec, M., Gruszka, D., Tylec, P., and Szarejko, I. (2016). Identification and functional analysis of the HvD14 gene involved in strigolactone signaling in Hordeum vulgare. Physiol. Plant. 158: 341–355.

Mashita, O., Koishihara, H., Fukui, K., Nakamura, H., and Asami, T. (2016). Discovery and identification of 2-methoxy-1-naphthaldehyde as a novel strigolactone-signaling inhibitor. J. Pestic. Sci. 41: 71–78.

Naim, F., Nakasugi, K., Crowhurst, R.N., Hilario, E., Zwart, A.B., Hellens, R.P., Taylor, J.M., Waterhouse, P.M., and Wood, C.C. (2012). Advanced engineering of lipid metabolism in Nicotiana benthamiana using a draft genome and the V2 viral silencing-suppressor protein. PLoS One 7: e52717.

Nakagawa, T., Kurose, T., Hino, T., Tanaka, K., Kawamukai, M., Niwa, Y., Toyooka, K., Matsuoka, K., Jinbo, T., and Kimura, T. (2007). Development of series of gateway binary vectors, pGWBs, for realizing efficient construction of fusion genes for plant transformation. J. Biosci. Bioeng. 104: 34–41.

Nakamura, H., Hirabayashi, K., Miyakawa, T., Kikuzato, K., Hu, W., Xu, Y., Jiang, K., Takahashi, I., Niiyama, R., Dohmae, N., Tanokura, M., and Asami, T. (2019). Triazole Ureas Covalently Bind to Strigolactone Receptor and Antagonize Strigolactone Responses. Molecular Plant 12: 44–58.

Napoli, C.A. and Ruehle, J. (1996). New Mutations Affecting Meristem Growth and Potential in Petunia hybridaVilm. J. Hered. 87: 371–377.

Nasir, F., Tian, L., Shi, S., Chang, C., Ma, L., Gao, Y., and Tian, C. (2019). Strigolactones positively regulate defense against Magnaporthe oryzae in rice (Oryza sativa). Plant Physiol. Biochem. 142: 106–116.

Nelson, D.C. (2021). The mechanism of host-induced germination in root parasitic plants. Plant Physiol. 185: 1353–1373.

Nelson, D.C., Flematti, G.R., Riseborough, J.-A., Ghisalberti, E.L., Dixon, K.W., and Smith, S.M. (2010). Karrikins enhance light responses during germination and seedling development in Arabidopsis thaliana. Proc. Natl. Acad. Sci. U. S. A. 107: 7095–7100.

Nelson, D.C., Riseborough, J.-A., Flematti, G.R., Stevens, J., Ghisalberti, E.L., Dixon, K.W., and Smith, S.M. (2009). Karrikins discovered in smoke trigger Arabidopsis seed germination by a mechanism requiring gibberellic acid synthesis and light. Plant Physiol. 149: 863–873.

Nelson, D.C., Scaffidi, A., Dun, E.A., Waters, M.T., Flematti, G.R., Dixon, K.W., Beveridge, C.A., Ghisalberti, E.L., and Smith, S.M. (2011). F-box protein MAX2 has dual roles in karrikin and strigolactone signaling in Arabidopsis thaliana. Proc. Natl. Acad. Sci. U. S. A. 108: 8897–8902.

Pang, Z., Zhang, X., Ma, F., Liu, J., Zhang, H., Wang, J., Wen, X., and Xi, Z. (2020). Comparative Studies of Potential Binding Pocket Residues Reveal the Molecular Basis of ShHTL Receptors in the Perception of GR24 in Striga. J. Agric. Food Chem. 68: 12729–12737.

Ruyter-Spira, C., Kohlen, W., Charnikhova, T., van Zeijl, A., van Bezouwen, L., de Ruijter, N., Cardoso, C., Lopez-Raez, J.A., Matusova, R., Bours, R., Verstappen, F., and Bouwmeester, H. (2011). Physiological effects of the synthetic strigolactone analog GR24 on root system architecture in Arabidopsis: another belowground role for strigolactones? Plant Physiol. 155: 721–734.

de Saint Germain, A. et al. (2016). An histidine covalent receptor and butenolide complex mediates strigolactone perception. Nat. Chem. Biol. 12: 787–794.

de Saint Germain, A. et al. (2020). A Phelipanche ramosa KAI2 Protein Perceives enzymatically Strigolactones and Isothiocyanates. bioRxiv: 2020.06.09.136473.

Samodelov, S.L., Beyer, H.M., Guo, X., Augustin, M., Jia, K.-P., Baz, L., Ebenhöh, O., Beyer, P., Weber, W., Al-Babili, S., and Zurbriggen, M.D. (2016). StrigoQuant: A genetically encoded biosensor for quantifying strigolactone activity and specificity. Sci Adv 2: e1601266.

Sanchez, E. et al. (2018). Structure-activity relationships of strigolactones via a novel, quantitative in planta bioassay. J. Exp. Bot. 69: 2333–2343.

Scaffidi, A., Waters, M.T., Ghisalberti, E.L., Dixon, K.W., Flematti, G.R., and Smith, S.M. (2013). Carlactone-independent seedling morphogenesis in Arabidopsis. Plant J. 76: 1–9.

Scaffidi, A., Waters, M.T., Sun, Y.K., Skelton, B.W., Dixon, K.W., Ghisalberti, E.L., Flematti, G.R., and Smith, S.M. (2014). Strigolactone Hormones and Their Stereoisomers Signal through Two Related Receptor Proteins to Induce Different Physiological Responses in Arabidopsis. Plant Physiol. 165: 1221–1232.

Seto, Y. et al. (2019). Strigolactone perception and deactivation by a hydrolase receptor DWARF14. Nat. Commun. 10: 191.

Shabek, N., Ticchiarelli, F., Mao, H., Hinds, T.R., Leyser, O., and Zheng, N. (2018). Structural plasticity of D3-D14 ubiquitin ligase in strigolactone signalling. Nature 563: 652–656.

Shen, H., Luong, P., and Huq, E. (2007). The F-box protein MAX2 functions as a positive regulator of photomorphogenesis in Arabidopsis. Plant Physiol. 145: 1471–1483.

Shindo, M., Yamamoto, S., Shimomura, K., and Umehara, M. (2020). Strigolactones Decrease Leaf Angle in Response to Nutrient Deficiencies in Rice. Front. Plant Sci. 11: 135.

Shinohara, N., Taylor, C., and Leyser, O. (2013). Strigolactone can promote or inhibit shoot branching by triggering rapid depletion of the auxin efflux protein PIN1 from the plasma membrane. PLoS Biol. 11: e1001474.

Snowden, K.C., Simkin, A.J., Janssen, B.J., Templeton, K.R., Loucas, H.M., Simons, J.L., Karunairetnam, S., Gleave, A.P., Clark, D.G., and Klee, H.J. (2005). The Decreased apical dominance1/Petunia hybrida CAROTENOID CLEAVAGE DIOXYGENASE8 gene affects branch production and plays a role in leaf senescence, root growth, and flower development. Plant Cell 17: 746–759.

Song, C., Zhao, J., Guichard, M., Shi, D., Grossmann, G., Schmitt, C., Jouannet, V., and Greb, T. (2021). Strigo-D2 – a bio-sensor for monitoring the spatio-temporal pattern of strigolactone signaling in intact plants. bioRxiv: 2021.08.03.454859.

Soundappan, I., Bennett, T., Morffy, N., Liang, Y., Stanga, J.P., Abbas, A., Leyser, O., and Nelson, D.C. (2015). SMAX1-LIKE/D53 Family Members Enable Distinct MAX2-Dependent Responses to Strigolactones and Karrikins in Arabidopsis. Plant Cell 27: 3143–3159.

Stanga, J.P., Morffy, N., and Nelson, D.C. (2016). Functional redundancy in the control of seedling growth by the karrikin signaling pathway. Planta 243: 1397–1406.

Stanga, J.P., Smith, S.M., Briggs, W.R., and Nelson, D.C. (2013). SUPPRESSOR OF MORE AXILLARY GROWTH2 1 controls seed germination and seedling development in Arabidopsis. Plant Physiol. 163: 318–330.

Stanic, M., Hickerson, N.M.N., Arunraj, R., and Samuel, M.A. (2021). Gene-editing of the strigolactone receptor BnD14 confers promising shoot architectural changes in Brassica napus (canola). Plant Biotechnol. J. 19: 639–641.

Sun, X.-D. and Ni, M. (2011). HYPOSENSITIVE TO LIGHT, an alpha/beta fold protein, acts downstream of ELONGATED HYPOCOTYL 5 to regulate seedling de-etiolation. Mol. Plant 4: 116–126.

Sun, Y.K., Flematti, G.R., Smith, S.M., and Waters, M.T. (2016). Reporter Gene-Facilitated Detection of Compounds in Arabidopsis Leaf Extracts that Activate the Karrikin Signaling Pathway. Front. Plant Sci. 7: 1799.

Swarbreck, S.M., Guerringue, Y., Matthus, E., Jamieson, F.J.C., and Davies, J.M. (2019). Impairment in karrikin but not strigolactone sensing enhances root skewing in Arabidopsis thaliana. Plant J. 98: 607–621.

Toh, S., Holbrook-Smith, D., Stogios, P.J., Onopriyenko, O., Lumba, S., Tsuchiya, Y., Savchenko, A., and McCourt, P. (2015). Structure-function analysis identifies highly sensitive strigolactone receptors in Striga. Science 350: 203–207.

Toh, S., Holbrook-Smith, D., Stokes, M.E., Tsuchiya, Y., and McCourt, P. (2014). Detection of parasitic plant suicide germination compounds using a high-throughput Arabidopsis HTL/KAI2 strigolactone perception system. Chem. Biol. 21: 988–998.

Tsuchiya, Y., Yoshimura, M., Sato, Y., Kuwata, K., Toh, S., Holbrook-Smith, D., Zhang, H., McCourt, P., Itami, K., Kinoshita, T., and Hagihara, S. (2015). PARASITIC PLANTS. Probing strigolactone receptors in Striga hermonthica with fluorescence. Science 349: 864–868.

Ueda, H. and Kusaba, M. (2015). Strigolactone Regulates Leaf Senescence in Concert with Ethylene in Arabidopsis. Plant Physiol. 169: 138–147.

Umehara, M., Hanada, A., Yoshida, S., Akiyama, K., Arite, T., Takeda-Kamiya, N., Magome, H., Kamiya, Y., Shirasu, K., Yoneyama, K., Kyozuka, J., and Yamaguchi, S. (2008). Inhibition of shoot branching by new terpenoid plant hormones. Nature 455: 195–200.

Uraguchi, D. et al. (2018). A femtomolar-range suicide germination stimulant for the parasitic plant Striga hermonthica. Science 362: 1301–1305.

Van Ha, C. et al. (2014). Positive regulatory role of strigolactone in plant responses to drought and salt stress. Proc. Natl. Acad. Sci. U. S. A. 111: 851–856.

Villaécija-Aguilar, J.A., Hamon-Josse, M., Carbonnel, S., Kretschmar, A., Schmid, C., Dawid, C., Bennett, T., and Gutjahr, C. (2019). SMAX1/SMXL2 regulate root and root hair development downstream of KAI2-mediated signalling in Arabidopsis. PLOS Genetics 15: e1008327.

Wang, L. et al. (2020). Strigolactone and Karrikin Signaling Pathways Elicit Ubiquitination and Proteolysis of SMXL2 to Regulate Hypocotyl Elongation in Arabidopsis. Plant Cell 32: 2251–2270.

Wang, L., Wang, B., Jiang, L., Liu, X., Li, X., Lu, Z., Meng, X., Wang, Y., Smith, S.M., and Li, J. (2015a). Strigolactone Signaling in Arabidopsis Regulates Shoot Development by Targeting D53-Like SMXL Repressor Proteins for Ubiquitination and Degradation. Plant Cell 27: 3128–3142.

Wang, P. et al. (2019). Functional analysis of the GbDWARF14 gene associated with branching development in cotton. PeerJ 7: e6901.

Wang, Y., Yao, R., Du, X., Guo, L., Chen, L., Xie, D., and Smith, S.M. (2021). Molecular basis for high ligand sensitivity and selectivity of strigolactone receptors in Striga. Plant Physiol. 185: 1411–1428.

Wang, Z.-P., Xing, H.-L., Dong, L., Zhang, H.-Y., Han, C.-Y., Wang, X.-C., and Chen, Q.-J. (2015b). Egg cell-specific promoter-controlled CRISPR/Cas9 efficiently generates homozygous mutants for multiple target genes in Arabidopsis in a single generation. Genome Biol. 16: 144.

Waters, M.T., Gutjahr, C., Bennett, T., and Nelson, D.C. (2017). Strigolactone Signaling and Evolution. Annu. Rev. Plant Biol. 68: 291–322.

Waters, M.T., Nelson, D.C., Scaffidi, A., Flematti, G.R., Sun, Y.K., Dixon, K.W., and Smith, S.M. (2012). Specialisation within the DWARF14 protein family confers distinct responses to karrikins and strigolactones in Arabidopsis. Development 139: 1285–1295.

Waters, M.T., Scaffidi, A., Moulin, S.L.Y., Sun, Y.K., Flematti, G.R., and Smith, S.M. (2015). A Selaginella moellendorffii Ortholog of KARRIKIN INSENSITIVE2 Functions in Arabidopsis Development but Cannot Mediate Responses to Karrikins or Strigolactones. Plant Cell 27: 1925–1944.

Wen, C., Xi, L., Gao, B., Wang, K., Lv, S., Kou, Y., Ma, N., and Zhao, L. (2015). Roles of DgD14 in regulation of shoot branching in chrysanthemum (Dendranthema grandiflorum “Jinba”). Plant Physiol. Biochem. 96: 241–253.

Yamada, Y., Furusawa, S., Nagasaka, S., Shimomura, K., Yamaguchi, S., and Umehara, M. (2014). Strigolactone signaling regulates rice leaf senescence in response to a phosphate deficiency. Planta 240: 399–408.

Yao, J., Mashiguchi, K., Scaffidi, A., Akatsu, T., Melville, K.T., Morita, R., Morimoto, Y., Smith, S.M., Seto, Y., Flematti, G.R., Yamaguchi, S., and Waters, M.T. (2018). An allelic series at the KARRIKIN INSENSITIVE 2 locus of Arabidopsis thaliana decouples ligand hydrolysis and receptor degradation from downstream signalling. Plant J. 96: 75–89.

Yao, R. et al. (2016). DWARF14 is a non-canonical hormone receptor for strigolactone. Nature 536: 469–473.

Yao, R., Wang, F., Ming, Z., Du, X., Chen, L., Wang, Y., Zhang, W., Deng, H., and Xie, D. (2017). ShHTL7 is a non-canonical receptor for strigolactones in root parasitic weeds. Cell Res. 27: 838–841.

Yoshimura, M., Sato, A., Kuwata, K., Inukai, Y., Kinoshita, T., Itami, K., Tsuchiya, Y., and Hagihara, S. (2018). Discovery of Shoot Branching Regulator Targeting Strigolactone Receptor DWARF14. ACS Cent Sci 4: 230–234.

Zhao, L.-H. et al. (2015). Destabilization of strigolactone receptor DWARF14 by binding of ligand and E3-ligase signaling effector DWARF3. Cell Res. 25: 1219–1236.

Zheng, J. et al. (2020). Karrikin Signaling Acts Parallel to and Additively with Strigolactone Signaling to Regulate Rice Mesocotyl Elongation in Darkness. Plant Cell 32: 2780–2805.

Zheng, K. et al. (2016). Characterization of DWARF14 Genes in Populus. Sci. Rep. 6: 21593.

Zhou, F. et al. (2013). D14-SCF(D3)-dependent degradation of D53 regulates strigolactone signalling. Nature 504: 406–410.

Figures:

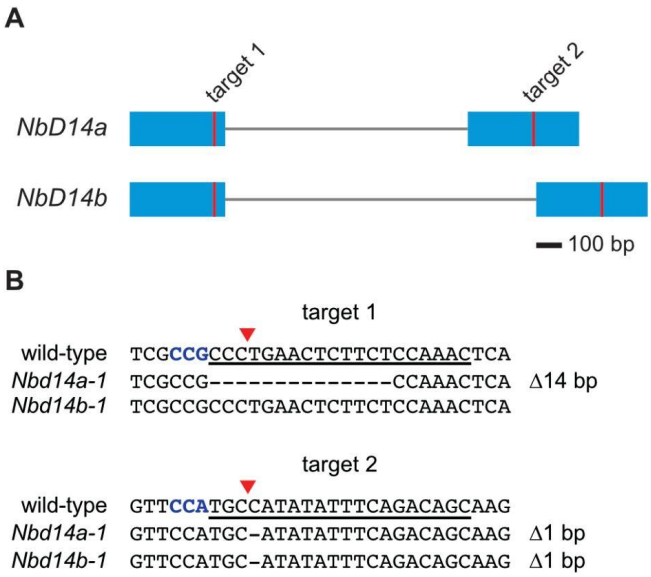


Figure 1.1 Mutation of two *D14* genes in *Nicotiana benthamiana* with CRISPR-Cas9

(A) Diagram of *D14a* and *D14b* genes in *N. benthamiana*. Blue boxes represent exons. Vertical red lines indicate gRNA target sites. (B) Sequences of Cas9-induced frameshift alleles of *NbD14a* and *NbD14b*. gRNA target sequence is underlined. Protospacer adjacent motif (PAM) sequence (5'-NGG-3') is indicated in bold blue font. Red triangles denote predicted Cas9 cleavage sites.

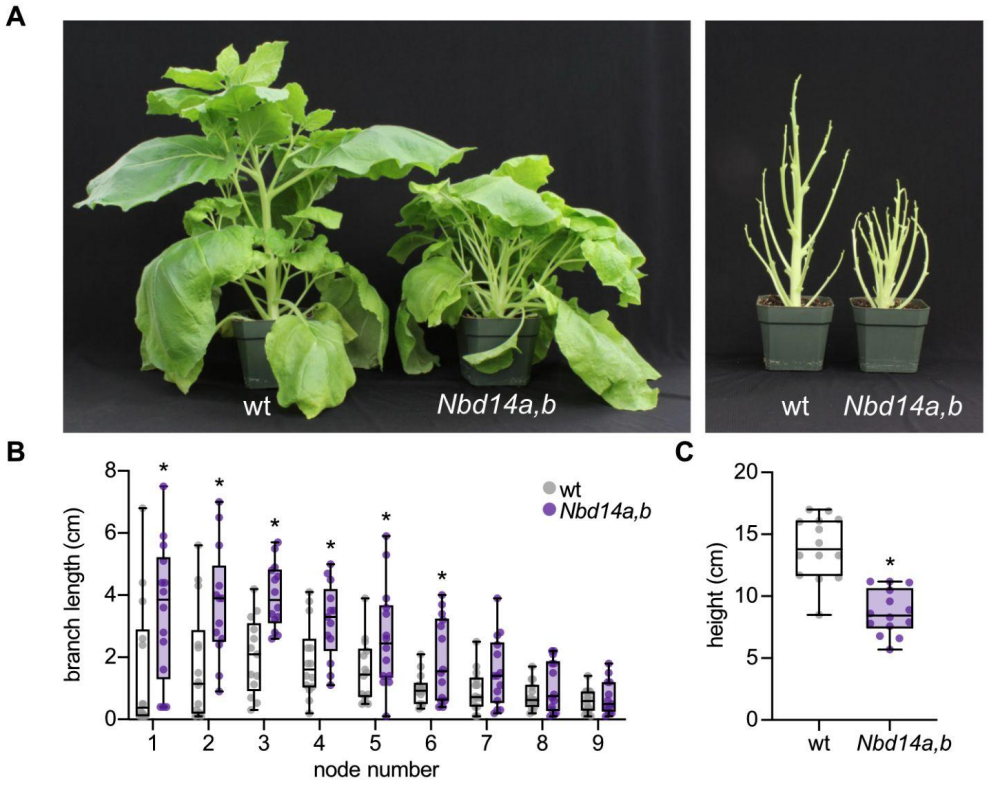


Figure 1.2 *Nbd14a,b* has more axillary bud outgrowth and reduced height
(A) Photographs of 10-week old wt and *Nbd14a,b N. benthamiana* plants with (right) and without (left) leaves. (B) Bud outgrowth of the first nine axillary nodes of 58-day old wt and *Nbd14a,b* plants. (C) Primary shoot height of wt and 58-day old *Nbd14a,b*. Box plots show median with 25th and 75th percentiles, and whiskers represent minimum and maximum values; n=10-12 plants; *, p <0.05, unpaired t-test with Welch correction, comparison of *Nbd14a,b* to wt.

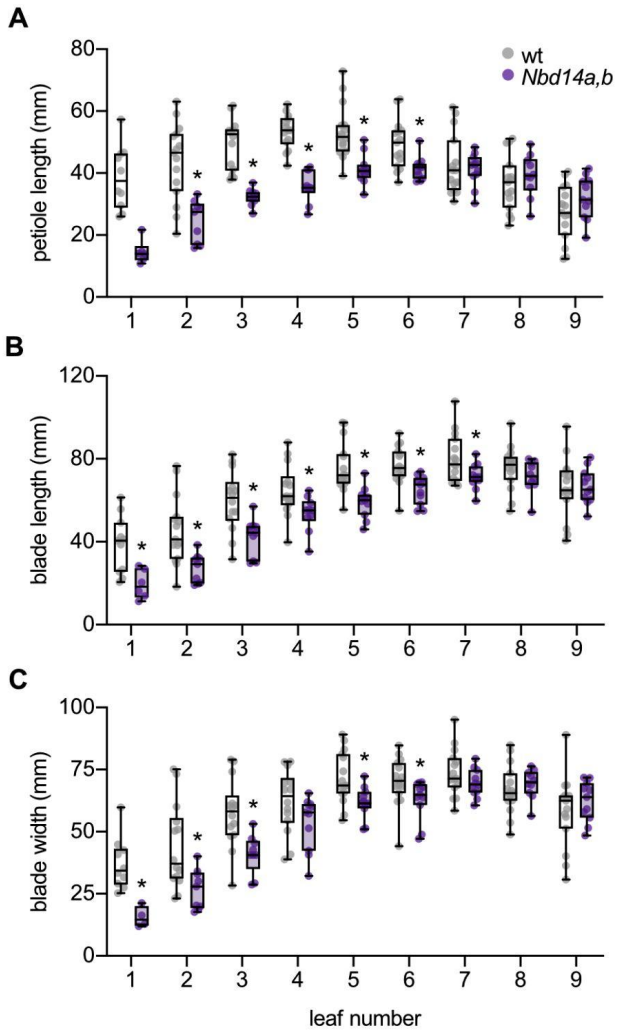


Figure 1.3 *Nbd14a,b* has smaller leaves and petioles
(A) Petiole lengths (B) blade lengths, and (C) blade widths of the first nine leaves of 58-day old wt and *Nbd14a,b* plants. Box plots show median with 25th and 75th percentiles, and whiskers represent minimum and maximum values; n=10-12 plants; *, p <0.05, unpaired t-test with Welch correction, comparison of *Nbd14a,b* to wt.

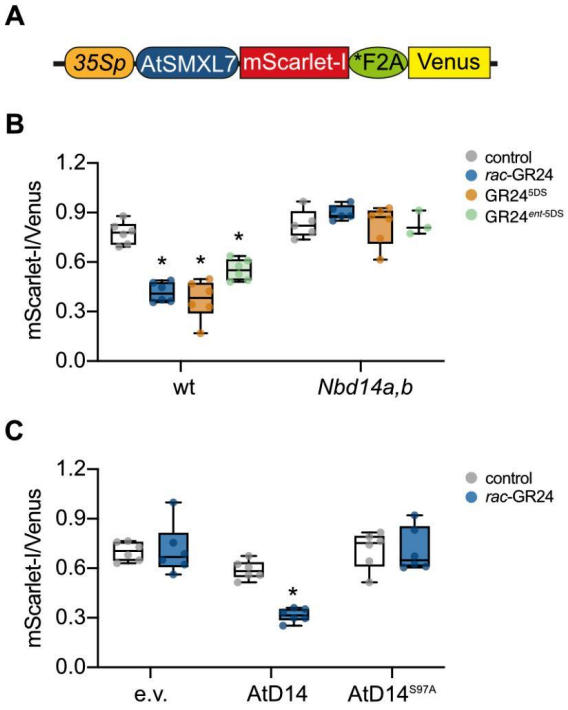


Figure 1.4 AtSMXL7 degradation in *N. benthamiana* is *NbD14*-dependent

(A) Diagram of the ratiometric AtSMXL7 reporter expressed in pRATIO3212. mScarlet-I is a fluorescent reporter protein translationally fused to the C-terminus of AtSMXL7, *F2A is a modified "self-cleaving" peptide, and Venus is a yellow fluorescent protein used for normalization. Diagram adapted from (Khosla et al., 2020b). (B) Background-corrected AtSMXL7-mScarlet-I to Venus fluorescence in *N. benthamiana* wt and *Nbd14a,b* leaf discs after 16 h treatments with solvent control (0.02% acetone (v/v)), or 10µM *rac*-GR24, GR24^{5DS}, or GR24$^{ent\text{-}5DS}$. (C) Background-corrected AtSMXL7-mScarlet-I to Venus fluorescence in *Nbd14a,b* leaf discs after 16 h treatments with solvent control (0.02% acetone (v/v)), or 10µM *rac*-GR24. pRATIO3212-AtSMXL7 was coexpressed with pGWB415 empty vector (e.v.), AtD14, or AtD14^{S97A}. Box plots show median with 25th and 75th percentiles, and whiskers represent minimum and maximum values; n=3-6 leaf discs; *, p <0.05, unpaired t-test with Welch correction, comparison of treatment to control.

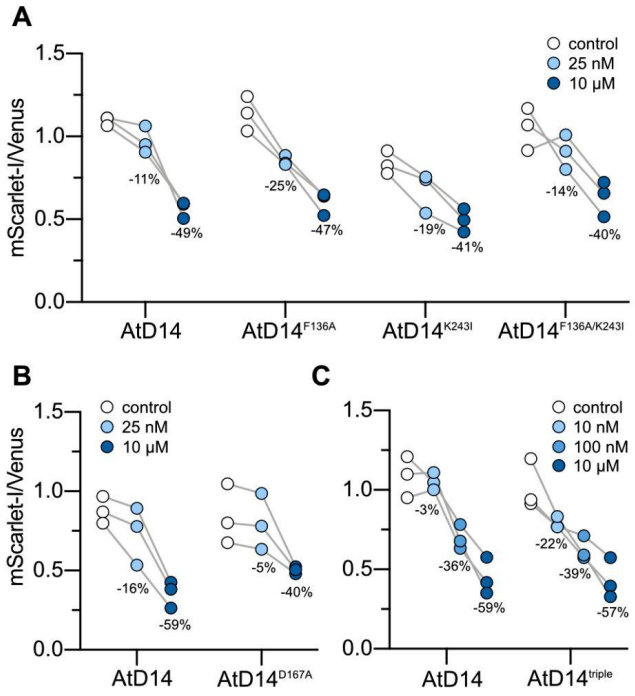


Figure 1.5 AtSMXL7 degradation is altered when co-expressed with AtD14 variants. Background-corrected AtSMXL7-mScarlet-I to Venus fluorescence in *Nbd14a,b* leaf discs after 16 h treatments with solvent control (0.02% acetone (v/v)), 10 nM, 25 nM, 100 nM, or 10 µM *rac*-GR24. pRATIO3212-AtSMXL7 was coexpressed with pGWB415-AtD14, (A) pGWB415-AtD14^{F136A}, -AtD14^{K243I}, or -AtD14$^{F136A/K243I}$; (B) pGWB415-AtD14^{D167A}; or (C) AtD14$^{F159T/A163L/G165A}$ (AtD14^{triple}). Each point represents the mean of n=3-6 treated discs from an individually transformed leaf. Paired data are linked by lines. Percentages indicate mean percent reduction in mScarlet-I/Venus ratio of each treatment compared to control.

Supplementary figures and legends:

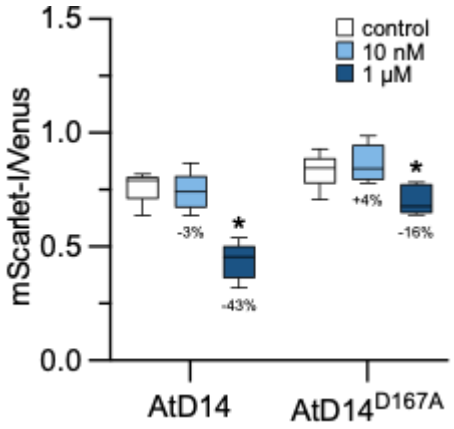


Figure S1. AtD14^{D167A} is less sensitive to *rac*-GR24 than wt AtD14.

Background-corrected AtSMXL7-mScarlet-I to Venus fluorescence in *Nbd14a,b* leaf discs after 16 h treatments with solvent control, 10 nM *rac*-GR24, or 1 µM *rac*-GR24. pRATIO3212-AtSMXL7 was coexpressed with pGWB415-AtD14 or pGWB415-AtD14^{D167A}. Box plots show median with 25th and 75th percentiles, and Tukey's whiskers (n = 5 independently transformed leaves, where each leaf value is the mean value of 3-6 discs). *, $p < 0.05$, repeated-measures two-way ANOVA with Dunnett's multiple comparisons test, comparing GR24 treatments to control for each genotype. Percentages below box plots indicate the percent change in the mean mScarlet-I/Venus ratio of each treatment compared to control.

Supplementary Table S1. Primers used in this study

Primer name	Sequence	Use
NbD14-DT1-BsF	5'-ATATATGGTCTCGATT**G**TTTGGAGAAGAGTTCAGGGGTT-3'	gRNA cloning
NbD14-DT1-F0	5'-T**G**TTTGGAGAAGAGTTCAGGGGTTTTAGAGCTAGAAATAGC-3'	
NbD14-DT2-R0	5'-AACTGCCATATATTTCAGACAG**C**AATCTCTTAGTCGACTCTAC-3'	
NbD14-DT2-BsR	5'-ATTATTGGTCTCGAAACTGCCATATATTTCAGACAG**C**AA-3'	
U6-26p-F	5'-TGTCCCAGGATTAGAATGATTAGGC-3'	colony PCR & sequencing of CRISPR-Cas9 construct
U6-29p-R	5'-AGCCCTCTTCTTTCGATCCATCAAC-3'	
U6-29p-F	5'-TTAATCCAAACTACTGCAGCCTGAC-3'	
pHEE401EhygB-F	5'-CGTGCTTTCAGCTTCGATGTAG-3'	transgene detection
pHEE401EhygB-R	5'-CAGTCAATGACCGCTGTTATGC-3'	
NbD14a,b-F	5'-CTGAACGTACGAGTCGTAGGTTC-3'	genotyping
NbD14a-3'UTR-R	5'-TGGGAGGATATGATACGAGAGC-3'	
NbD14a-R	5'-AAGAGCTCTTCTAAGCTCTTGAGTC-3'	
NbD14b-Intron-R	5'-CGAACATCACACATCACACG-3'	
NbD14b-Intron-F	5'-TGCATCTCATTAACGGCAAG-3'	
NbD14b-R	5'-AAGAGCTCTTCTAAGCTCTTGAGCT-3'	

Chapter 2: Identification of residues required for receptor-target interactions during strigolactone signaling

Abstract:

The strigolactone hormone (SL) and karrikin (KAR, smoke-derived compounds) signaling pathways in plants affect critical processes such as drought tolerance, nutrient acquisition, shoot branching, germination; seedling, root, and leaf development, and beneficial associations with soil microbes. Although the SL and KAR signaling pathways mainly regulate different traits, they use the same or related protein components. In *Arabidopsis thaliana*, the receptors of each pathway are homologous α/β-fold hydrolases: DWARF14 (D14) for SLs and KARRIKIN INSENSITIVE2 (KAI2) for KARs. When activated, each receptor interacts with and targets a different set of transcriptional co-repressor proteins in the SMAX1-LIKE (SMXL) family for polyubiquitination and degradation, leading to SL- or KAR-responsive changes in gene expression. However, **how D14 interacts with its SMXL protein targets is still unknown.** I hypothesize that one or more residues at the target-interaction surfaces of D14 and KAI2 specify selective interactions with SMXL protein partners, forming the basis of SL and KAR signaling fidelity.

To characterize the target-interaction surface, I identified highly conserved surface-exposed residues on D14 in the active conformation. I have used alanine-scanning mutagenesis to evaluate the function of 67 surface residues in the D14-SMXL7 interaction. In a first-pass screen, each D14 variant is tested for its ability to target a ratiometric SMXL7 reporter for degradation in a *Nicotiana benthamiana d14a,b* mutant background. I found 20 variants that differentially affect SMXL7 reporter accumulation and degradation compared to wild-type D14. When stably transformed into the *Arabidopsis*

thaliana d14 mutant background, the majority of these variants can rescue the mutant phenotype, except for one variant, D14D198A. However, the data for D14D198A suggests this residue is critical for protein structure and stability, not SMXL interaction. This research provides more profound knowledge of the intricate dynamics of SL signaling.

Introduction:

Plants, with their stationary life cycle, face a myriad of unpredictable environments, including temperature changes, shifts in light, availability of water and nutrients, exposure to pathogens, or physical damage. Yet, they maintain their growth and development using complex hormone-signaling pathway networks. These pathways enable plants to respond in a timely and coordinated manner to environmental stimuli, influencing their developmental processes(Vanstraelen & Benková, 2012). The crosstalk between these pathways adds another complexity to the plant's response to environmental factors(Vanstraelen & Benková, 2012). For example, the gibberellin (GA) and abscisic acid (ABA) pathways, by taking in light and water from the environment, determine the precise timing of seed germination(Liu & Hou, 2018). Many hormone signaling pathways utilize the same or similar components to facilitate this crosstalk(Blázquez et al., 2020). However, it remains unclear how plants can share the same components yet produce distinct physiological outputs depending on the hormone. One of the most enigmatic examples of this plant hormone signaling crosstalk is between the strigolactone (SL) and karrikin (KAR) signaling pathways, two homologous pathways that influence a wide range of plant processes.

SLs, carotenoid-derived phytohormones, were first investigated in root exudates as germination stimulants of parasitic weeds. This initial discovery sparked further research,

leading to the identification of SLs as signals that induce hyphal branching in arbuscular mycorrhizal fungi (AMF), and most recently as plant hormones regulating shoot and root architecture(Cook et al., 1966);(Akiyama et al., 2005; Akiyama & Hayashi, 2006)(Gomez-Roldan et al., 2008; Umehara et al., 2008)(Akiyama et al., 2005; Akiyama & Hayashi, 2006).

Scientists discovered KARs as the potent germination stimulant found in the smoke of burnt plant material(Chiwocha et al., 2009; Choi et al., 2020; W. Li et al., 2017; Merritt et al., 2009; Nelson et al., 2012; Stanga et al., 2016; Waters & Nelson, 2022)). When investigating the molecular mechanism of KAR-induced seed germination, researchers discovered the core KAR signaling components conserved amongst land plants(Bythell-Douglas et al., 2017; Machin et al., 2020). By analyzing KAR signaling mutants, it became evident the KAR signaling pathway regulates light-dependent seedling development, as well as drought tolerance, and components of the signaling pathway required for AMF associations(Chiwocha et al., 2009; Choi et al., 2020; W. Li et al., 2017; Merritt et al., 2009; Nelson et al., 2012; Stanga et al., 2016; Waters & Nelson, 2022). Because KARs are exogenous molecules, they are not considered plant hormones. However, there is an exceeding amount of data to suggest they mimic an endogenous signal that could be regarded as a plant hormone(Stirling et al., 2024; Waters & Nelson, 2022).

Different ligands typically activate the SL and KAR signaling pathways, have distinct expression profiles, and have distinctive phenotypic outputs, yet both share the same or related components(Nelson et al., 2010; Scaffidi et al., 2014; Waters et al., 2012; Waters, Scaffidi, Moulin, et al., 2015; Waters & Nelson, 2022). In *Arabidopsis thaliana*, the receptors of each pathway are homologous α/β-fold hydrolases: DWARF14 (D14) is the

receptor for SLs, and KARRIKIN INSENSITIVE2 (KAI2) is the receptor of KARs(Hamiaux et al., 2012; Waters et al., 2012). Both of these receptors have hydrolytic function via the conserved serine-histidine-aspartate catalytic triad; although KARs are not hydrolyzable, KAI2 can hydrolyze other molecules such as unnatural stereoisomers of SLs(Hamiaux et al., 2012; Nakamura et al., 2013; Scaffidi et al., 2012; Waters et al., 2014; Waters, Scaffidi, Moulin, et al., 2015; Zhao et al., 2013). The KAI2 lineage is maintained across land plants, and D14-type proteins diverged from the KAI2 lineage through gene duplication and emerged before the gymnosperm lineage(Bythell-Douglas et al., 2017). KAI2 signaling has probably been an important adaptation for land plants, and D14 signaling has been co-opted for more complex processes in seed plants(Bythell-Douglas et al., 2017; Machin et al., 2020). Interestingly, SL receptors responsible for sensing host-derived SLs in parasitic weeds are KAI2 proteins that have undergone a significant expansion only found in Orobanchaceae, and most species in this family have many copies of these genes. This rapidly evolving clade, known as the divergent clade of KAI2s (KAI2d), has evolved away from the conserved function of KL perception. KAI2d proteins evolved to perceive SLs through convergent evolution of the ligand binding pocket(Conn et al., 2015; Toh et al., 2015; Tsuchiya et al., 2015).

Both the SL and KAR pathways use one essential protein, MORE AXILLARY GROWTH2 (MAX2), an F-box protein involved in the SKP1-CULLIN-F-BOX (SCF) E3 ubiquitin ligase complex(Nelson et al., 2011; Soundappan et al., 2015; Stanga et al., 2016). This complex targets transcriptional regulatory proteins of each pathway for ubiquitination, leading to their degradation by the 26S proteasome (Abd-Hamid et al. 2020; Yu et al. 2007).

The SL pathway targets a clade of D53-type proteins (SMXL6/7/8 in *Arabidopsis*) in the SMAX1-LIKE (SMXL) family for degradation upon activation by SLs(Liang et al., 2016; Soundappan et al., 2015; Wang et al., 2015; Zhou et al., 2013). Similarly, the KAI2 signaling pathway targets SMAX1-type (SMAX1 and SMXL2 in *Arabidopsis*) proteins for degradation(Khosla, Morffy, et al., 2020; Wang et al., 2020). SMXL proteins act as key growth regulators through transcriptional co-repression(Temmerman et al., 2022). Similar to the diversification of the receptors of these pathways, SL-responsive SMXLs only emerged at the base of the angiosperm lineage, where the KAI2 signaling SMXLs have homologs found throughout land plants(Kodama et al., 2023; Mizuno et al., 2021; Moturu et al., 2018). Recent data suggests that D14 can target the KAR repressors SMAX1 and SMXL2 under specific physiological conditions, such as osmotic stress(Q. Li et al., 2022; Wang et al., 2020). However, it is unclear if this is due to non-natural experimental settings, actual physiological crosstalk between the two pathways, or an artifact of D14 promiscuity due to the recent evolution of D14-SMXL interactions. Nonetheless, genes involved in KAR/SL developmental regulation are activated after the degradation of the respective SMXL proteins for each pathway(Temmerman et al., 2022).

The formation of this complex is crucial for a coordinated response to each signal. It is important to understand how this complex forms and how each receptor and SMXL pair can distinguish themselves from each other for proper signal transduction. Numerous studies have aimed to clarify the interactions within this complex through targeted amino acid alterations, ranging from single to multiple substitutions.

A pivotal 2016 study resolved the crystal structure of D14 in complex with rice MAX2 (D3), revealing a substantial conformational change upon strigolactone binding compared to the apo structure(R. Yao et al., 2016; Zhao et al., 2013). Remarkably, the

D14-MAX2 interface is highly conserved in D14 and KAI2 around the helical lid domain with the same residues required between the two receptors(Bythell-Douglas et al., 2017; R. Yao et al., 2016). This interface consists of a minor and significant interaction area on D14 with the C-terminal leucine-rich repeat (LRR) region of MAX2(R. Yao et al., 2016). D14 undergoes a significant conformational change upon interaction, mainly in the lid domain and ligand binding pocket(R. Yao et al., 2016). In the apo structure, the lid domain consists of four alpha helices; however, in the structure with MAX2, this domain is reduced to three helices, and the fourth transitions into a coil loop(R. Yao et al., 2016; Zhao et al., 2013). The conformational change condenses the ligand binding pocket, keeping the catalytic serine and histidine residues in place. However, the loop containing catalytic aspartate residue moves out of the pocket and becomes disordered (R. Yao et al., 2016; Zhao et al., 2013). The study also identified a mutation, G158E, disrupting the D14-MAX2 interaction while preserving hydrolytic function and interactions with SMXL proteins(R. Yao et al., 2016).

In this model, the D-ring of the SL molecule becomes covalently bonded to the catalytic histidine, leading to a conformational change, allowing D14 to form a complex with MAX2(R. Yao et al., 2016). However, the intricacies of this process have been the subject of debate in the literature(Bürger & Chory, 2020; Carlsson et al., 2018; de Saint Germain et al., 2016). This model assumes SL hydrolysis occurs during complex formation and that SMXL degradation requires hydrolysis; however, *in vivo* studies have shown hydrolysis rates are slower than the rate of SMXL degradation(de Saint Germain et al., 2016; Hamiaux et al., 2012; Nakamura et al., 2013; Zhao et al., 2013; Zhou et al., 2013). At the same time, mutations in the serine and histidine residues of the catalytic triad render the receptors non-functional(Hamiaux et al., 2012; Khosla, Morffy, et al., 2020; Nakamura

et al., 2013; Seto et al., 2019; Waters, Scaffidi, Moulin, et al., 2015). Mutating the aspartate residue D218 into an alanine residue eliminates hydrolytic capability but rescues the bushy phenotype of *d14* mutants and shows hypersensitivity to SLs for branching inhibition(Seto et al., 2019). This data has led to an alternative model where mere interaction with the ligand leads to activation and interaction with MAX2. However, due to the strict conservation of the catalytic triad in D14 and KAI2 proteins, hydrolysis likely plays an important role in signal transduction that has yet to be fully resolved(Bürger & Chory, 2020).

MAX2 also displays post-SL targeting and ubiquitination of D14(Chevalier et al., 2014; Q. Hu et al., 2017; Martín-Fontecha et al., 2024). Genetic evidence suggests this step occurs after the SMXLs have been degraded as a form of negative feedback regulation(Chevalier et al., 2014). There is supporting evidence that D14 can undergo perception and hydrolysis more than once, suggesting that the cells use D14 degradation to prevent further SL signaling from occurring once the cascade has been activated (Seto et al., 2019). KAI2 also shows protein degradation post-KAR signaling but appears to be MAX2-independent(Waters, Scaffidi, Flematti, et al., 2015). A recent study found that D14-induced SL hydrolysis was unnecessary for D14 degradation, further supporting the model suggesting interaction with SLs triggers D14 activation(Chevalier et al., 2014; Q. Hu et al., 2017; Martín-Fontecha et al., 2024). Researchers in this study found that MAX2 and SMXLs were not necessary for D14 degradation, however, MAX2 accounted for most of the D14 degradation(Chevalier et al., 2014; Q. Hu et al., 2017; Martín-Fontecha et al., 2024). KAI2 also shows protein degradation post-KAR signaling but appears MAX2-independent(Waters, Scaffidi, Flematti, et al., 2015). MAX2 has also displayed different conformations when in complex with D14. Moreover, this occurs with the C-terminal helix

of MAX2, which binds D14 in either an engaged or dislodged conformation(Shabek et al., 2018; Tal et al., 2022). The dislodged conformation prevents D14 from transitioning into the active conformation (closed state) and prevents hydrolysis, while the engaged conformation occurs when SMXL proteins join the complex(Shabek et al., 2018; Tal et al., 2022).

Extensive research has been focused on understanding the different domains in SMXL proteins and their signaling dynamics. SMXL proteins have five distinct domains: N, D1, M, D2a, and D2b(Khosla, Morffy, et al., 2020). The N domain contains the nuclear localization signal (NLS) in D53/SMXL6,7,8 proteins; as transcriptional co-repressors, these proteins function within the nucleus(Choi et al., 2020; Liang et al., 2016). The D1 and M domains participate in receptor interaction(Khosla, Morffy, et al., 2020). Consequently, these are the most variable regions in conservation amongst this family of proteins, hinting at diversification due to receptor interactions(Khosla, Morffy, et al., 2020; Walker et al., 2019). The D2a domain is responsible for MAX2 interaction and contains the RGKT motif required for subsequent degradation(Jiang et al., 2013; Kerr et al., 2021; Khosla, Morffy, et al., 2020; Liang et al., 2016; Mizuno et al., 2021; Soundappan et al., 2015; Struk et al., 2018; Wang et al., 2015, 2020; Zheng et al., 2021; Zhou et al., 2013). Furthermore MAX2 interaction does not occur if this motif is mutated, leading to protein stability and a dominant negative phenotype(Khosla, Morffy, et al., 2020; Liang et al., 2016; Soundappan et al., 2015; Struk et al., 2018; Wang et al., 2015; Zhou et al., 2013). In between the D2a and D2b domains lies the ETHYLENE-RESPONSE FACTOR Amphiphilic Repression (EAR) motif required for transcriptional co-repression with TOPLESS (TPL)/TPL-Related (TPR), co-repressors(Jiang et al., 2013; Moturu et al., 2018; Plant et al., 2021; Soundappan et al., 2015; Struk et al., 2018; Walker et al., 2019;

Wang et al., 2015). Lastly, the C-terminal D2b domain is necessary for SMXL-SMXL hetero- and homodimer interactions, which has been demonstrated in yeast two-hybrud assays(Khosla, Morffy, et al., 2020; Liang et al., 2016; Q. Li et al., 2024; Ma et al., 2017). The biological importance of SMXL dimerization is currently unknown.

Elucidating how SMXL proteins interact with D14 or KAI2 and MAX2 has been more difficult due to the lack of structural data and the complexity of SMXL proteins. Some studies have utilized in vitro mutational analysis to map interaction surfaces. Before the D14-MAX2/D3-ASK1 crystal structure was solved, the research used an alpha screen approach to analyze D14 variants with mutations in potential MAX2 interacting residues(Zhao et al., 2015). While many residues seemingly affected the binding to D3/MAX2, only two of the residues they mutated proved to be important in the D14-D3/MAX2-ASK1 crystal structure(R. Yao et al., 2016; Zhao et al., 2015).

Similarly, a mutational analysis of DAD2/D14 in a yeast two-hybrid system was conducted to identify MAX2 and D53/SMXL interacting residues(Lee et al., 2020). However, the expression of these variants in *Arabidopsis* and *Petunia* led to conflicting results. Notably, the N242I DAD2/D14 variant exhibited a constitutive interaction with MAX2 in the yeast two-hybrid system. However, when expressed in *Arabidopsis*, as DAD2, not D14, it failed to rescue the *Atd14* mutant phenotype, nor did it induce a dominant negative effect when expressed in *Col-0(Drummond et al., 2023)*. DAD2 wild-type also did not fully restore the mutant phenotype, posing a challenge in interpreting the variant results(Drummond et al., 2023). When the equivalent mutant for AtD14, K243I, was tested in Chapter One, the variant was hypersensitive to targeting the SMXL7 reporter under low SL treatments, consistent with a constitutive interaction (White et al., 2022). When overexpressed in *Petunia*, each variant seemingly rescued the mutant

phenotype(Drummond et al., 2023). Therefore, consider mutations obtained from in vitro assays with caution.

Several mutations of D14 reduce interactions with SMXL proteins *in planta*. For example, R183H maintains hydrolytic capacity and MAX2 interaction but cannot interact with SMXL7 via yeast two-hybrid or rescue the *d14* mutant phenotype(Seto et al., 2019). Another mutation, d14-seto (P169L), a highly conserved residue on the lid domain, shows reduced SMXL7 interaction but constitutive interaction with SMAX1 in yeast two-hybrid, indicating a possible specificity determining residue(Chevalier et al., 2014). This variant also displays a higher SL-induced degradation rate than wild-type D14(Q. Li et al., 2022; Martín-Fontecha et al., 2024).

Recently, another research group analyzed the functional differences between two D14 homologs, SsD14a and *Ss*D14b, found in sugarcane(A. Hu et al., 2021). They found a conserved C-terminal arginine in SsD14a, a proline at the same location in SsD14b(A. Hu et al., 2021). Through yeast two-hybrid (Y2H) experiments, they found that SsD14a could interact with SsMAX2, SsSMXL7, and AtSMXL7, while SsD14b only interacted with SsMAX2(A. Hu et al., 2021). Upon mutating the proline residue in SsD14b to arginine (P304R), it gained interactions with SsMAX2, SsSMXL7, and AtSMXL7(A. Hu et al., 2021). Conversely, mutating R310P in SsD14a and R262P in AtD14 abolished interactions with SsMAX2, SsSMXL7, and AtSMXL7 while still maintaining interaction with SsMAX2(A. Hu et al., 2021). Notably, overexpressing P304R SsD14b in the *Atd14* mutant background rescued the branching phenotype, whereas SsD14b could not(A. Hu et al., 2021).

There is still limited understanding of SMXL interacting residues on KAI2. Several *kai2* alleles were identified through an EMS screen, and one of the causal mutations, D184N, resulted in a hydrolytically active and stable protein. However, it exhibited the

typical long hypocotyl phenotype of *kai2* mutants(J. Yao et al., 2018). Interestingly, this variant was more prone to degradation initiated by karrikin and a non-natural stereoisomer SL(J. Yao et al., 2018). Although it is not clear how this mutation prevents signal transduction from proceeding, the authors speculate it impairs MAX2 due to the residue's proximity to the MAX2 binding interface(J. Yao et al., 2018).

Most of these mutations were tested *in vitro* assays or mutant populations without deeply understanding how they affect D14 and KAI2-mediated signal transduction. While many of these mutations provide insight into the residues important for interaction, it is unclear whether that is due to stabilizing effects or direct contact with SMXLs. This chapter aims to map the SMXL interacting residues on the surface of D14 and evaluate how each residue impacts SMXL degradation as a proxy for signal transduction. I have individually mutated 67 highly conserved amino acids on D14 into alanine residues. Using these variants, I tested their ability to target SMXL7 for degradation in a transient fluorescent assay in *Nicotiana benthamiana*. While most residues displayed similar degradation patterns compared to wild-type D14, some residue changes displayed increased SMXL7 stability while others decreased SMXL7 stability and increased and decreased SMXL7 degradation. For those that displayed altered SMXL7 degradation patterns compared to the wild-type, I stably transformed them into the *Atd14* mutant background and assayed their ability to rescue the bushy mutant phenotype. Lastly, I expressed some of these variants in the ratiometric system to evaluate their stability and SL-induced degradation. While many variants displayed intriguing responses regarding SMXL7 reporter degradation, many were able to rescue the *Atd14* mutant phenotype or displayed instability when expressed in *N. benthamiana.* This data suggested that the D14 interaction with SMXL7 is not easily perturbed by single mutations, perhaps because it

involves multiple residues or interfaces. The ratiometric assay in *N. benthamiana* potentially reveals differences in the efficiency of D14-mediated degradation of SMXL7 that would not be observed through transgenic shoot branching assays in *Arabidopsis*, where overexpression of a *d14* variant may adequately compensate for its partial loss-of-function. These findings have potential implications for our understanding of SL signal transduction mechanisms, paving the way for further research in this field.

Materials and methods:

Amino acid conservation analysis

69 *D14* and 91 *KAI2* sequences were collected from published datasets (Bythell-Douglas et al., 2017; Conn et al., 2015). Protein sequence alignments were performed in MEGA 11 using the MUSCLE multiple sequence alignment algorithms (Tamura et al., 2021). Residues with over 70% identity conservation amongst D14 sequences were plotted onto the AtD14-OsD3-ASK1 (R. Yao et al., 2016) structure using ChimeraX (Pettersen et al., 2021) and analyzed for solvent-accessible surfaces to determine surface-exposed residues with a sasa score greater than 20. In total 69 residues were selected, this includes the catalytic mutant S97A, and the previously published amino acid change R183H (Seto et al., 2019).

Plant growth conditions

Arabidopsis thaliana seeds were incubated at -80 °C for 12h, and surface sterilized using 0.05% (v/v) Triton X-100, 70% EtOH solution, a 70% and 95% EtOH wash, and air dried. Seeds were grown on 0.5X Murashige and Skoog (MS) media, pH 5.7 with 1% (w/v) agar, and stratified for 3 days at 4 °C in the dark. One week old seedlings were transplanted to Sungro Professional Growing Mix, supplemented with Gnatrol WDG, Marathon (imidacloprid), and Osmocote 14-14-14 fertilizer. Plants were grown under long-day conditions (16 h white light, 120 µmol m^{-2} s^{-1} ; 8 h dark) at ~22 °C *N. benthamiana* seeds were incubated at -80 °C for 12h, germinated on Sungro Professional Growing Mix, supplemented with Gnatrol WDG, Marathon (imidacloprid), and Osmocote 14-14-14 fertilizer. Seedlings were transferred to pots at ~7-10 d old. *N. benthamiana* plants were grown under long-day conditions (16 h white light, 120 µmol m^{-2} s^{-1} ; 8 h dark) at ~22 °C.

Cloning

The CDSs for *AtD14* (AT3G03990) and *AtSMXL7* (AT3G03990) were cloned into the pDONR221a entry vector modified to have ampicillin resistance using Gateway BP cloning (Invitrogen). Each pDONR221a-D14 alanine variant was created using the Q5 Site-Directed Mutagenesis kit (New England Biolabs) and Sanger-sequence verified. For the *N. benthamiana* SMXL7 degradation assays, D14 variants were moved into the plant transformation vector pGWB512 (Nakagawa et al., 2007) and AtSMXL7 cloned into the pRATIO3212 ratiometric reporter vector (Khosla, Rodriguez-Furlan, et al., 2020)) using Gateway LR cloning (Invitrogen). For the *N. benthamiana* D14 degradation assays, D14 variants were moved into the pRATIO1212 ratiometric reporter vector (Khosla, Rodriguez-Furlan, et al., 2020)) using Gateway LR cloning (Invitrogen) *Phtheirospermum japonicum (Pj) MAX2* CDS was PCR-amplified and cloned into pENTR D-TOPO entry vector to generate entry vectors, then cloned into the pGWB402 (Nakagawa et al., 2007). For stable *A. thaliana* lines, D14 variants were moved into the plant transformation vector pGWB402 (Nakagawa et al., 2007) modified to have a seed coat YFP marker from pYUU (pGWBcitr-p35S destination vector) (Angulo et al., 2020).

Degradation assays

pGWB512-D14 and pGWB402-PjMAX2 vectors were transformed into *A. tumefaciens* strain GV3101 via electroporation. pRATIO3212-SMXL7 and pRATIO1212-D14 vectors were transformed into *A. tumefaciens* strain GV3101 carring a plasmid expressing p19, suppressor of gene-silencing, via electroporation. Transient transformation of *N. benthamiana* and measurement of mScarlet-I and Venus was performed as described previously (Khosla & Nelson, 2020), with the following modifications for the cell densities

of *A. tumefaciens* cultures resuspended in infiltration media before injection of *N. benthamiana* leaves: *A. tumefaciens* containing pRATIO3212-SMXL7 vectors at OD_{600} 0.8, cotransformed with *A. tumefaciens* containing pGWB512-D14 at OD_{600} 0.1, and injected at a final OD_{600} 0.9. *A. tumefaciens* containing pRATIO1212-D14 vectors at OD_{600} 0.5, cotransformed with *A. tumefaciens* containing pGWB402-PjMAX2 at OD_{600} 0.5, and injected at a final OD_{600} 1.

Production of transgenic Arabidopsis lines

pGWBcitr-p35S-D14 vectors were transformed into *A. tumefaciens* (GV3101). Each vector was transformed into *Arabidopsis thaliana d14-1 (Waters et al., 2012)* mutant background using the floral dip method (Clough & Bent, 1998). Lines were selected under a $\sim 470\text{nm}$ blue light flashlight and T1 and single insertion T3 homozygous lines were used for branching assays.

Branching assay

Arabidopsis thaliana seeds were incubated at -80 °C for 12h, and surface sterilized surface sterilized using 0.05% (v/v) Triton X-100, 70% EtOH solution, a 70% and 95% EtOH wash, and air dried. Seeds were grown on 0.5X Murashige and Skoog (MS) media, pH 5.7 with 1% (w/v) agar, and stratified for 3 days at 4 °C in the dark. One-week-old seedlings were transferred onto Sungro Professional Growing Mix, supplemented with Gnatrol WDG, Marathon (imidacloprid), and Osmocote 14-14-14 fertilizer. Plants were grown under long-day conditions (16 h white light, 120 µmol m^{-2} s^{-1} ; 8 h dark) at ~22 °C. Branches for hemizygous T1 assay were counted at ~7 and 10 week old stage. For T3

branching assay, each plant was noted for the day of anthesis. Plant height was measured and axillary branches were counted at 28 days post-anthesis.

Results and Discussion:

Determination of amino acids involved in D14-SMXL7 interaction:

To understand the amino acids required for SMXL interaction, I looked at amino acid sequence conservation across D14 proteins. Residues involved in the MAX2 interaction interface are highly conserved amongst D14 and KAI2 proteins; therefore, I hypothesized this is true for SMXL interaction(Bythell-Douglas et al., 2017; R. Yao et al., 2016). I aligned 69 annotated D14 sequences from angiosperms, obtained from Phytozome and previously published data sets, and focused on highly conserved residues, initially with >90% conservation, before widening my list of residues with the help of students in the Dynamic Genome course(Bythell-Douglas et al., 2017; Conn et al., 2015). To determine which residues to test, I set the conservation cutoff to >70%; however, this only eliminated 54 of the 267 residues comprising AtD14. I then filtered out any residues buried within the protein, assuming amino acids with low solvent exposure scores are inside the protein and unlikely to be involved in protein-protein interactions. Highly conserved residues on the interior of D14 are likely necessary for protein structure, the ligand binding pocket, and the catalytic triad, as these residues are 100% conserved.

Because D14 undergoes a significant conformational change post ligand binding and MAX2 interaction, residues buried in the apo structure may become exposed in the active or “closed” state(R. Yao et al., 2016). To address this, I calculated the solvent-accessible scores (sasa) in Chimera X for all residues in both the apo and active structure(Goddard et al., 2018; R. Yao et al., 2016; Zhao et al., 2013) (Figure 2.1A, Table S2.1). Arbitrarily setting the cutoff at a score of >20 shortened the list to 91 conserved and surface-exposed residues. Based on biochemical and genetic evidence, D14 is in complex with MAX2 when interacting with SMXL7, for example, the G158E mutation

impairs MAX2 interaction but not SMXL7 interaction and leads to the stereotypical *d14* mutant phenotype, suggesting that SMXL degradation requires D14-MAX2 interaction(Goddard et al., 2018; R. Yao et al., 2016; Zhao et al., 2013). I focused on the conformation D14 is in when interacting with MAX2 as this is likely the conformation it is in when interacting with SMXL7.

I eliminated all glycine, proline, and alanine residues from testing from this list. Prolines and glycines are structurally crucial for proteins, and therefore, mutating highly conserved prolines or glycines could potentially disrupt proper protein formation if mutated(Krieger et al., 2005). Conversely, mutating these residues does not always affect protein stability, as demonstrated by the *d14seto* mutant, caused by the P169L mutation, and the G158E mutation(Chevalier et al., 2014; Q. Li et al., 2022; R. Yao et al., 2016). Both residue mutations maintain enzymatic function, indicating proper protein formation, but have impaired signaling function. These three types of residues may assist in SMXL interaction. They, therefore, could be tested in the future with the caveat that such mutations could compromise the structural integrity of the protein. Lastly, there are some residues in the MAX2 binding interface with a sasa score greater than 20 that I eliminated from the list as they are unlikely to be involved in both interactions. These filtering processes led to a list of 67 residues (Table 2.1). However, I eliminated one residue, D167, as I tested this in chapter one (Figure 1.5B). Previously reported residues critical for SMXL interaction, R183 and R262, were included, as neither were substituted with alanine(A. Hu et al., 2021; Seto et al., 2019).

Evaluation of D14 variants to target SMXL7 for degradation:

In a collaborative effort, the students in the Dynamic Genome course individually mutated 40 of the residues of interest by designing mutagenic primers and using the New

England Biolabs Q5 site-directed mutagenesis kit. The students also sequenced and cloned the mutated entry clones into *E. coli* for further usage. My undergraduate student Xitlalli Zavala and I created the remaining 20 residues using the same process.

To evaluate how these mutations affect D14-SMXL7 interaction, I tested their ability to change SMXL7 stability and degradation. To observe SMXL7 degradation in response to each D14 variant, I employed the same ratiometric system described in Chapter One, where the ratiometric SMXL7 reporter is transiently co-transformed with D14 expressed in the *Nbd14a,b* mutant background with leaf discs are treated with a 0.02% (v/v) acetone control or a synthetic SL, 10 µM *rac*-GR24, overnight and the fluorescent signal is detected the following day(Khosla, Rodriguez-Furlan, et al., 2020; White et al., 2022). I then categorized SMXL7 responses for each variant by changes in the SMXL7 reporter accumulation and degradation compared to when the reporter is co-transformed with wild-type AtD14. Surprisingly, more than half, 46, of the residue changes made no apparent change in SMXL7 reporter accumulation or degradation compared to leaves co-transformed with wild-type D14 (Figure 2.2). I re-evaluated the 20 variants with responses different from the D14 wild-type. (Figure 2.3).

Interestingly, among these was $D14^{R183A}$, which unlike its counterpart, $D14^{R183H}$, had no obvious change in the SMXL7 reporter compared to leaves co-transformed with D14 wild-type (Seto et al., 2019) (Figure 2.2R). Alanine has a small nonpolar side chain, a single methyl group, where histidine is a positively charged residue with a bulkier imidazole side chain. This sidechain may create steric hindrance with the residue on SMXL7 with which the arginine interacts. The $D14^{R183H}$ variant showed apparent degradation of the reporter, however when co-transformed together, this variant consistently displayed overaccumulation of the SMXL7 reporter in the acetone control

compared to leaves co-transformed with D14 wild-type (Figure 2.2G, P, R, Figure 2.3A). This disagrees with previous evidence that suggests the R183H mutation abolishes SMXL7 interaction (Seto et al., 2019). SMXL7 reporter overaccumulation is also obvious in the catalytic mutant, $D14^{S97A}$, which does not exhibit degradation. Therefore, it is used as a negative control in each experiment.

Another example of SMXL7 reporter overaccumulation is when the reporter is co-expressed with the $D14^{R262A}$ variant; a previous study showed that when mutated to proline, this variant can no longer interact with SMXL7 (A. Hu et al., 2021). Similar to the R183H mutation, this variant still displays apparent SMXL7 reporter degradation when co-expressed (Figure 2.2A, Figure 2.3A). Three other variants initially showed a similar SMXL7 reporter overaccumulation phenotype when co-expressed together; however, when tested again, $D14^{L7A}$, $D14^{T71A}$, and $D14^{V202A}$ did not display this SMXL7 reporter overaccumulation when co-expressed together (Figure 2.2B, G, F, Figure 2.3A). The co-expression of $D14^{L7A}$ with the SMXL7 reporter demonstrated a slight increase in the SMXL7 reporter in the acetone control compared to the D14 wild-type but was not significantly different (Figure 2.3A). It is conceivable that endogenous SLs in the *N. benthamiana* leaves induce background degradation of the reporter before treatments. I conducted these experiments separately so slightly different phenotypes might appear, possibly due to the age of the *N. benthamiana* plants or the growth of the *Agrobacterium* cells. D14 variants that have a weaker interaction with SMXL7, such as $D14^{R183H}$, may hinder MAX2 from polyubiquitinating SMXL7 or have impaired flexibility moving from the open to closed state that might cause the SMXL7 reporter to accumulate more. Another possibility is that these variants require a higher concentration of a ligand or more time for activation and subsequent degradation. As the D14 variants and SMXL7 reporter are over-

expressed, it is plausible that these proteins have weak interactions but can degrade enough SMXL7 to observe a noticeable change in the mScarlet to Venus ratio. MAX2 is the limiting factor in this system as it is the only component not overexpressed; therefore, an ample amount of "weak" D14 may still facilitate recruiting SCF^{MAX2} to the SMXL7 reporter. I argue this is also true in the case of variants that exhibit reduced SMXL7 degradation after SL treatment but do not completely abolish SL-induced degradation of the SMXL7 reporter.

Conversely, the coexpression of some variants, for example, $D14^{L127A}$, leads to under-accumulation of the SMXL7 reporter (Figure 2.2, Figure 2.3C). Under-accumulation could be due to mutations that increase the signaling dynamics of D14, for example, making the protein more flexible between the open and closed states. This increased flexibility could make D14 variants more active toward the endogenous SLs, increasing the amount of degradation before overnight treatments. Furthermore, if the constitutive degradation of the SMXL7 reporter occurs before treatments, it could mislead the *rac*-GR24 results when the signal is read post-treatment. These reasons could be the case for the $D14^{L127A}$, $D14^{Y152A}$, and $D14^{F159A}$ variants, as they all have decreased Mscarlet-I-to-Venus ratios in the acetone treated leaf discs compared to leaves co-transformed with D14 wild-type (Figure 2.2G, L, P, Q, Figure 2.3C). Depending on the experiment, leaves co-transformed with these variants slightly reduce or abolish the SL-induced degradation of the reporter mScarlet-to-Venus ratio in the *rac*-GR24 treatment compared to the acetone treatment. F159 is neighboring the D14-MAX2 interface, so this residue may help facilitate that interaction, and mutating it to an alanine could create a weaker interaction with MAX2 (R. Yao et al., 2016).

As discussed earlier, some variants, when co-expressed with the reporter, some variants caused either an increase or decrease in SMXL7 degradation relative to D14 wild-type induced degradation. Variants $D14^{V15A}$ and $D14^{V168A}$ have consistently demonstrated an increase in the SMXL7 reporter degradation, indicating that these mutations could have a stronger interaction with SMXL7 or make it more available for SCF^{MAX2} to polyubiquitinate the protein (Figure 2.2G, S, Figure 2.3C). Some variants, such as $D14^{N128A}$ and $D14^{R192A}$, present a reduction in the SMXL7 reporter degradation under the *rac*-GR24 treatment (Figure 2.2P, Q, Figure 2.3B). These mutations suggest a weaker interaction with SMXL7, making it hard to target for degradation. One variant, $D14^{D198A}$, consistently showed a significant reduction or complete abolishment of SMXL7 reporter degradation, which implied that this residue is critical for D14-SMXL interaction (Figure 2.2O, U, Figure 2.3C).

It was shocking that so many residue switches did not appear to affect D14-induced SMXL7 for degradation. Protein-protein interactions often have many chemical requirements to facilitate a strong interaction. Such requirements can be through a hydrophobic surface on one protein interacting with a hydrophobic surface on the partner protein. Of the 67 residues mutated, 28 fall within the hydrophobic class of amino acids, while many of these have large side chains; switching to an alanine residue could maintain the hydrophobicity in that region and not impair SMXL7 binding. For example, residues I105, I108, V202, and L205 form a hydrophobic patch on the surface of D14. Only leaves co-transformed with $D14^{V202A}$ exhibited an interesting SMXL7 reporter response of over-accumulation during the initial degradation assay; however, subsequent testing of $D14^{V202A}$ in the SMXL7 degradation assay revealed a D14 wild-type-like response (Figure 2.2F, Figure 2.3A). Although several of these residues did not evoke a significant

response, substituting them with a hydrophilic residue such as serine could result in a more pronounced impairment of SMXL7 reporter degradation. Using a similar argument, replacing positively or negatively charged residues with negatively and positively charged residues, respectively, could dramatically hinder the D14-SMXL7 interaction.

Because SMXL7 is a large protein (112kD), and D14 is small by comparison (30kD), it is conceivable that there are many regions on D14 that SMXL7 interacts with. Therefore, mutating one of these regions does not fully impair the necessary interaction, leading to SMXL7 degradation. Combining these mutations could lead to a more in-depth understanding of the SMXL7 interaction regions on D14.

Although transient assays in *N. benthamiana* provided valuable insights, it was unclear if these mutations could rescue the highly branched phenotype of *Atd14*. Therefore, I stably transformed variants that altered the SMXL7 reporter accumulation and variants that had an increased or decreased SMXL7 reporter degradation compared to the D14 wild-type from the initial degradation assay into the *Atd14* mutant background under the control of the constitutive 35S promoter. As the selectable marker for these lines is a mCitrine expressed in the seed coat, there was no need for selection on antibiotic or herbicide-containing media. This allowed me to assess the ability of hemizygous D14 variant transgenes to reverse the *d14* mutant phenotype in the T1 generation. Surprisingly, most variants reversed the bushy phenotype (see Figure 2.4). It is conceivable that the phenotypes observed in homozygous single insertion T3 lines will be more evident in rescuing the branching phenotype or displaying a more robust branching phenotype than in the T1 generation experiments. Rosette branches of the T1 plants were measured on the same day rather than 28 days after anthesis, which was performed in the T3 branching assay. Therefore, the T1 plants were not necessarily at equivalent developmental stages

when branching was counted. This may result in increased phenotypic variation in this experiment.

In line with the degradation assay, it is probable that many of these D14 variants have weakened interactions with SMXL proteins. However, overexpressing them may still allow for proper signaling function to be maintained. Utilizing the *D14* native promoter to drive the expression of these variants may provide more accurate evidence of a weak interaction.

If D14 mutants have a dominant-negative effect on signaling, as could be true for D14 variants causing the SMXL7 reporter to over accumulate, this effect may not be evident in the *Atd14* mutant background. Dominant-negative variants would be more apparent if tested in wild type (*Col-0*). If a mutation caused D14 to interact with SMXLs without SL, it could sequester SMXLs from MAX2-targeted degradation. Sequestering SMXLs or preventing MAX2-dependent degradation of SMXLs could block native D14 function, resulting in increased SMXL abundance and a highly branched phenotype

I assayed homozygous transgenic lines for several D14 variants in the T3 generation: $D14^{N128A}$, $D14^{Y152A}$, $D14^{R183H}$, and $D14^{D198A}$, along with the wild-type and $D14^{S97A}$ controls. In this assay, monitoring anthesis allowed the developmental stage of each plant to be equal when branches and height were measured to produce more consistent data. $D14^{N128A}$ and $D14^{Y152A}$ fully rescued the height and branching phenotype in this assay. Similar to what is reported in the literature, R183H could not fully rescue the branching and height phenotype. However, both phenotypes were less severe than the S97A variant (Figure 2.5) (Seto et al., 2019). The discrepancies between the data from (Seto et al., 2019) and mine may be due to differences in experimental conditions as they counted branches earlier and under hydroponic conditions.

The D14^{D198A} variant displayed similar phenotypes to those of the *Atd14* mutant background and the D14^{S97A} variant, agreeing with data from the degradation assay (Figure 2.5). D198 shows high conservation in D14 and KAI2 proteins, which implies a critical role (Table S2.1). While my evidence suggests it is vital for SMXL interaction, it is unclear if altering this residue alters protein folding, rendering it non-functional, is required for MAX2-mediated degradation, or affects ligand interaction.

To determine whether the reduced activity of D14 variants on SL-induced degradation of SMXL7 might be due to instability or degradation of D14, I used the ratiometric system to express 11 of the D14 variants, including D14 wild-type and D14^{S97A}. If a mutation affects protein stability, the mScarlet-I reporter will have a much lower signal than the Venus reference. If the mutation affects MAX2-mediated degradation, the reporter will be stabilized under SL treatment or have altered degradation compared to the D14 wild-type reporter.

D14 wild-type and D14^{S97A} reporters had high expression when transformed into the *N. benthamiana* leaves; however, degradation under the SL treatment was not evident for the D14 wild-type reporter (Figure 2.6A). The reporter stability could be due to limited amounts of MAX2 in the *N. benthamiana* leaves. To address this, I co-transformed the leaves with the D14 reporters and a vector containing the MAX2 gene from the hemiparasitic plant *Phtheirospermum japonicum,* driven by the 35S promoter. The results demonstrated a 4x reduction in the D14 wild-type reporter under SL treatment and stability of the D14^{S97A} reporter under both the control and SL treatments (Figure 2.6B). Moving forward, the variants tested in this assay were co-transformed with the MAX2-containing agrobacteria.

The D14^{D198A} reporter had a highly reduced mScarlet-I to Venus signal compared to the D14 wild-type and D14^{S97A} reporters, and did not exhibit a further reduction post-SL treatment (Figure 2.6C). The D14^{D198A} response suggests that this mutation reduces the stability of the protein and is likely the cause of the inability to target SMXL7 for degradation and rescue the *Atd14* mutant phenotype.

Intriguingly, other variants reduced the D14 reporter signal and degradation compared to the D14 wild-type reporter, which displayed a rescuing phenotype in the Arabidopsis assays. For example, D14^{Y132A} and D14^{Y152A} displayed a lowered mScarlet-I signal in the control treatment and a slight response to the SL treatment. It is unclear whether these results are due to increased reporter degradation or the mutation causes protein instability.

I used DynaMut to gain insight into the structural effects of these mutations on D14. DynaMut is a web-based program that visualizes protein dynamics and predicts mutational effects on protein dynamics and stability (Rodrigues et al., 2018). Inputting D14^{Y132A}, D14^{Y152A}, and D14^{D198A} into the program for both the apo/open and active/closed confirmations provided evidence that these mutations alter the flexibility and overall stability of D14 by calculating the ΔΔ G of each mutation (Rodrigues et al., 2018; R. Yao et al., 2016; Zhao et al., 2013) (Figure 2.7). ΔΔ G values are based on changes in folding free energy between the D14 structure and the mutated structure, where a negative value indicates a destabilizing effect and a positive value indicates a stabilizing effect (Rodrigues et al., 2018). The D14^{Y132A} and D14^{Y152A} predictions suggest these mutations increase the flexibility and are destabilizing in both conformations of D14 (Figure 2.7 A-B). It is plausible that these mutations cause D14 to fluctuate between the open and closed conformations more easily. In that case, it is conceivable that they could interact with SMXLs without SL,

explaining why both of these mutations demonstrate under-accumulation of the SMXL7 reporter (Figure 2.3C).

The D198A mutation, as per the DynaMut predictions, presents intriguing results. The open conformation exhibits a stabilizing effect on the overall structure of $D14^{D198A}$. However, this mutation also significantly increases the relative flexibility of the loop where the residue is located and the adjacent loop, as denoted by the red coloring (Figure 2.7C). In contrast, in the closed state, the D198A mutation shows an overall destabilizing effect, yet it reduces the relative flexibility around the residue, as indicated by the blue coloring (Figure 2.7C). These findings raise the possibility that the D198A mutation could have a profound impact on protein stability, potentially leading to rapid protein degradation, which warrants further investigation.

Conclusion:

This chapter aimed to determine the SMXL interacting regions of D14. I identified 67 highly conserved and surface-exposed D14 amino acid residues and individually mutated each residue into alanine residues to assess how each residue influences SMXL interaction. I then tested each D14 variant in a transient SMXL7 degradation assay. The results indicated that many residues affected the SMXL7 reporter response with or without SL treatment. However, most variants rescued the branching phenotype when overexpressed in *Atd14*.

One variant, $D14^{D198A}$, displayed a severe reduction in SMXL7 reporter degradation and did not rescue the mutant phenotype in *Atd14*. To better understand how D198A and other mutations affected protein stability and post-signaling degradation, I tested them in the transient degradation system as the target protein. All variants in the

transient assay, except $D14^{S97A}$ and $D14^{D198A}$, displayed SL-induced degradation. Low reporter expression in the acetone control was observed in leaves expressing $D14^{N128A}$, $D14^{Y132A}$, $D14^{Y152A}$, $D14^{R183H}$, $D14^{D198A}$, and $D14^{V221A}$. A molecular modeling program, Dynamut, predicts the mutations Y132A, Y152A, and D198A to have destabilizing effects and changes in protein flexibility between the open and closed conformations.

The data gathered presents more questions than answers. Interestingly, most of these single-point mutations seem to have no effect on D14-induced SMXL7 degradation. While it is possible that some mutations do impact D14, they might be too subtle to be detected in the assays conducted in this chapter. This leads me to hypothesize that the lack of a strong phenotype from the variants could be due to the fact that SMXLs interact through multiple residues and/or regions on D14. This could have significant implications for our understanding of D14-SMXL interactions if confirmed.

Given the recent advancements in protein modeling with AlphaFold, we have a unique opportunity to delve deeper into protein-protein interactions. AlphaFold could be especially useful here, where understanding the D14-SMXL7 interaction is challenging. I propose modeling this interaction in AlphaFold, identifying potential interaction regions of D14, and testing them by mutating a single residue in each predicted region.

Suppose we assume that the degradation assay results are accurate and that the absence of a branching phenotype in Arabidopsis is simply due to overexpression. In that case, many of the "interesting" variants, those that affected SMXL7 reporter stability and degradation, are located on the lid domain of D14. The lid domain consists of roughly residues 125-200 and is the region that undergoes the most significant conformational change between the open and closed states(R. Yao et al., 2016; Zhao et al., 2013). The lid region is next to the MAX2 binding interface. If SMXLS requires this conformation for

interaction, I hypothesize that the lid domain is crucial for such interaction. Residues located on the lid domain might even provide specificity for SMXL proteins, as many residues in this region are highly conserved among KAI2 proteins but have different residues. I propose residue swaps on KAI2 in this region with the respective residues found on D14 and test if KAI2 can switch protein partners, SMAX1 for SMXL7. Understanding the crucial role of the lid domain and specific residues in the interaction between receptor protein partners could provide valuable insights into the underlying mechanisms of the SL and KAR signaling pathways.

References:

Akiyama, K., & Hayashi, H. (2006). Strigolactones: chemical signals for fungal symbionts and parasitic weeds in plant roots. Annals of Botany, 97(6), 925–931.

Akiyama, K., Matsuzaki, K.-I., & Hayashi, H. (2005). Plant sesquiterpenes induce hyphal branching in arbuscular mycorrhizal fungi. Nature, 435(7043), 824–827.

Angulo, J., Astin, C. P., Bauer, O., Blash, K. J., Bowen, N. M., Chukwudinma, N. J., Dinofrio, A. S., Faletti, D. O., Ghulam, A. M., Gusinde-Duffy, C. M., Horace, K. J., Ingram, A. M., Isaack, K. E., Jeong, G., Kiser, R. J., Kobylanski, J. S., Long, M. R., Manning, G. A., Morales, J. M., … Lukowitz, W. (2020). Targeted mutagenesis of the Arabidopsis GROWTH-REGULATING FACTOR (GRF) gene family suggests competition of multiplexed sgRNAs for Cas9 apoprotein. In bioRxiv (p. 2020.08.16.253203). https://doi.org/10.1101/2020.08.16.253203

Blázquez, M. A., Nelson, D. C., & Weijers, D. (2020). Evolution of Plant Hormone Response Pathways. Annual Review of Plant Biology, 71, 327–353.

Bürger, M., & Chory, J. (2020). The Many Models of Strigolactone Signaling. Trends in Plant Science, 25(4), 395–405.

Bythell-Douglas, R., Rothfels, C. J., Stevenson, D. W. D., Graham, S. W., Wong, G. K.-S., Nelson, D. C., & Bennett, T. (2017). Evolution of strigolactone receptors by gradual neo-functionalization of KAI2 paralogues. BMC Biology, 15(1), 52.

Carlsson, G. H., Hasse, D., Cardinale, F., Prandi, C., & Andersson, I. (2018). The elusive ligand complexes of the DWARF14 strigolactone receptor. Journal of Experimental Botany, 69(9), 2345–2354.

Chevalier, F., Nieminen, K., Sánchez-Ferrero, J. C., Rodríguez, M. L., Chagoyen, M., Hardtke, C. S., & Cubas, P. (2014). Strigolactone promotes degradation of DWARF14, an α/β hydrolase essential for strigolactone signaling in Arabidopsis. The Plant Cell, 26(3), 1134–1150.

Chiwocha, S. D. S., Dixon, K. W., Flematti, G. R., Ghisalberti, E. L., Merritt, D. J., Nelson, D. C., Riseborough, J.-A. M., Smith, S. M., & Stevens, J. C. (2009). Karrikins: A new family of plant growth regulators in smoke. Plant Science: An International Journal of Experimental Plant Biology, 177(4), 252–256.

Choi, J., Lee, T., Cho, J., Servante, E. K., Pucker, B., Summers, W., Bowden, S., Rahimi, M., An, K., An, G., Bouwmeester, H. J., Wallington, E. J., Oldroyd, G., & Paszkowski, U. (2020). The negative regulator SMAX1 controls mycorrhizal symbiosis and strigolactone biosynthesis in rice. Nature Communications, 11(1), 2114.

Clough, S. J., & Bent, A. F. (1998). Floral dip: a simplified method for Agrobacterium-mediated transformation of Arabidopsis thaliana. The Plant Journal: For Cell and Molecular Biology, 16(6), 735–743.

Conn, C. E., Bythell-Douglas, R., Neumann, D., Yoshida, S., Whittington, B., Westwood, J. H., Shirasu, K., Bond, C. S., Dyer, K. A., & Nelson, D. C. (2015). PLANT EVOLUTION. Convergent evolution of strigolactone perception enabled host detection in parasitic plants. Science, 349(6247), 540–543.

Cook, C. E., Whichard, L. P., Turner, B., Wall, M. E., & Egley, G. H. (1966). Germination of Witchweed (Striga lutea Lour.): Isolation and Properties of a Potent Stimulant. Science, 154(3753), 1189–1190.

de Saint Germain, A., Clavé, G., Badet-Denisot, M.-A., Pillot, J.-P., Cornu, D., Le Caer, J.-P., Burger, M., Pelissier, F., Retailleau, P., Turnbull, C., Bonhomme, S., Chory, J., Rameau, C., & Boyer, F.-D. (2016). An histidine covalent receptor and butenolide complex mediates strigolactone perception. Nature Chemical Biology, 12(10), 787–794.
Drummond, R. S. M., Lee, H. W., Luo, Z., Dakin, J. F., Janssen, B. J., & Snowden, K. C. (2023). Varying the expression pattern of the strigolactone receptor gene DAD2 results in phenotypes distinct from both wild type and knockout mutants. Frontiers in Plant Science, 14, 1277617.

Goddard, T. D., Huang, C. C., Meng, E. C., Pettersen, E. F., Couch, G. S., Morris, J. H., & Ferrin, T. E. (2018). UCSF ChimeraX: Meeting modern challenges in visualization and analysis. Protein Science: A Publication of the Protein Society, 27(1), 14–25.

Gomez-Roldan, V., Fermas, S., Brewer, P. B., Puech-Pagès, V., Dun, E. A., Pillot, J.-P., Letisse, F., Matusova, R., Danoun, S., Portais, J.-C., Bouwmeester, H., Bécard, G., Beveridge, C. A., Rameau, C., & Rochange, S. F. (2008). Strigolactone inhibition of shoot branching. Nature, 455(7210), 189–194.

Hamiaux, C., Drummond, R. S. M., Janssen, B. J., Ledger, S. E., Cooney, J. M., Newcomb, R. D., & Snowden, K. C. (2012). DAD2 is an α/β hydrolase likely to be involved in the perception of the plant branching hormone, strigolactone. Current Biology: CB, 22(21), 2032–2036.

Hu, A., Zhao, Q., Chen, L., Zhao, J., Wang, Y., Feng, K., Wu, L., Xie, M., Zhou, X., Xiao, L., Ming, Z., Zhang, M., & Yao, R. (2021). Identification of Conserved and Divergent Strigolactone Receptors in Sugarcane Reveals a Key Residue Crucial for Plant Branching Control. Frontiers in Plant Science, 12, 2489.

Hu, Q., He, Y., Wang, L., Liu, S., Meng, X., Liu, G., Jing, Y., Chen, M., Song, X., Jiang, L., Yu, H., Wang, B., & Li, J. (2017). DWARF14, A Receptor Covalently Linked with the Active Form of Strigolactones, Undergoes Strigolactone-Dependent Degradation in Rice. Frontiers in Plant Science, 8, 1935.

Jiang, L., Liu, X., Xiong, G., Liu, H., Chen, F., Wang, L., Meng, X., Liu, G., Yu, H., Yuan, Y., Yi, W., Zhao, L., Ma, H., He, Y., Wu, Z., Melcher, K., Qian, Q., Xu, H. E., Wang, Y., & Li, J. (2013). DWARF 53 acts as a repressor of strigolactone signalling in rice. Nature, 504(7480), 401–405.

Kerr, S. C., Patil, S. B., de Saint Germain, A., Pillot, J.-P., Saffar, J., Ligerot, Y., Aubert, G., Citerne, S., Bellec, Y., Dun, E. A., Beveridge, C. A., & Rameau, C. (2021). Integration of the SMXL/D53 strigolactone signalling repressors in the model of shoot branching regulation in Pisum sativum. The Plant Journal: For Cell and Molecular Biology, 107(6), 1756–1770.

Khosla, A., Morffy, N., Li, Q., Faure, L., Chang, S. H., Yao, J., Zheng, J., Cai, M. L., Stanga, J., Flematti, G. R., Waters, M. T., & Nelson, D. C. (2020). Structure–Function Analysis of SMAX1 Reveals Domains That Mediate Its Karrikin-Induced Proteolysis and Interaction with the Receptor KAI2. The Plant Cell, 32(8), 2639–2659.

Khosla, A., & Nelson, D. C. (2020). Ratiometric Measurement of Protein Abundance after Transient Expression of a Transgene in Nicotiana benthamiana. Bio-Protocol, 10(17), e3747.

Khosla, A., Rodriguez-Furlan, C., Kapoor, S., Van Norman, J. M., & Nelson, D. C. (2020). A series of dual-reporter vectors for ratiometric analysis of protein abundance in plants. Plant Direct, 4(6), e00231.

Kodama, K., Xie, X., & Kyozuka, J. (2023). The D14 and KAI2 Orthologs of Gymnosperms Sense Strigolactones and KL Mimics, Respectively, and the Signals Are Transduced to Control Downstream Genes. Plant & Cell Physiology. https://doi.org/10.1093/pcp/pcad072

Krieger, F., Möglich, A., & Kiefhaber, T. (2005). Effect of proline and glycine residues on dynamics and barriers of loop formation in polypeptide chains. Journal of the American Chemical Society, 127(10), 3346–3352.

Lee, H. W., Sharma, P., Janssen, B. J., Drummond, R. S. M., Luo, Z., Hamiaux, C., Collier, T., Allison, J. R., Newcomb, R. D., & Snowden, K. C. (2020). Flexibility of the petunia strigolactone receptor DAD2 promotes its interaction with signaling partners. The Journal of Biological Chemistry, 295(13), 4181–4193.
Liang, Y., Ward, S., Li, P., Bennett, T., & Leyser, O. (2016). SMAX1-LIKE7 Signals from the Nucleus to Regulate Shoot Development in Arabidopsis via Partially EAR Motif-Independent Mechanisms. The Plant Cell, 28(7), 1581–1601.

Li, Q., Martín-Fontecha, E. S., Khosla, A., White, A. R. F., Chang, S., Cubas, P., & Nelson, D. C. (2022). The strigolactone receptor D14 targets SMAX1 for degradation in response to GR24 treatment and osmotic stress. Plant Communications, 3(2), 100303.

Li, Q., Yu, H., Chang, W., Chang, S., Guzmán, M., Faure, L., Wallner, E.-S., Yan, H., Greb, T., Wang, L., Yao, R., & Nelson, D. C. (2024). SMXL5 attenuates strigolactone signaling in Arabidopsis thaliana by inhibiting SMXL7 degradation. Molecular Plant, 17(4), 631–647.

Liu, X., & Hou, X. (2018). Antagonistic Regulation of ABA and GA in Metabolism and Signaling Pathways. Frontiers in Plant Science, 9, 251.

Li, W., Nguyen, K. H., Chu, H. D., Van Ha, C., Watanabe, Y., Osakabe, Y., Leyva-González, M. A., Sato, M., Toyooka, K., Voges, L., Tanaka, M., Mostofa, M. G., Seki, M., Seo, M., Yamaguchi,

S., Nelson, D. C., Tian, C., Herrera-Estrella, L., & Tran, L.-S. P. (2017). The karrikin receptor KAI2 promotes drought resistance in Arabidopsis thaliana. PLoS Genetics, 13(11), e1007076.

Machin, D. C., Hamon-Josse, M., & Bennett, T. (2020). Fellowship of the rings: a saga of strigolactones and other small signals. The New Phytologist, 225(2), 621–636.

Ma, H., Duan, J., Ke, J., He, Y., Gu, X., Xu, T.-H., Yu, H., Wang, Y., Brunzelle, J. S., Jiang, Y., Rothbart, S. B., Xu, H. E., Li, J., & Melcher, K. (2017). A D53 repression motif induces oligomerization of TOPLESS corepressors and promotes assembly of a corepressor-nucleosome complex. Science Advances, 3(6), e1601217.

Martín-Fontecha, E. S., Cardinale, F., Bürger, M., Prandi, C., & Cubas, P. (2024). Novel Mechanisms of Strigolactone-Induced DWARF14 Degradation in Arabidopsis thaliana. In bioRxiv (p. 2024.01.10.574527). https://doi.org/10.1101/2024.01.10.574527

Merritt, D. J., Dixon, K. W., Flematti, G. R., & Ghisalberti, E. L. (2009). Karrikinolide - A phytoreactive compound derived from smoke with applications in horticulture, ecological restoration and agriculture. Acta Horticulturae, 813, 155–170.

Mizuno, Y., Komatsu, A., Shimazaki, S., Naramoto, S., Inoue, K., Xie, X., Ishizaki, K., Kohchi, T., & Kyozuka, J. (2021). Major components of the KARRIKIN INSENSITIVE2-dependent signaling pathway are conserved in the liverwort Marchantia polymorpha. The Plant Cell, 33(7), 2395–2411.

Moturu, T. R., Thula, S., Singh, R. K., Nodzyński, T., Vařeková, R. S., Friml, J., & Simon, S. (2018). Molecular evolution and diversification of the SMXL gene family. Journal of Experimental Botany, 69(9), 2367–2378.

Nakagawa, T., Kurose, T., Hino, T., Tanaka, K., Kawamukai, M., Niwa, Y., Toyooka, K., Matsuoka, K., Jinbo, T., & Kimura, T. (2007). Development of series of gateway binary vectors, pGWBs, for realizing efficient construction of fusion genes for plant transformation. Journal of Bioscience and Bioengineering, 104(1), 34–41.

Nakamura, H., Xue, Y.-L., Miyakawa, T., Hou, F., Qin, H.-M., Fukui, K., Shi, X., Ito, E., Ito, S., Park, S.-H., Miyauchi, Y., Asano, A., Totsuka, N., Ueda, T., Tanokura, M., & Asami, T. (2013). Molecular mechanism of strigolactone perception by DWARF14. Nature Communications, 4, 2613.

Nelson, D. C., Flematti, G. R., Ghisalberti, E. L., Dixon, K. W., & Smith, S. M. (2012). Regulation of seed germination and seedling growth by chemical signals from burning vegetation. Annual Review of Plant Biology, 63, 107–130.
Nelson, D. C., Flematti, G. R., Riseborough, J.-A., Ghisalberti, E. L., Dixon, K. W., & Smith, S. M. (2010). Karrikins enhance light responses during germination and seedling development in Arabidopsis thaliana. Proceedings of the National Academy of Sciences of the United States of America, 107(15), 7095–7100.

Nelson, D. C., Scaffidi, A., Dun, E. A., Waters, M. T., Flematti, G. R., Dixon, K. W., Beveridge, C. A., Ghisalberti, E. L., & Smith, S. M. (2011). F-box protein MAX2 has dual roles in karrikin and strigolactone signaling in Arabidopsis thaliana. Proceedings of the National Academy of Sciences of the United States of America, 108(21), 8897–8902.

Pettersen, E. F., Goddard, T. D., Huang, C. C., Meng, E. C., Couch, G. S., Croll, T. I., Morris, J. H., & Ferrin, T. E. (2021). UCSF ChimeraX: Structure visualization for researchers, educators, and developers. Protein Science: A Publication of the Protein Society, 30(1), 70–82.

Plant, A. R., Larrieu, A., & Causier, B. (2021). Repressor for hire! The vital roles of TOPLESS-mediated transcriptional repression in plants. The New Phytologist, 231(3), 963–973.

Rodrigues, C. H., Pires, D. E., & Ascher, D. B. (2018). DynaMut: predicting the impact of mutations on protein conformation, flexibility and stability. Nucleic Acids Research, 46(W1), W350–W355.

Scaffidi, A., Waters, M. T., Bond, C. S., Dixon, K. W., Smith, S. M., Ghisalberti, E. L., & Flematti, G. R. (2012). Exploring the molecular mechanism of karrikins and strigolactones. Bioorganic & Medicinal Chemistry Letters, 22(11), 3743–3746.

Scaffidi, A., Waters, M. T., Sun, Y. K., Skelton, B. W., Dixon, K. W., Ghisalberti, E. L., Flematti, G. R., & Smith, S. M. (2014). Strigolactone Hormones and Their Stereoisomers Signal through Two Related Receptor Proteins to Induce Different Physiological Responses in Arabidopsis. Plant Physiology, 165(3), 1221–1232.

Seto, Y., Yasui, R., Kameoka, H., Tamiru, M., Cao, M., Terauchi, R., Sakurada, A., Hirano, R., Kisugi, T., Hanada, A., Umehara, M., Seo, E., Akiyama, K., Burke, J., Takeda-Kamiya, N., Li, W., Hirano, Y., Hakoshima, T., Mashiguchi, K., … Yamaguchi, S. (2019). Strigolactone perception and deactivation by a hydrolase receptor DWARF14. Nature Communications, 10(1), 191.

Shabek, N., Ticchiarelli, F., Mao, H., Hinds, T. R., Leyser, O., & Zheng, N. (2018). Structural plasticity of D3-D14 ubiquitin ligase in strigolactone signalling. Nature, 563(7733), 652–656.

Soundappan, I., Bennett, T., Morffy, N., Liang, Y., Stanga, J. P., Abbas, A., Leyser, O., & Nelson, D. C. (2015). SMAX1-LIKE/D53 Family Members Enable Distinct MAX2-Dependent Responses to Strigolactones and Karrikins in Arabidopsis. The Plant Cell, 27(11), 3143–3159.

Stanga, J. P., Morffy, N., & Nelson, D. C. (2016). Functional redundancy in the control of seedling growth by the karrikin signaling pathway. Planta, 243(6), 1397–1406.

Stirling, S. A., Guercio, A. M., Patrick, R. M., Huang, X.-Q., Bergman, M. E., Dwivedi, V., Kortbeek, R. W. J., Liu, Y.-K., Sun, F., Tao, W. A., Li, Y., Boachon, B., Shabek, N., & Dudareva, N. (2024). Volatile communication in plants relies on a KAI2-mediated signaling pathway. Science, 383(6689), 1318–1325.

Struk, S., Braem, L., Walton, A., De Keyser, A., Boyer, F.-D., Persiau, G., De Jaeger, G., Gevaert, K., & Goormachtig, S. (2018). Quantitative Tandem Affinity Purification, an Effective Tool to Investigate Protein Complex Composition in Plant Hormone Signaling: Strigolactones in the Spotlight. Frontiers in Plant Science, 9, 528.

Tal, L., Palayam, M., Ron, M., Young, A., Britt, A., & Shabek, N. (2022). A conformational switch in the SCF-D3/MAX2 ubiquitin ligase facilitates strigolactone signalling. Nature Plants, 8(5), 561–573.
Tamura, K., Stecher, G., & Kumar, S. (2021). MEGA11: Molecular Evolutionary Genetics Analysis Version 11. Molecular Biology and Evolution, 38(7), 3022–3027.
Temmerman, A., Guillory, A., Bonhomme, S., Goormachtig, S., & Struk, S. (2022). Masks Start to Drop: Suppressor of MAX2 1-Like Proteins Reveal Their Many Faces. Frontiers in Plant Science, 13, 887232.

Toh, S., Holbrook-Smith, D., Stogios, P. J., Onopriyenko, O., Lumba, S., Tsuchiya, Y., Savchenko, A., & McCourt, P. (2015). Structure-function analysis identifies highly sensitive strigolactone receptors in Striga. Science, 350(6257), 203–207.

Tsuchiya, Y., Yoshimura, M., Sato, Y., Kuwata, K., Toh, S., Holbrook-Smith, D., Zhang, H., McCourt, P., Itami, K., Kinoshita, T., & Hagihara, S. (2015). PARASITIC PLANTS. Probing strigolactone receptors in Striga hermonthica with fluorescence. Science, 349(6250), 864–868.

Umehara, M., Hanada, A., Yoshida, S., Akiyama, K., Arite, T., Takeda-Kamiya, N., Magome, H., Kamiya, Y., Shirasu, K., Yoneyama, K., Kyozuka, J., & Yamaguchi, S. (2008). Inhibition of shoot branching by new terpenoid plant hormones. Nature, 455(7210), 195–200.

Vanstraelen, M., & Benková, E. (2012). Hormonal interactions in the regulation of plant development. Annual Review of Cell and Developmental Biology, 28, 463–487.

Walker, C. H., Siu-Ting, K., Taylor, A., O'Connell, M. J., & Bennett, T. (2019). Strigolactone synthesis is ancestral in land plants, but canonical strigolactone signalling is a flowering plant innovation. BMC Biology, 17(1), 70.

Wang, L., Wang, B., Jiang, L., Liu, X., Li, X., Lu, Z., Meng, X., Wang, Y., Smith, S. M., & Li, J. (2015). Strigolactone Signaling in Arabidopsis Regulates Shoot Development by Targeting D53-Like SMXL Repressor Proteins for Ubiquitination and Degradation. The Plant Cell, 27(11), 3128–3142.

Wang, L., Xu, Q., Yu, H., Ma, H., Li, X., Yang, J., Chu, J., Xie, Q., Wang, Y., Smith, S. M., Li, J., Xiong, G., & Wang, B. (2020). Strigolactone and Karrikin Signaling Pathways Elicit Ubiquitination and Proteolysis of SMXL2 to Regulate Hypocotyl Elongation in Arabidopsis. The Plant Cell, 32(7), 2251–2270.

Waters, M. T., & Nelson, D. C. (2022). Karrikin perception and signalling. The New Phytologist. https://doi.org/10.1111/nph.18598

Waters, M. T., Nelson, D. C., Scaffidi, A., Flematti, G. R., Sun, Y. K., Dixon, K. W., & Smith, S. M. (2012). Specialisation within the DWARF14 protein family confers distinct responses to karrikins and strigolactones in Arabidopsis. Development , 139(7), 1285–1295.

Waters, M. T., Scaffidi, A., Flematti, G., & Smith, S. M. (2015). Substrate-Induced Degradation of the α/β-Fold Hydrolase KARRIKIN INSENSITIVE2 Requires a Functional Catalytic Triad but Is Independent of MAX2. Molecular Plant, 8(5), 814–817.

Waters, M. T., Scaffidi, A., Moulin, S. L. Y., Sun, Y. K., Flematti, G. R., & Smith, S. M. (2015). A Selaginella moellendorffii Ortholog of KARRIKIN INSENSITIVE2 Functions in Arabidopsis Development but Cannot Mediate Responses to Karrikins or Strigolactones. The Plant Cell, 27(7), 1925–1944.

Waters, M. T., Scaffidi, A., Sun, Y. K., Flematti, G. R., & Smith, S. M. (2014). The karrikin response system of Arabidopsis. The Plant Journal: For Cell and Molecular Biology, 79(4), 623–631.

White, A. R. F., Mendez, J. A., Khosla, A., & Nelson, D. C. (2022). Rapid analysis of strigolactone receptor activity in a Nicotiana benthamiana dwarf14 mutant. Plant Direct, 6(3), e389.

Yao, J., Mashiguchi, K., Scaffidi, A., Akatsu, T., Melville, K. T., Morita, R., Morimoto, Y., Smith, S. M., Seto, Y., Flematti, G. R., Yamaguchi, S., & Waters, M. T. (2018). An allelic series at the KARRIKIN INSENSITIVE 2 locus of Arabidopsis thaliana decouples ligand hydrolysis and receptor degradation from downstream signalling. The Plant Journal: For Cell and Molecular Biology, 96(1), 75–89.

Yao, R., Ming, Z., Yan, L., Li, S., Wang, F., Ma, S., Yu, C., Yang, M., Chen, L., Chen, L., Li, Y., Yan, C., Miao, D., Sun, Z., Yan, J., Sun, Y., Wang, L., Chu, J., Fan, S., … Xie, D. (2016). DWARF14 is a non-canonical hormone receptor for strigolactone. Nature, 536(7617), 469–473.

Zhao, L.-H., Zhou, X. E., Wu, Z.-S., Yi, W., Xu, Y., Li, S., Xu, T.-H., Liu, Y., Chen, R.-Z., Kovach, A., Kang, Y., Hou, L., He, Y., Xie, C., Song, W., Zhong, D., Xu, Y., Wang, Y., Li, J., … Xu, H. E. (2013). Crystal structures of two phytohormone signal-transducing α/β hydrolases: karrikin-signaling KAI2 and strigolactone-signaling DWARF14. Cell Research, 23(3), 436–439.

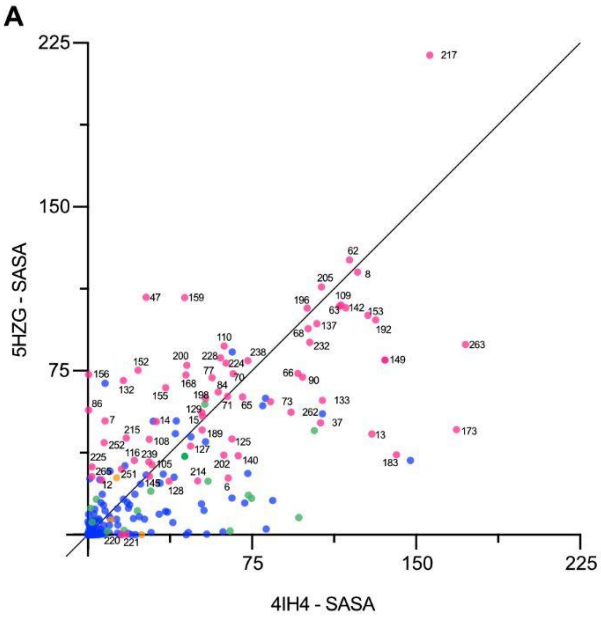
Zhao, L.-H., Zhou, X. E., Yi, W., Wu, Z., Liu, Y., Kang, Y., Hou, L., de Waal, P. W., Li, S., Jiang, Y., Scaffidi, A., Flematti, G. R., Smith, S. M., Lam, V. Q., Griffin, P. R., Wang, Y., Li, J., Melcher, K., & Xu, H. E. (2015). Destabilization of strigolactone receptor DWARF14 by binding of ligand and E3-ligase signaling effector DWARF3. Cell Research, 25(11), 1219–1236.

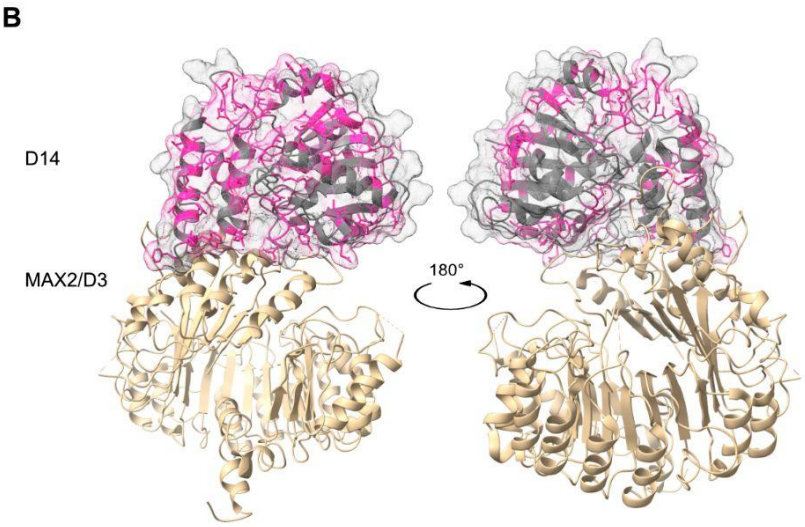
Zheng, X., Yang, X., Chen, Z., Xie, W., Yue, X., Zhu, H., Chen, S., & Sun, X. (2021). Arabidopsis SMAX1 overaccumulation suppresses rosette shoot branching and promotes leaf and petiole elongation. Biochemical and Biophysical Research Communications, 553, 44–50.

Zhou, F., Lin, Q., Zhu, L., Ren, Y., Zhou, K., Shabek, N., Wu, F., Mao, H., Dong, W., Gan, L., Ma, W., Gao, H., Chen, J., Yang, C., Wang, D., Tan, J., Zhang, X., Guo, X., Wang, J., … Wan, J.

(2013). D14-SCF(D3)-dependent degradation of D53 regulates strigolactone signalling. Nature, 504(7480), 406–410

Figures:





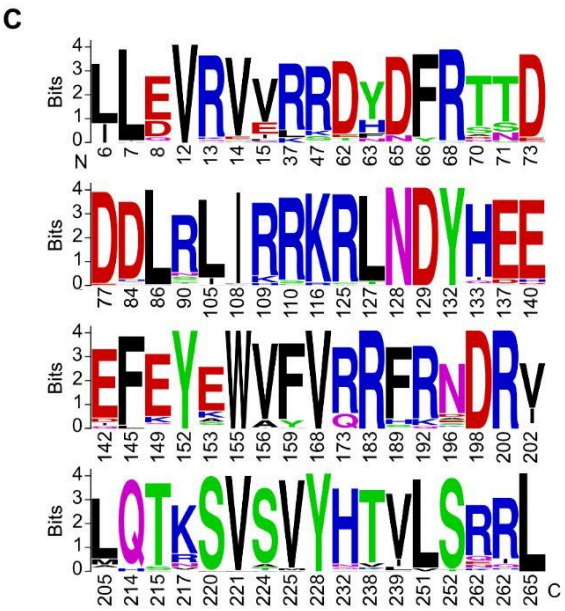
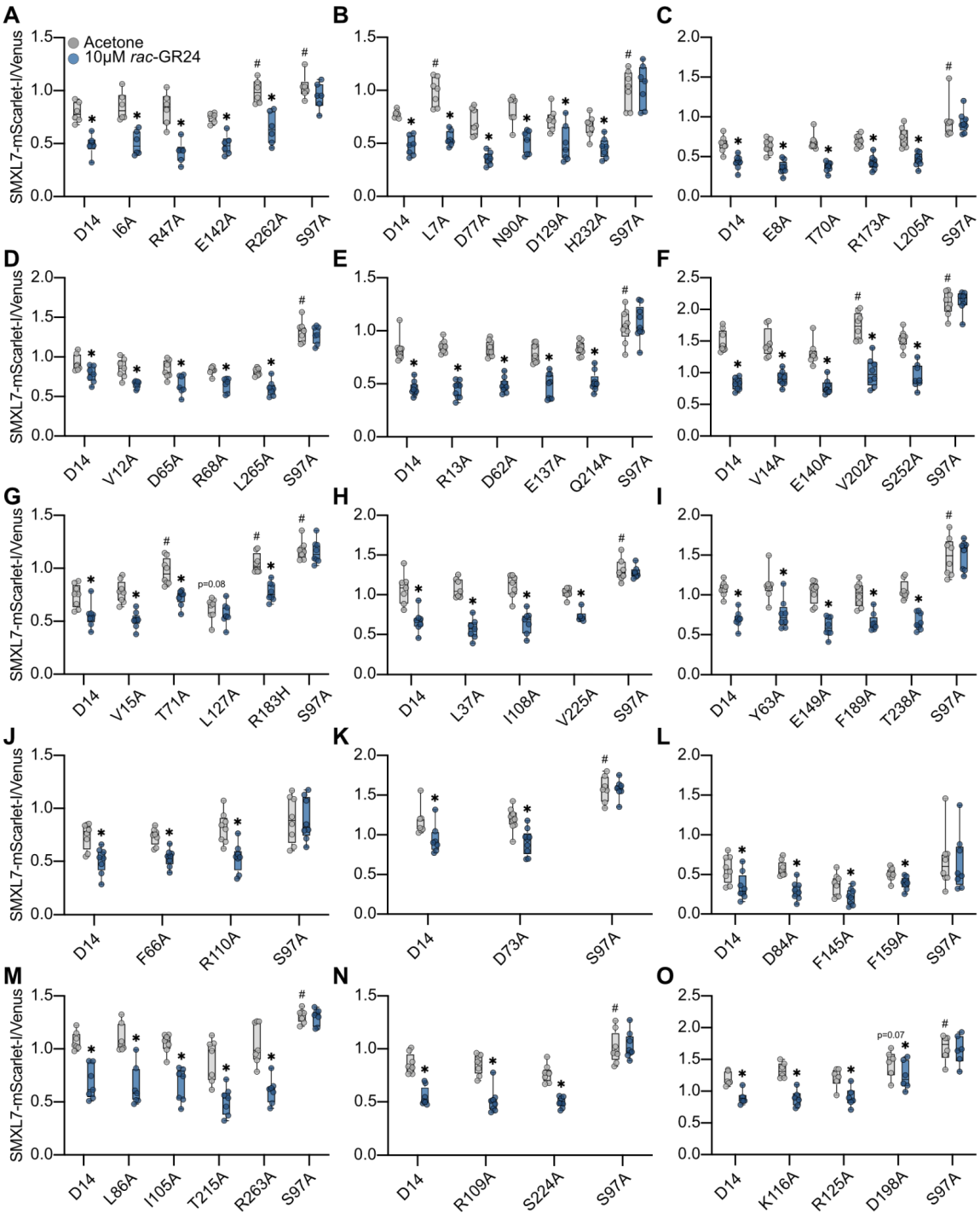


Figure 2.1: Identifying amino acid residues to assess their role in SMXL7 interaction

(A) Dot plot describing solvent accessibility scores (SASA) of D14 amino acid residues with a conservation >70% for the apo (4IH4, Zhao et al 2013) crystal structure of *AtD14* and active (5HZG, Yao et al 2016) AtD14 in complex with OsD14 crystal structure, determined in ChimeraX (UCSF). Residues highlighted in pink are residues chosen for SMXL7 interaction analysis, residues highlighted in green are involved in the MAX2 interaction interface, residues highlighted in orange are the catalytic triad, and residues highlighted in blue were not selected for further analysis. (B) residues (pink) chosen to be analyzed plotted onto the active AtD14 structure (5HZG, Yao et al 2016). (C) Seqlogo describing conservation of residues chosen for analysis.


A
B
C
D
E
F
G
H
I
J
K
L
M
N
O
SMXL7-mScarlet-I/Venus
Acetone
10μM rac-GR24
D14
I6A
R47A
E142A
R262A
S97A
L7A
D77A
N90A
D129A
H232A
E8A
T70A
R173A
L205A
V12A
D65A
R68A
L265A
R13A
D62A
E137A
Q214A
V14A
E140A
V202A
S252A
V15A
T71A
L127A
R183H
p=0.08
L37A
I108A
V225A
Y63A
E149A
F189A
T238A
F66A
R110A
D73A
D84A
F145A
F159A
L86A
I105A
T215A
R263A
R109A
S224A
K116A
R125A
D198A
p=0.07

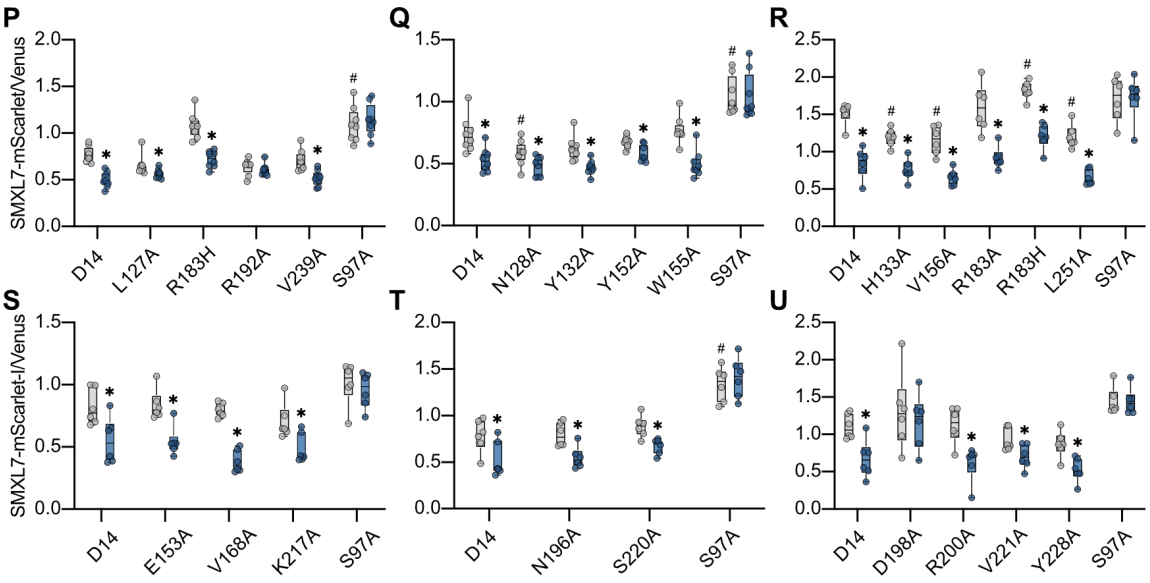


Figure 2.2: Assessment of D14 variant ability to target SMXL7 for degradation

Evaluation of ratiometric SMXL7 reporter when co-transformed with D14 variants (A-U). Leaf discs treated with 0.02% (v/v) acetone or 10 µM *rac*-GR24 treatment. n = 5-7 leaves per construct, mean ratio of 3-6 discs per leaf. *P < 0.05, paired two-way ANOVA, comparison of treatments to acetone control with Bonferroni correction for multiple comparisons. $^{\#}P < 0.05$ one-way ANOVA, comparison of variant acetone control to D14 acetone control with Bonferroni correction for multiple comparisons. Box plot whiskers indicate minimum and maximum values.

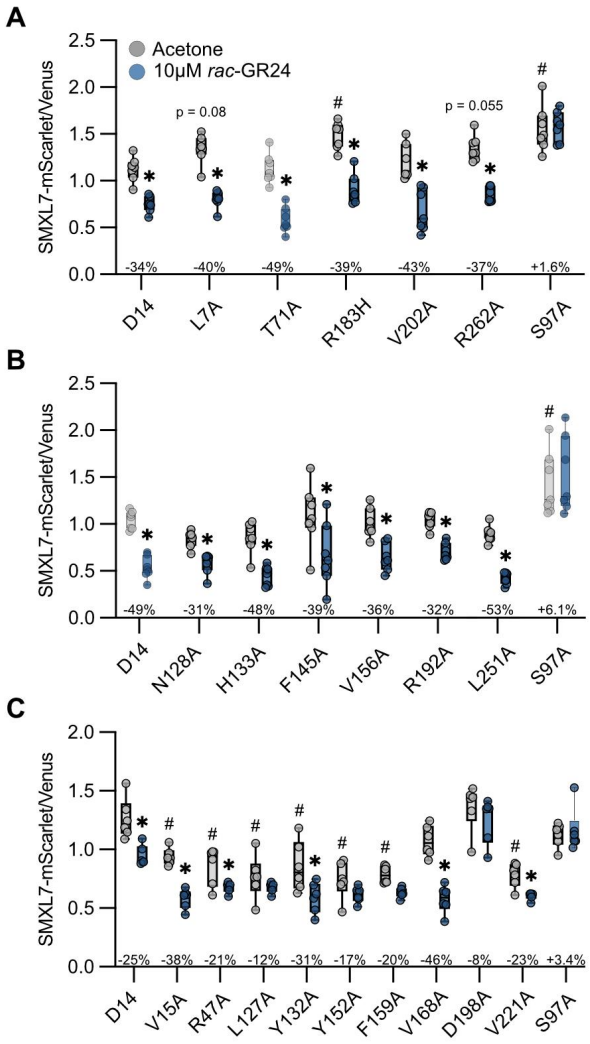


Figure 2.3: Reevaluation of interesting D14 variants in SMXL7 degradation assay

Evaluation of ratiometric SMXL7 reporter when co-transformed with D14 variants previously determined to affect SMXL7 reporter accumulation or degradation (A-C). Leaf discs treated with 0.02% (v/v) acetone or 10 μM *rac*-GR24 treatment. n = 5-7 leaves per construct, mean ratio of 3-6 discs per leaf. *P < 0.05, paired two-way ANOVA, comparison of treatments to acetone control with Bonferroni correction for multiple comparisons. $^{\#}$P < 0.05 one-way ANOVA, comparison of variant acetone control to D14 acetone control with Bonferroni correction for multiple comparisons. percentages displayed indicate %degradation relative to acetone control. Box plot whiskers indicate minimum and maximum values.

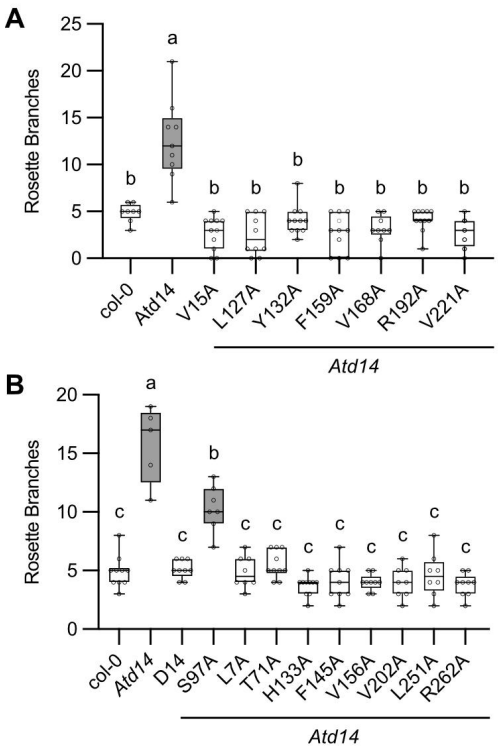


Figure 2.4: Majority of D14 variants rescue *Atd14* branching phenotype in T1 generation

Assessment of branching phenotypes for 35S:D14 variants in *Atd14* mutant background in the T1 generation. (A) Rosette branches were counted at 7 weeks old and (B) 10 weeks old. box plots with the same number are not significantly different. One-way ANOVA, comparison of genotypes Bonferroni correction for multiple comparisons. Box plot whiskers indicate minimum and maximum values.

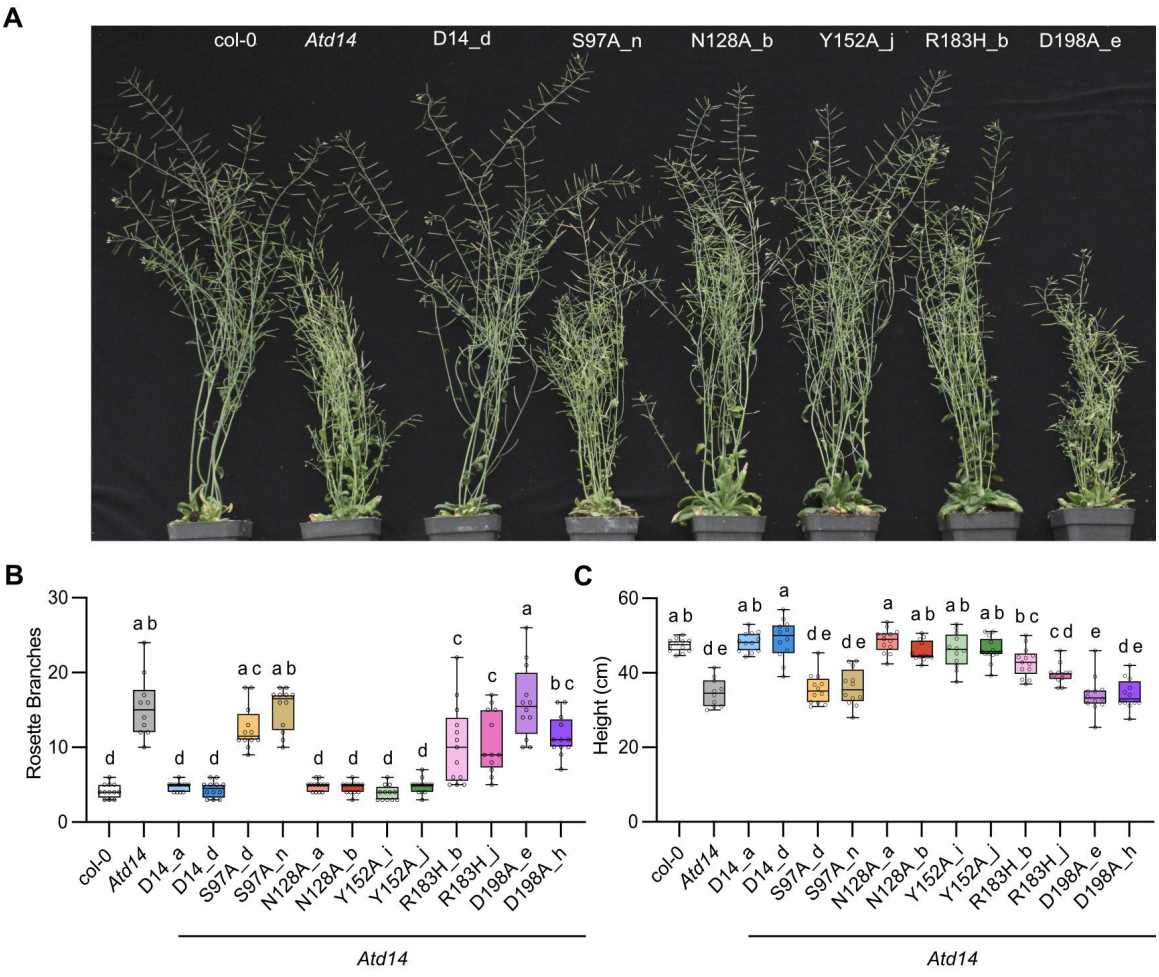


Figure 2.5: The D198A mutation does not rescue the branching or height phenotype of *Atd14*

Assessment of branching and height phenotypes for 35S:D14 variants in *Atd14* mutant background in the T3 generation. (A) Representative photos of mutant plants (B) Rosette branches were counted and (C) height measured 28 days post anthesis. box plots with the same number are not significantly different. One-way ANOVA, comparison of genotypes Bonferroni correction for multiple comparisons. Box plot whiskers indicate minimum and maximum values.

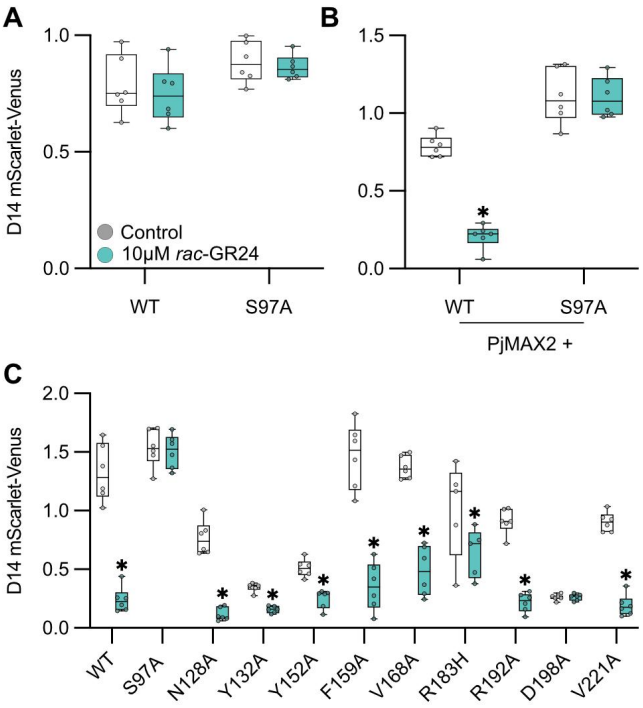


Figure 2.6: Analysis of D14 variant stability and MAX2 induced degradation

Determination of D14 ratiometric reporters in the *Nbd14a,b* mutant background without (A) and with (B) the addition of 35S:PjMAX2. Leaf discs treated with 0.02% (v/v) DMSO or 10 μM *rac*-GR24 treatment. (C) Activity of D14 variant ratiometric reporters when co-transformed with 35S:PjMAX2. Leaf discs treated with 0.02% (v/v) acetone or 10 μM *rac*-GR24 treatment. n = 5-6 leaves per construct, mean ratio of 3-6 discs per leaf. *P < 0.05, paired two-way ANOVA, comparison of treatments to DMSO or acetone control with Bonferroni correction for multiple comparisons. Box plot whiskers indicate minimum and maximum values.

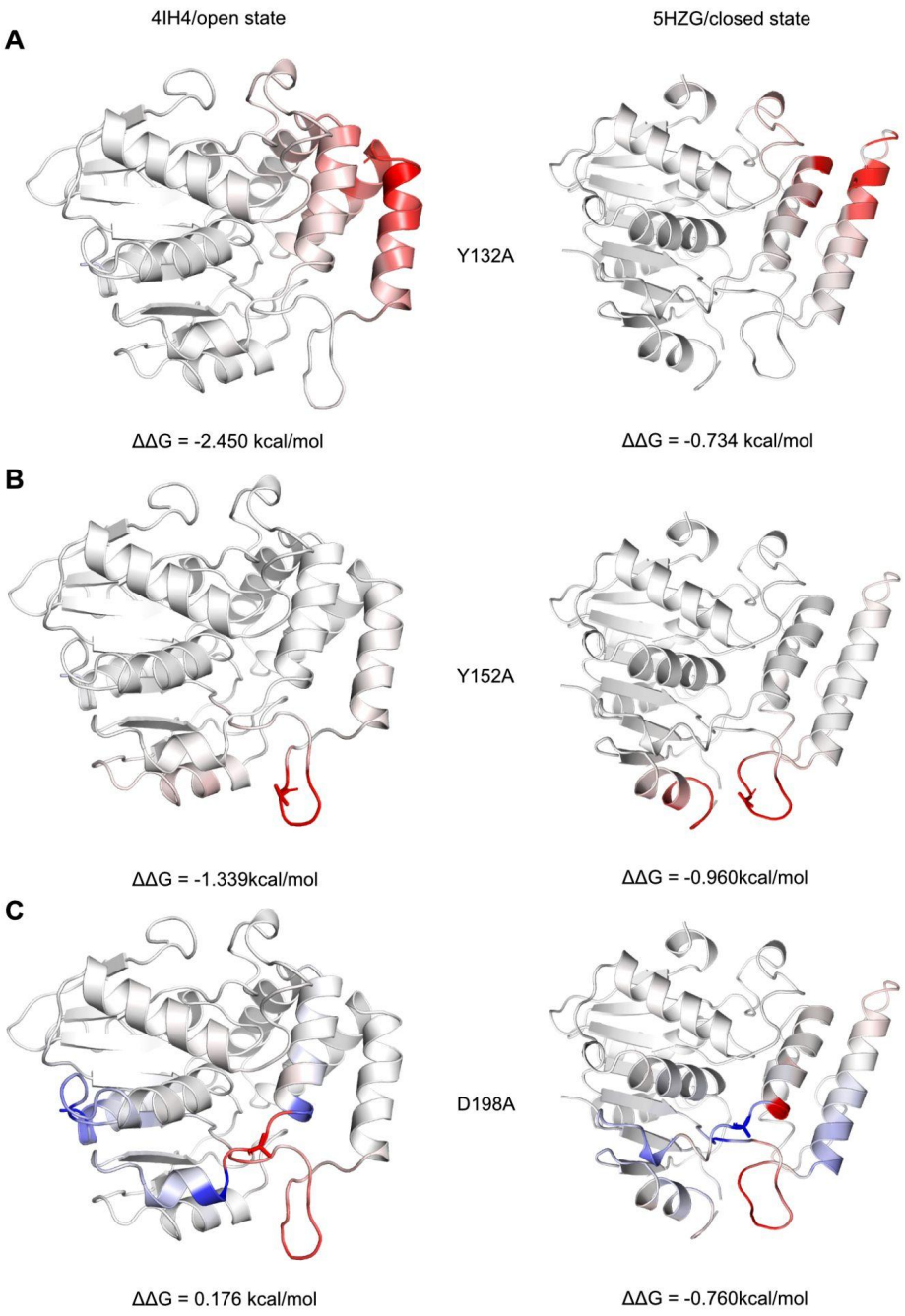


Figure 2.7: DynaMut predictions suggest stabilizing and destabilizing effects of mutations

Flexibility modeling of the Y132A (A), Y152A (B), and D198A (C) in the open (4IH4) and closed (5HZG) states by DynaMut. ΔΔ G calculations are changes in folding free energy between the D14 structure and the mutated structure. Red coloring indicate regions with increased flexibility from the mutation and blue coloring indicate regions with increased rigidity from the mutation.

Supplementary tables:

Table S2.1 Selected residues and values

Residue and position in AtD14	Most conserved residue and conservation of position for D14 proteins	4IH4 sasa score (apo/open state)	5HZG sasa score (active/closed state)	Residue and position in AtKAI2	Most conserved residue and conservation of position for KAI2 proteins
I6	L 81%	64.11	25.96	V4	V 48%
L7	L 99%	7.87	52.02	E5	E 79%
E8	E 70%	123.23	120.10	E6	E 88%
V12	V 100%	6.25	25.01	V10	V 91%
R13	R 93%	129.75	46.10	K11	R 49%
V14	V 91%	31.29	51.76	V12	V 74%
V15	V 71%	52.45	54.23	I13	L 63%
L37	R 83%	106.43	51.23	H35	H 84%
R47	R 86%	26.63	108.58	R44	R 79%
D62	D 88%	119.63	125.69	D59	D 87%
Y63	Y 62%	115.09	104.51	Y60	Y 99%
D65	D 93%	70.66	63.06	D62	D 95%
F66	F 96%	98.15	72.14	F63	F 98%
R68	R 97%	100.64	94.22	R65	R 100%
T70	T 74%	66.40	73.72	S67	S 76%
T71	T 70%	63.81	63.28	N68	T 73%
D73	D 96%	83.45	60.90	E70	E 90%
D77	D 97%	56.72	71.88	F74	Y 68%
D84	D 91%	59.54	65.22	E81	E 74%
L86	L 99%	0.32	57.00	L83	L 82%
N90	R 80%	96.01	73.78	S87	S 79%
I105	L 90%	29.37	32.06	L102	I 75%
I108	I 97%	27.97	43.61	L105	I 82%
R109	R 87%	115.68	105.14	N106	S 30%
R110	R 93%	62.32	86.36	R107	R 97%
K116	K 96%	21.15	34.05	K113	K 100%
R125	R 96%	65.80	43.88	R122	R 100%
L127	L 93%	46.91	40.51	V124	Y 72%
N128	N 99%	37.15	24.41	N125	N 99%

D129	D 99%	52.05	55.94	D126	D 76%
Y132	Y 100%	16.30	70.51	Y129	Y 99%
H133	H 88%	107.23	61.37	Q130	Y 53%
E137	E 91%	104.69	96.55	E134	E 80%
E140	E 91%	68.72	36.11	D137	D 50%
E142	E 86%	117.91	103.87	N139	D 36%
F145	F 96%	28.18	26.79	F142	F 72%
E149	E 83%	135.83	79.93	R146	K 29%
Y152	Y 100%	22.96	75.23	Y149	Y 96%
E153	E 71%	127.96	100.42	K150	K 91%
W155	W 100%	35.59	67.21	W152	W 100%
V156	V 88%	0.27	73.18	C153	C 77%
F159	F 88%	44.19	108.55	F156	F 93%
V168	V 100%	44.85	73.08	M165	M 89%
R173	R 80%	168.54	48.11	Q170	Q 100%
R183	R 100%	141.09	36.55	R180	R 100%
F189	F 87%	52.23	47.91	S186	S 92%
R192	R 87%	131.48	98.32	Q189	Q 76%
N196	N 77%	100.24	103.61	Q193	Q 34%
D198	D 100%	53.73	62.33	D195	D 100%
R200	R 100%	45.19	77.50	R197	R 100%
V202	V 72%	62.19	36.35	I199	I 32%
L205	L 81%	106.81	113.29	F202	H 39%
Q214	Q 96%	50.18	24.65	Q211	Q 100%
T215	T 93%	17.56	44.30	S212	S 95%
K217	K 74%	156.27	219.34	K214	K 88%
S220	S 99%	17.45	N/A	A217	A 97%
V221	V 99%	15.36	N/A	V218	V 97%
S224	S 90%	63.10	78.55	V221	V 52%
V225	V 96%	1.91	31.05	V222	V 92%
Y228	Y 100%	60.63	80.85	Y225	Y 95%
H232	H 90%	101.36	88.03	N229	N 58%
T238	T 90%	73.04	79.60	V235	I 77%
V239	V 86%	27.86	33.30	V236	V 91%
L251	L 96%	15.38	30.03	L248	L 100%
S252	S 97%	7.49	42.08	S249	S 100%
R262	R 78%	92.80	56.04	L259	L 98%
R263	R 86%	172.65	87.06	R260	R 82%

L265	L 100%	1.78	26.56	I262	I 98%

Table S2.2 Primer sequences

Primer name	Sequence	Use
I6A	FP: 5'-TCAACACAACgccTTAGAAGCTCTAAATG-3' RP: 5'-CTCATTCACCGAGGAAGAG-3'	Primers for mutagenesis, lower case letters indicate codon mutation
L7A	FP: 5'-ACACAACATCgcaGAAGCTCTAAATGTC-3' RP: 5'-TGACTCATTCACCGAGGAAG-3'	
E8A	FP: 5'-CAACATCTTAgcaGCTCTAAATGTC-3' RP: 5'-TGTTGACTCATGAAGCCTG-3'	
V12A	FP: 5'-GCTCTAAATGcCCGGGTCGTG-3' RP: 5'-TCTAAGATGTTGTGTTGACTC-3'	
R13A	FP: 5'-TCTAAATGTCgcgGTCGTGGGTAC-3' RP: 5'-GCTTCTAAGATGTTGTGTTG-3'	
V14A	FP: 5'-AAATGTCCGGgccGTGGGTACGG-3' RP: 5'-AGAGCTTCTAAGATGTTGTGTTGACTCATTC-3'	
V15A	FP: 5'-TGTCCGGGTCgcgGGTACGGGTG-3' RP: 5'-TTTAGAGCTTCTAAGATGTTGTGTTGACTCATTCACC-3'	
L37A	FP: 5'-AGCTTGGCACgcgATCCTTCCTTAC-3' RP: 5'-GATTGGTCAGTACCGAATC-3'	
R47A	FP: 5'-TCAAAACTACgcaGTCGTCCTCTATG-3' RP: 5'-GTGAAGTAAGGAAGGATC-3'	
D62A	FP: 5'-TGTCAACCCCgctTACTTCGATTTCAATC-3' RP: 5'-CTGCCGGCGCAAACTAGG-3'	
Y63A	FP: 5'-CAACCCCGATgccTTCGATTTCAATCGTTACACAA-3' RP: 5'-ACACTGCCGGCGCAAACT-3'	
D65A	FP: 5'-GATTACTTCGcTTTCAATCGTTACACAACTCTCGATC-3' RP: 5'-GGGGTTGACACTGCCGGC-3'	
F66A	FP: 5'-TTACTTCGATgcCAATCGTTACACAACTCTCGATC-3' RP: 5'-TCGGGGTTGACACTGCCG-3'	
R68A	FP: 5'-CGATTTCAATgcTTACACAACTCTCGATCC-3' RP: 5'-AAGTAATCGGGGTTGACAC-3'	

T70A	FP: 5’-CAATCGTTACgcgACTCTCGATC-3’ RP: 5’-AAATCGAAGTAATCGGGG-3’
T71A	FP: 5’-TCGTTACACAgctCTCGATCCTT-3’ RP: 5’-TTGAAATCGAAGTAATCGGG-3’
D73A	FP: 5’-CACAACTCTCgcTCCTTACGTC-3’ RP: 5’-TAACGATTGAAATCGAAGTAATC-3’
D77A	FP: 5’-TCCTTACGTCgctGATCTTCTCAAC-3’ RP: 5’-TCGAGAGTTGTGTAACGATTG-3’
D84A	FP: 5’-CAACATCGTTgctTCACTCGGAATC-3’ RP: 5’-AGAAGATCATCGACGTAAG-3’
L86A	FP: 5’-CGTTGATTCAgccGGAATCCAAAAC-3’ RP: 5’-ATGTTGAGAAGATCATCG-3’
N90A	FP: 5’-CGGAATCCAAgccTGTGCTTACG-3’ RP: 5’-AGTGAATCAACGATGTTG-3’
I105A	FP: 5’-GATCGGAATCgccGCTTCGATTC-3’ RP: 5’-ATAGCGGAAACAGAGTGAC-3’
I108A	FP: 5’-CATCGCTTCGgctCGTCGGCCGG-3’ RP: 5’-ATTCCGATCATAGCGGAAAC-3’
R109A	FP: 5’-CGCTTCGATTgctCGGCCGGAGC-3’ RP: 5’-ATGATTCCGATCATAGCG-3’
R110A	FP: 5’-TTCGATTCGTgcGCCGGAGCTTTTC-3’ RP: 5’-GCGATGATTCCGATCATAG-3’
K116A	FP: 5’-GCTTTTCTCCgcGCTTATCTTGATCGGATTTTCGC-3’ RP: 5’-TCCGGCCGACGAATCGAA-3’
R125A	FP: 5’-ATTTTCGCCTgcGTTTCTCAACG-3’ RP: 5’-CCGATCAAGATAAGCTTG-3’
L127A	FP: 5’-GCCTAGGTTTgccAACGACGAGG-3’ RP: 5’-GAAAATCCGATCAAGATAAGC-3’
N128A	FP: 5’-TAGGTTTCTCgcCGACGAGGATTATC-3’ RP: 5’-GGCGAAAATCCGATCAAG-3’
D129A	FP: 5’-GTTTCTCAACgccGAGGATTATC-3’ RP: 5’-CTAGGCGAAAATCCGATC-3’
Y132A	FP: 5’-CGACGAGGATgcTCATGGAGGATTC-3’ RP: 5’-TTGAGAAACCTAGGCGAAAATC-3’

H133A	FP: 5’-CGAGGATTATgctGGAGGATTCGAAG-3’ RP: 5’-TCGTTGAGAAACCTAGGC-3’
E137A	FP: 5’-TGGAGGATTCgcaGAAGGTGAGA-3’ RP: 5’-TGATAATCCTCGTCGTTG-3’
E140A	FP: 5’-CGAAGAAGGTgcgATTGAGAAAG-3’ RP: 5’-AATCCTCCATGATAATCC-3’
E142A	FP: 5’-AGGTGAGATTgcgAAAGTTTTCTC-3’ RP: 5’-TCTTCGAATCCTCCATGATAATC-3’
F145A	FP: 5’-TGAGAAAGTTgccTCAGCTATGG-3’ RP: 5’-TATCTCACCTTCTTCGAATC-3’
E149A	FP: 5’-CTCAGCTATGgcaGCTAATTACG-3’ RP: 5’-AAAACTTTCTCAATCTCACC-3’
Y152A	FP: 5’-GGAAGCTAATgcCGAAGCTTGG-3’ RP: 5’-ATAGCTGAGAAAACTTTCTC-3’
E153A	FP: 5’-AGCTAATTACgcaGCTTGGGTTC-3’ RP: 5’- TCCATAGCTGAGAAAACTTTC-3’
W155A	FP: 5’-TTACGAAGCTgcGGTTCATGGATTTG-3’ RP: 5’-TTAGCTTCCATAGCTGAG-3’
V156A	FP: 5’-CGAAGCTTGGgctCATGGATTTG-3’ RP: 5’-TAATTAGCTTCCATAGCTGAGAAAAC-3’
F159A	FP: 5’-GGTTCATGGAgcTGCTCCGCTTG-3’ RP: 5’-CAAGCTTCGTAATTAGCTTC-3’
V168A	FP: 5’-TGGAGCTGATgctCCGGCGGCGG-3’ RP: 5’-ACAGCAAGCGGAGCAAATCCATGAACC-3’
R173A	FP: 5’-GGCGGCGGTTgcaGAATTTAGCC-3’ RP: 5’-GGAACATCAGCTCCAACAG-3’
R183A	FP: 5’-GTTTAATATGgcTCCGGATATATCTCTGTTTG-3’ RP: 5’-AAAGTCCGGCTAAATTCTC-3’
R183H	FP: 5’-GTTTAATATGcaTCCGGATATATC-3’ RP: 5’-AAAGTCCGGCTAAATTCTC-3’
F189A	FP: 5’-TATATCTCTGgctGTTTCGAGGACG-3’ RP: 5’-TCCGGACGCATATTAAAC-3’
R192A	FP: 5’-GTTTGTTTCGgcgACGGTTTTCAAC-3’ RP: 5’-AGAGATATATCCGGACGC-3’
N196A	FP: 5’-GACGGTTTTCgccAGCGATCTGAG-3’ RP: 5’-CTCGAAACAAACAGAGATATATC-3’
D198A	FP: 5’-TTCAACAGCGcTCTGAGAGGTG-3’ RP: 5’-AACCGTCCTCGAAACAAAC-3’
R200A	FP: 5’-CAGCGATCTGgcAGGTGTGCTTG-3’ RP: 5’-TTGAAAACCGTCCTCGAAAC-3’
V202A	FP: 5’-TCTGAGAGGTgcgCTTGGGTTAG-3’ RP: 5’-TCGCTGTTGAAAACCGTC-3’

L205A	FP: 5'-TGTGCTTGGGgcaGTTAGAGTTC-3' RP: 5'-CCTCTCAGATCGCTGTTG-3'	
Q214A	FP: 5'-GTGTGTGATTgcgACGGCGAAGG-3' RP: 5'-GTCGGAACTCTAACTAAC-3'	
T215A	FP: 5'-TGTGATTCAGgcgGCGAAGGATG-3' RP: 5'-CACGTCGGAACTCTAACTAACC3'	
K217A	FP: 5'-TCAGACGGCGgcgGATGTTTCTG-3' RP: 5'-ATCACACACGTCGGAACT3'	
S220A	FP: 5'-GAAGGATGTTgCTGTGCCGGC-3' RP: 5'-GCCGTCTGAATCACACAC-3'	
V221A	FP: 5'-GATGTTTCTGcGCCGGCTTCG-3' RP: 5'-CTTCGCCGTCTGAATCAC-3'	
S224A	FP: 5'-TGTGCCGGCTgcgGTGGCGGAGT-3' RP: 5'-GAAACATCCTTCGCCGTCTGAATCACACACGTCG-3'	
V225A	FP: 5'-GCCGGCTTCGgcgGCGGAGTATC-3' RP: 5'-ACAGAAACATCCTTCGCCGTCTG-3'	
Y228A	FP: 5'-GGTGGCGGAGgcTCTTAGGTCTCATC-3' RP: 5'-GAAGCCGGCACAGAAACA-3'	
H232A	FP: 5'-TCTTAGGTCTgctCTCGGTGGAGATACTACTGTG-3' RP: 5'-TACTCCGCCACCGAAGCC-3'	
T238A	FP: 5'-TGGAGATACTgctGTGGAGACTC-3' RP: 5'-CCGAGATGAGACCTAAGATAC-3'	
V239A	FP: 5'-AGATACTACTgcgGAGACTCTTAAAAC-3' RP: 5'-CCACCGAGATGAGACCTA-3'	
L251A	FP: 5'-TTTGCCGCAGgctAGTGCTCCGG-3' RP: 5'-TGTCCTTCAGTTTTAAGAGTCTC-3'	
S252A	FP: 5'-GCCGCAGCTTgctGCTCCGGCGC-3' RP: 5'- AAATGTCCTTCAGTTTTAAGAGTCTCC-3'	
R262A	FP: 5'- TCAGTTTCTCgcgCGAGCTCTTCCTCGGTGAATGAGTC-3' RP: 5'- GCAAGCTGCGCCGGAGCA-3'	
R263A	FP: 5'-GTTTCTCCGGgcaGCTCTTCCTCGGTG-3' RP: 5'- AAATGTCCTTCAGTTTTAAGAGTCTCC-3'	
L265A	FP: 5'-CCGGCGAGCTgcTCCTCGGTGA-3' RP: 5'-TGAGCAAGCTGCGCCGGA-3'	
M13puc_F M13_R	5'-CCCAGTCACGACGTTGTAAAACG-3' 5'-GGAAACAGCTATGACCATG-3'	pDONR221a D14 variant colony PCR and genotyping

35s_F	5’-CTATCCTTCGCAAGACCCTTC-3’	pGWB512 or pGWBcitr D14 variant colony PCR and genotyping
M13puc_R	5’-AGCGGATAACAATTTCACACAGG-3’	
pGWBseq_3R	5’-GAACGATCGGGGAAATTCGAGC-3’	
35s_F	5’-CTATCCTTCGCAAGACCCTTC-3’	pRATIO1212 D14 variant colony PCR and genotyping
MScarlet-I_R	5’-TAATCACAGCTTCGCCCTTG-3’	
D14_seq1_F	5’-CGTTGGTCACTCTGTTTCCGCTATG-3’	D14 specific primers for sequencing
D14_seq2_F	5’-CGGTTAGAGAATTTAGCCGGAC-3’	
D14_seq_R	5’-CACCTCTCAGATCGCTGTTG-3’	

Chapter 3:

An Atypical Subclade of KAI2d Proteins Attenuate Responses to Host-derived Strigolactones in a Hemiparasitic Plant, *Phtheirospermum japonicum*

Abstract:

Many root parasitic plants in the Orobanchaceae use host-derived strigolactones as germination cues. This adaptation facilitates attachment to a host and is particularly important for the success of obligate parasitic weeds that cause substantial crop losses globally. Parasite seeds sense strigolactones through "divergent" KARRIKIN INSENSITIVE2 (KAI2d)/HYPOSENSITIVE TO LIGHT (HTL) α/β-hydrolases that have undergone substantial duplication and diversification in Orobanchaceae genomes. After germination, chemotropic growth of parasite roots toward a strigolactone source also occurs in some species. We investigated which of the seven *KAI2d* genes found in a facultative hemiparasite, *Phtheirospermum japonicum*, may enable chemotropic responses to strigolactones. To do so, we developed a triple mutant *Nbd14a,b kai2i* line of *Nicotiana benthamiana* in which strigolactone-responsive degradation of SMAX1 - a direct consequence of KAI2d activation - is disrupted. In combination with a transiently expressed, ratiometric reporter of SMAX1 protein abundance, this mutant forms a system for the functional analysis of parasite KAI2d proteins in a plant cellular context. Using this system, we found that three PjKAI2d proteins do not trigger SMAX1 degradation in the presence of strigolactones. Instead, these PjKAI2d inhibit the perception of low strigolactone concentrations by strigolactone-responsive PjKAI2d in a dominant-negative manner that depends upon an active catalytic triad. This mechanism for attenuating

strigolactone signaling potentially enhances the perception of strigolactone gradients during growth toward a host.

Introduction:

Root parasitic plants in the Orobanchaceae have adapted to sense chemical signals exuded into soil from plant roots (Bouwmeester et al., 2021). Typically, these signals are strigolactones (SLs), a family of carotenoid-derived compounds that have roles in hormonal regulation of plant development and recruitment of beneficial symbiotic associations with microbes (Clark and Bennett, 2024; Kee et al., 2023; Waters et al., 2017). Many of the obligate parasites in the Orobanchaceae use SLs as a cue for germination, which makes it more likely for a nascent seedling to find and attach to a potential host before it exhausts its supply of nutrients (Cook et al., 1966; Mutuku et al., 2021; Ogawa and Shirasu, 2022). Chemicals exuded from host roots are also used by parasitic seedlings to orient the direction of radicle elongation (Krupp et al., 2021; Whitney and Carsten, 1981; Williams, 1961). Chemotropic growth toward SLs has been observed in an obligate hemiparasite, *Striga hermonthica*, which requires a host to complete its life cycle, as well as in a facultative hemiparasite, *Ptheirospermum japonicum*, which can grow independently of a host or engage in parasitism opportunistically (Ogawa et al., 2022).

Host-derived SLs are perceived by the seed of root parasites through a mechanism that has been adapted from karrikin signaling (Conn et al., 2015; Nelson, 2021; Toh et al., 2015; Tsuchiya et al., 2015). Karrikins (KARs) are butenolide compounds found in smoke that stimulate germination of many plants in the soil seed bank after fire (Flematti et al., 2004; Nelson et al., 2012). KAR perception is mediated by an α/β-hydrolase, KARRIKIN INSENSITIVE2 (KAI2), also known as HYPOSENSITIVE TO LIGHT (HTL) (Sun and Ni, 2011; Waters et al., 2012). Activation of KAI2 stimulates interactions with an F-box protein,

MORE AXILLARY GROWTH2 (MAX2)/DWARF3 (D3), and putative transcriptional co-repressor proteins, SUPPRESSOR OF MAX2 1 (SMAX1) and SMAX1-LIKE2 (SMXL2) (Khosla et al., 2020a; Stanga et al., 2013; Wang et al., 2020; Zheng et al., 2020). MAX2 acts as an adapter that confers substrate specificity to an SCF-type (Skp1, Cullin, F-box) E3 ubiquitin ligase complex (Stirnberg et al., 2007). KAI2–SCF^{MAX2} polyubiquitinates SMAX1 and SMXL2, marking them for rapid degradation by the 26S proteasome (Khosla et al., 2020a; Wang et al., 2020; Zheng et al., 2020). Degradation of SMAX1 and SMXL2 then initiates various downstream growth responses including seed germination (Bunsick et al., 2022; Stanga et al., 2016, 2013; Waters and Nelson, 2022). A very similar mechanism is used by spermatophytes in the perception of endogenous SL hormones. A paralog of KAI2, DWARF14 (D14)/DECREASED APICAL DOMINANCE2 (DAD2), is a SL receptor that works with SCF^{MAX2} to target several SMAX1-LIKE (SMXL) proteins for degradation (Blázquez et al., 2020; Hamiaux et al., 2012; Yao et al., 2016). In *Arabidopsis thaliana*, SMXL6, SMXL7, and SMXL8 (orthologs of DWARF53 in *Oryza sativa*) are the primary targets of D14–SCF^{MAX2}, but SMAX1 and SMXL2 can also be targeted when SL is applied or putatively increased during osmotic stress (Jiang et al., 2013; Li et al., 2022; Soundappan et al., 2015; L. Wang et al., 2015; Wang et al., 2020; Zhou et al., 2013).

Mounting evidence suggests that although KAI2 can mediate responses to KARs (or, more likely, a KAR metabolite), its usual function is the perception of an unknown endogenous signal(s) known as “KAI2 ligand” (KL) (Conn and Nelson, 2015; Waters and Nelson, 2022). One to a few copies of *KAI2* are typically present in angiosperm genomes. *KAI2* paralogs have shown varied ligand preferences for KL, different KARs, (–)-germacrene D, or synthetic KAI2 agonists that suggests adaptation for perceiving different signals (Carbonnel et al., 2020; Martinez et al., 2022; Stirling et al., 2024; Sun et al., 2020).

In the parasitic Orobanchaceae, *KAI2* has undergone an unusual expansion in copy number that is particularly dramatic among obligate parasites such as *Striga* spp. (Conn et al., 2015; Nelson, 2021; Toh et al., 2015; Yoshida et al., 2019). The majority of the new *KAI2* paralogs fall into a rapidly evolving, "divergent" clade, *KAI2d (Conn et al., 2015; Nelson, 2021)*. KAI2d proteins from the root parasitic species *S. hermonthica*, *Phelipanche aegyptiaca*, *Phelipanche ramosa*, *Orobanche minor*, and *Orobanche cumana* have been demonstrated to perceive SLs (Conn et al., 2015; Larose et al., 2022; de Saint Germain et al., 2021; Takei et al., 2023; Toh et al., 2015; Tsuchiya et al., 2015; Wang et al., 2021; Yao et al., 2017). In addition, a KAI2d protein from *P. ramosa* responds to isothiocyanates (de Saint Germain et al., 2021). Therefore, the *KAI2d* clade arose from gene duplication and underwent neofunctionalization that changed the ligand preferences of KAI2 proteins, similar to the evolution of D14. The transition to SL perception in KAI2 proteins can evolve through as few as three mutations in the ligand-binding pocket (Arellano-Saab et al., 2021). It is also remarkable that some KAI2d proteins, such as *S. hermonthica* HTL7 (ShHTL7), confer sensitivity to extraordinarily low (e.g. picomolar) concentrations of SLs, although this is more a consequence of unusually high affinity for MAX2 rather than for SL (Toh et al., 2015; Tsuchiya et al., 2015; Wang et al., 2021).

Why parasite genomes contain so many *KAI2d* paralogs remains an unresolved question. One potential explanation is that individual KAI2d proteins may specialize in perception of different SLs, of which more than 30 have been identified (Bouwmeester et al., 2021; Conn et al., 2015; Nelson, 2021). This would putatively enable a parasite to respond to a specific chemical fingerprint that corresponds to a compatible host. Indeed, variable affinities for different SLs have been observed in the germination responses of some parasites as well as among KAI2d proteins *in vitro* and *in vivo* (Fernández-Aparicio

et al., 2011; Toh et al., 2015; Tsuchiya et al., 2015; Wang et al., 2021). Broadening the range of SLs that can be perceived, putatively through *KAI2d* evolution, can lead to rapid expansions in the host range, as illustrated by the recent emergence of a race of sunflower broomrape, *O. cumana*, that can also attack tomato (Dor et al., 2020). Thus, the antagonistic coevolution of hosts and plant parasites could drive diversification of SL biosynthesis and SL detection mechanisms, respectively.

A second idea is that *KAI2d* simply may be prone to gene duplication. The observation of localized duplication of *KAI2d* genes in different parasite genomes suggests they have arisen through mechanisms such as unequal crossing over, which is facilitated by repetitive genetic sequences (Xu et al., 2022; Yoshida et al., 2019). It is possible that very few *KAI2d* genes in a genome are involved in host perception and that most *KAI2d* copies are either pseudogenes or have little or no adaptive value. Notably, chemical stimulation of ShHTL7 alone is sufficient to trigger germination of *S. hermonthica*, implying that other KAI2d proteins may be unnecessary in that species, at least in seed *(Uraguchi et al., 2018)*.

A third possibility, which has not yet been tested, is that some KAI2d proteins may have antagonistic effects on parasite germination (Nelson, 2021). This idea arose from the observation that closely related root parasites, such as *S. hermonthica* and *Striga gesnerioides* or species within the *Orobanche/Phelipanche* genera, can show quite different responses to various SLs or host exudates during germination despite having large and highly similar sets of *KAI2d* genes (Fernández-Aparicio et al., 2011, 2009; Nomura et al., 2013; Tsuchiya et al., 2015). For obligate parasites, many of which are specialists with a restricted host range, positive germination responses to SLs made by a compatible host combined with inhibitory responses to SLs made by a non-compatible

host would have obvious advantages. Putatively, the most direct route for the evolution of inhibitory responses to a detrimental SL would be through the emergence of a dominant-negative (antimorphic) KAI2d protein that is activated by that SL, rather than through accruing loss-of-function mutations in all *KAI2d* paralogs that can recognize that SL (Nelson, 2021). Several *KAI2d* genes from *S. hermonthica*, *Orobanche cernua*, and *O. cumana* have failed to confer SL responses to *A. thaliana* in cross-species complementation assays (Conn et al., 2015; Larose et al., 2022; Nelson, 2021; Toh et al., 2015). It is unknown, however, whether any of these proteins are dominant-negative forms of KAI2d, inactive, or only seem to be inactive for other reasons (e.g. an appropriate SL agonist was not tested, or the protein cannot form functional interactions with *Arabidopsis* SCF^{MAX2} and SMAX1/SMXL2 proteins).

Additional examples of unusual *KAI2d* have been described recently in *P. japonicum*. Under nutrient-deprived conditions, *P. japonicum* seedlings show chemotropic root growth toward artificial and biological SL sources (Ogawa et al., 2022). Putatively, this response is mediated by one or more *KAI2d* genes, of which up to seven are present in the *P. japonicum* genome, as *SMAX1* overexpression blocks chemotropism (Ogawa et al., 2022). *PjKAI2d1*, *PjKAI2d4*, *PjKAI2d4.2*, and *PjKAI2d5* form a clade that has generally low expression in seedlings. *PjKAI2d2*, *PjKAI2d3*, and *PjKAI2d3.2* form a sister clade that has comparably high expression in seedlings prior to infection of the host. Furthermore, *PjKAI2d2* and *PjKAI2d3.2* expression is induced by *rac*-strigol treatment or the absence of nutrients. These expression patterns suggested that the members of this clade are the most likely candidates for SL perception in *P. japonicum* seedlings. Indeed, overexpression of *PjKAI2d2* increases chemotropism of *P. japonicum* hairy roots toward *rac*-strigol (Ogawa et al., 2022). However, *Arabidopsis d14 kai2* lines carrying *PjKAI2d2*,

PjKAI2d3, and *PjKAI2d3.2* transgenes show little or no germination response to *rac*-strigol treatment (Ogawa et al., 2022). This raises the question of whether these KAI2d proteins function differently than typical SL receptors.

The options are currently limited for evaluating the function of KAI2d proteins from parasitic plants within a plant cellular context. A commonly used approach has been cross-species complementation, in which a *KAI2d* transgene from a parasite is introduced into a *kai2* or *d14 kai2* mutant background in *A. thaliana*, which is easily transformed, and then evaluated for its ability to rescue seed germination or seedling growth phenotypes in the presence of candidate signaling molecules (Conn et al., 2015; Toh et al., 2015). This approach has identified KAI2d proteins with high sensitivity to strigolactones, although its success as a bioassay is probably influenced by the affinity of each KAI2d for *Arabidopsis* MAX2 and SMAX1/SMXL2 proteins (Wang et al., 2021). One drawback is that it takes several months to more than a year to develop homozygous transgenic lines for phenotypic assays.

An alternative approach involves assaying SL responses in a transient expression system in plants. We previously made a set of vectors, pRATIO, for ratiometric analysis of protein abundance (Khosla et al., 2020b). In this system, the coding sequence for a target protein of interest is fused to that of a reporter protein (e.g. the bright, red fluorescent protein mScarlet-I), a modified “self-cleaving” 2A peptide from foot-and-mouth disease virus, and a reference reporter protein (e.g. the yellow fluorescent protein Venus). During translation, the target-reporter fusion protein is separated from the reference reporter protein due to ribosomal skipping induced by the 2A peptide. The ratio of target reporter signal to reference reporter signal provides a convenient readout of relative target protein abundance *in vivo*. The system is deployed through injection of *Agrobacterium*

tumefaciens cells carrying pRATIO plasmids into *N. benthamiana* leaves ("agroinfiltration") and measured through fluorescence or luminescence scanning of excised leaf discs for each reporter protein a few days later. This method has enabled monitoring of AtSMAX1 and AtSMXL7 degradation following KAR or SL treatments (Khosla et al., 2020a, 2020b; Li et al., 2022; White et al., 2022).

An extension of this approach is to measure the ability of co-expressed KAI2 or D14 receptor proteins to trigger SMAX1/SMXL reporter degradation, but it requires removal of the native *N. benthamiana* KAR or SL receptors. We previously isolated loss-of-function mutations in the two copies of *D14* in the *N. benthamiana* genome through CRISPR-Cas9 gene editing (White et al., 2022). The resulting *Nbd14a,b* mutant line shows developmental phenotypes that are consistent with SL insensitivity. In addition, degradation of AtSMXL7 ratiometric reporter protein after treatment with *rac*-GR24 (a racemic mixture of a synthetic SL analog, $GR24^{5DS}$, and its enantiomer, $GR24^{ent\text{-}5DS}$) or its enantiopure components is blocked (White et al., 2022). This genetic background makes it possible to assay the SL signaling activity of transiently co-expressed *D14* variants. However, it is not suitable for analyzing KAI2d function, as some degradation of SMAX1 and SMXL2 ratiometric reporters still occurs after $GR24^{5DS}$ treatment (Li et al., 2022). Putatively, this is because one or more of the KAI2 proteins in *N. benthamiana* can mediate responses to $GR24^{5DS}$.

We set out to examine the functions of the seven *P. japonicum KAI2d* genes. To do so, we improved the *N. benthamiana* platform to enable characterization of *P. japonicum* KAI2d proteins. In this heterologous, plant-based assay, we found that PjKAI2d2, PjKAI2d3, and PjKAI2d3.2 do not activate SMAX1 degradation in response to

SL perception, in contrast to PjKAI2d proteins from the low-expression clade. Instead, PjKAI2d2 and PjKAI2d3.2 antagonize SL signal transduction by other PjKAI2d proteins, potentially providing a mechanism to attenuate SL responses that might be useful for perceiving shallow chemical gradients during chemotropism.

Materials and methods:

Plant growth conditions

N. benthamiana seeds were incubated at -80 °C for 12h, germinated on Sungro Professional Growing Mix, supplemented with Gnatrol WDG, Marathon (imidacloprid), and Osmocote 14-14-14 fertilizer. Seedlings were transferred to pots at ~7-10 d old. *N. benthamiana* plants were grown under long day conditions (16 h white light, 120 µmol m^{-2} s^{-1} ; 8 h dark) at ~22 °C.

Gene editing

Guide RNAs to target *NbKAI2* genes were designed manually. Both gRNA-encoding genes were cloned into a single pHEE401E construct as described previously, but with Q5 high-fidelity DNA polymerase (New England Biolabs) and NEBridge Golden Gate Assembly Kit (BsaI-HF v2, New England Biolabs) (Z.-P. Wang et al., 2015; White et al., 2022; Xing et al., 2014). Transformation of *Nbd14a,b* was performed by the Plant Transformation Facility at the University of California, Davis, as described previously (White et al., 2022).

Genotyping

DNA was extracted from *N. benthamiana* leaf tissue ground in liquid N_2 and incubated with 250 µl buffer (0.35 M sorbitol, 5 mM EDTA, 100 mM Tris-Cl) and kept at 4 °C for 20 min. Tissue mixtures were centrifuged for 10 min at 6000 rpm at 4 °C. The pellet was resuspended with 350 µL lysis buffer (250 mM NaCl, 25 mM EDTA, 200 mM Tris-Cl, 0.5% SDS). Lysate was incubated at 95 °C for 15 min, then 400 µL ice-cold 100% isopropanol was added. Lysate was centrifuged for 10 min at 12000 rpm. Pellet was washed in 400 µL ice-cold 70% ethanol, centrifuged for 5 min at 12000 rpm, and ethanol was removed. DNA was air dried and resuspended with 50 µL buffer (10 mM Tris-HCl, 1 mM EDTA, pH 8). Genotyping was performed with Taq polymerase (New England Biolabs) using standard PCR reaction conditions supplemented with $MgCl_2$ and primers described in Table S1.

PjSMAX1 degradation assays

Gateway entry clones containing each coding sequence (CDS) of *PjKAI2d2*, *PjKAI2d3*, and *PjKAI2d3.2* were previously described (Ogawa et al., 2022). Each CDS of *PjSMAX1.1* and *PjSMAX1.2* CDS was PCR-amplified and cloned into pENTR D-TOPO entry vector to generate entry vectors, then cloned into the pRATIO1212 ratiometric reporter vector (Khosla et al., 2020b). *Agrobacterium tumefaciens* GV3101 that also carries a plasmid expressing p19, suppressor of gene-silencing, was transformed with pRATIO1212-SMAX1.1 and pRATIO1212-SMAX1.2 by electroporation. The CDSs for *PjKAI2d1*, *PjKAI2d4*, *PjKAI2d4.2*, and *PjKAI2d5*, described in (Ogawa et al., 2022), were synthesized (Twist Bioscience). *OcKAI2d1* was previously described in (Larose et al., 2022). CDSs were Gateway cloned into an ampicillin-resistant pDONR221 entry vector, and Sanger sequence-verified. PjKAI2d2^{S94A} and PjKAI2d3.2^{S94A} ampicillin-resistant pDONR221 entry

vectors were created using a Q5 Site-Directed Mutagenesis kit (New England Biolabs). The *KAI2d* CDSs were transferred into the plant transformation vector pGWB402 (Nakagawa et al., 2007) using Gateway LR cloning (Invitrogen). pGWB402-KAI2d vectors were transformed into *A. tumefaciens* strain GV3101 via electroporation. Transient transformation of *N. benthamiana* and measurement of mScarlet-I and Venus was performed as described previously (Khosla and Nelson, 2020), with the following modifications for the cell densities of *A. tumefaciens* cultures resuspended in infiltration media prior to injection of *N. benthamiana* leaves: Figures 1-2, *A. tumefaciens* containing pRATIO1212-*PjSMAX1* vectors were injected at OD_{600} 0.8. Figure 2, *A. tumefaciens* containing *KAI2* vectors or pGWB402 alone was injected at OD_{600} 0.1. Figures 3-4, *A. tumefaciens* containing pRATIO1212-*PjSMAX1.1* was injected at OD_{600} 0.7 and *A. tumefaciens* containing *PjKAI2d1* and *PjKAI2d4* vectors was injected at OD_{600} 0.05. Final OD_{600} was brought to 1.2 with *A. tumefaciens* containing empty vector (pGWB402). Figure 3, *A. tumefaciens* containing *PjKAI2d2* and *PjKAI2d3.2* vectors was injected at OD_{600} 0.087, 0.15, or 0.45. Figure 4, *A. tumefaciens* containing *PjKAI2d2* and *PjKAI2d3.2* vectors was injected at OD_{600} 0.45. Racemic GR24 and racemic strigol were synthesized by Strigolab. KAR_1 was synthesized and kindly supplied by Dr. Adrian Scaffidi and Dr. Gavin Flematti (University of Western Australia). Treatments of excised leaf discs per each assay are as follows: Figure 1, 0.02% (v/v) acetone, 10 µM *rac*-GR24, 10 µM KAR_1. Figure 2, **(A)**Figure 1, 0.02% (v/v) acetone or 10 µM *rac*-GR24, **(B)** 0.01% (v/v) acetone or 1 µM *rac*-strigol. Figure 3, 0.01% (v/v) acetone, 1 nM *rac*-strigol, 10 nM *rac*-strigol, or 100 nM *rac*-strigol. Figure 4, 0.01% (v/v) acetone, 1 nM *rac*-strigol, or 100 nM *rac*-strigol. Fluorescence was read ~16h post treatment. Each data point represents the average ratio

of mScarlet-I to Venus fluorescence of 4-8 leaf discs from a single transformed leaf. n = 4-7 leaves.

Phylogenetic analysis

KAI2 sequences were collected from published datasets (Conn et al., 2015; Stirling et al., 2024; Toh et al., 2015; Yoshida et al., 2019). Protein sequence alignments were performed in MEGA 11 using the MUSCLE multiple sequence alignment algorithms (Tamura et al., 2021a). The multiple sequence alignment was trimmed using ClipKIT "smart-gap" (Steenwyk et al., 2020). 128 out of 421 positions were trimmed. The phylogenetic tool IQ TREE inferred the evolutionary history using the Maximum Likelihood method and JTT matrix-based model (Trifinopoulos et al., 2016). The tree with the highest negative log likelihood was selected. The gamma model was used to estimate evolutionary rate differences among sites (8 categories). The alpha parameter was estimated from the dataset. There were a total of 293 amino acid positions and 228 sequences in the final dataset. Bootstrap values were calculated using UltraFast (10,000 iterations). Tree search settings were 0.5 perturbation strength and 100 iterations to stop. Tree was viewed in MEGA 11 (Tamura et al., 2021b) and branches are not scaled.

Statistical analysis and data presentation

All data was analyzed and graphs produced using Prism 10 (GraphPad) with figure assembly in Affinity Designer.

Results:

Generation of a strigolactone-insensitive mutant in *Nicotiana benthamiana*

We identified four potentially functional *KAI2* genes and one pseudogene in the allotetraploid genome of *N. benthamiana* (assembly version 1.0.1) (Bombarely et al., 2012). Based on phylogenetic analysis, three genes are “conserved”-type *KAI2* (*KAI2c*), members of a clade under strong purifying selection that has been associated with KL perception, while one is an “intermediate”-type *KAI2* (*KAI2i*) from a less well-conserved group that has been associated with perception of KAR_1 or (–)-germacrene D (Conn et al., 2015; Stirling et al., 2024) (Figure S1).

With the goal of eliminating SL-induced degradation of SMAX1 in *N. benthamiana* leaves, we used CRISPR-SpCas9 to introduce mutations in the four *NbKAI2* genes in the *Nbd14a,b* mutant background. We selected two gRNAs that could potentially target the second exon of multiple *NbKAI2* genes (Figure 1A), and then transformed *Nbd14a,b* with pHEE401E, a binary plasmid that expresses maize-codon-optimized *SpCas9* from an egg cell-specific promoter and both gRNAs from U6 promoters (Z.-P. Wang et al., 2015). To monitor SMAX1 degradation, we introduced coding sequences for the two copies of *SMAX1* that have been identified in *P. japonicum*, *PjSMAX1.1* and *PjSMAX1.2*, into the ratiometric reporter vector pRATIO1212 (Khosla et al., 2020b; Ogawa et al., 2022) (Figure 1B). The reporter ratios for both PjSMAX.1 and PjSMAX1.2 declined after *rac*-GR24 treatment in wild-type *N. benthamiana* and *Nbd14a,b* leaves, suggesting they are regulated similarly (Figure 1C,D). We identified a CRISPR-Cas9 transgenic line that showed little or no degradation of PjSMAX1.1 ratiometric reporter in response to *rac*-GR24 treatment, although it was still responsive to KAR_1 (Figure 1E). This line has a one base-pair insertion mutation in *NbKAI2i* that causes a frameshift, but the other three *NbKAI2* genes are unaffected (Figure 1F). Therefore, NbKAI2i is putatively responsible for the remaining *rac*-GR24 response in *Nbd14a,b*.

Functional analysis of PjKAI2d proteins

We isolated a transgene-free, homozygous *Nbd14a,b kai2i* line through segregation. We then investigated the ability of the seven PjKAI2d proteins to trigger degradation of PjSMAX1.1 ratiometric reporter in *Nbd14a,b kai2i* leaves in response to SL treatment. The coding sequence for each gene was cloned into a binary vector, pGWB402, which drives transgene expression under the control of a *35S* promoter, and co-transformed with pRATIO1212-PjSMAX1.1. We tested the empty pGWB402 vector and pGWB402 containing the coding sequence of *OcKAI2d1* from the obligate holoparasite *O. cumana* as negative and positive controls, respectively (Conn et al., 2015; Larose et al., 2022).

We observed a significant decrease in the PjSMAX1.1 reporter ratio after 10 µM *rac*-GR24 treatment when *OcKAI2d1*, but not any of the *PjKAI2d*, was co-expressed in *Nbd14a,b kai2i* (Figure 2A). Because *rac*-GR24 may not be an effective ligand for PjKAI2d proteins, we also tested *rac*-strigol, a racemic mixture of a naturally occurring SL and its enantiomer that attracts chemotropic growth of *P. japonicum* (Ogawa et al., 2022). In contrast to *rac*-GR24, 1 µM *rac*-strigol stimulated PjSMAX1.1 degradation in the presence of several KAI2d (Figure 2B). Co-expression of *PjKAI2d1*, *PjKAI2d4*, and *PjKAI2d5* caused significant reductions in the PjSMAX1.1 reporter ratio after *rac*-strigol treatment, suggesting that they are functional SL receptors. In mock-treated conditions, the PjSMAX1.1 reporter ratio was also reduced by all three co-expressed genes relative to the empty vector control (Figure 2). This may be because PjKAI2d1, PjKAI2d4, and PjKAI2d5 respond to endogenous SLs in *Nbd14a,b Nbkai2* leaves. *PjKAI2d4.2* co-expression produced a particularly low PjSMAX1.1 reporter ratio, implying that PjKAI2d4.2

has constitutive signaling activity or is even more sensitive to endogenous SLs than the other PjKAI2d proteins. In contrast, we did not observe any evidence of PjSMAX1.1 reporter degradation after *rac*-strigol treatment when *PjKAI2d2*, *PjKAI2d3*, or *PjKAI2d3.2* were co-expressed (Figure 2B). Furthermore, the PjSMAX1.1 reporter ratio remained similar to the empty vector control in mock-treated leaves when these genes were co-expressed (Figure 2). These results suggest that PjKAI2d2, PjKAI2d3, and PjKAI2d3.2 are insensitive to SL and/or unable to transduce SL signals.

These observations conflicted with our initial hypothesis that *PjKAI2d2*, *PjKAI2d3*, and *PjKAI2d3.2* are responsible for SL responses in *P. japonicum* seedlings (Ogawa et al., 2022). Therefore, we considered that PjKAI2d2, PjKAI2d3, and PjKAI2d3.2 may have atypical functions instead. Specifically, we hypothesized that these proteins may competitively inhibit PjSMAX1 degradation by SL-responsive PjKAI2d proteins. To test this idea, we co-expressed *PjKAI2d2* and *PjKAI2d3.2* with the SL-responsive genes *PjKAI2d1* and *PjKAI2d4* and tested the PjSMAX1.1 degradation response to different concentrations of *rac*-strigol.

Expression of *PjKAI2d1* and *PjKAI2d4* alone conferred significant reductions in the PjSMAX1.1 reporter ratio after treatment with *rac*-strigol concentrations as low as 1 to 10 nM, suggesting that the receptors encoded by these genes are highly sensitive to SL (Figure 3). We then co-transformed *PjKAI2d2* or *PjKAI2d3.2* with *PjKAI2d1* or *PjKAI2d4* by mixing *A. tumefaciens* strains at different ratios. The amount of *A. tumefaciens* cells carrying *PjKAI2d1* or *PjKAI2d4* plasmids was kept constant, and supplementation with an empty vector strain was used to keep the overall concentration of *A. tumefaciens* cells used in each agroinfiltration of *N. benthamiana* leaves the same.

Co-transformation of *PjKAI2d1* cells with a 1:9 concentration of *PjKAI2d2* cells blocked degradation of the PjSMAX1.1 reporter in the presence of 10 nM or 100 nM *rac*-strigol treatments (Figure 3A). At lower ratios of *PjKAI2d1* to *PjKAI2d2*, the response to 10 nM, but not 100 nM, *rac*-strigol was blocked. A similar effect was observed at 1:3 and 1:9 mixtures of *PjKAI2d1* and *PjKAI2d3.2* cells; degradation of the PjSMAX1.1 reporter after 1 nM *rac*-strigol treatment was blocked, but higher concentrations of *rac*-strigol overcame the inhibitory effect of *PjKAI2d3.2* co-expression (Figure 3B). When PjKAI2d4 was used as the SL receptor, PjSMAX1.1 reporter degradation by 1 nM rac-strigol was inhibited by 1:3 and 1:9 mixtures with PjKAI2d2, and PjKAI2d3.2 did not block responses to any concentration of *rac*-strigol (Figure 3C,D). This suggested that PjKAI2d4 activity was less affected than PjKAI2d1 by co-expression of *PjKAI2d2* and *PjKAI2d3.2*, perhaps because PjKAI2d4 is more sensitive to SL than PjKAI2d1. However, it is notable that in almost all cases, the addition of *PjKAI2d2* or *PjKAI2d3.2* caused a significant increase in the PjSMAX1.1 reporter ratio in mock-treated leaf discs compared to *PjKAI2d1* or *PjKAI2d4* alone (Figure 3). Overall, these observations suggest that PjKAI2d2 and PjKAI2d3.2 inhibit SL signaling by PjKAI2d1 and PjKAI2d4 at low concentrations of SL, whether endogenous or applied. Therefore, PjKAI2d2 and PjKAI2d3.2 may shift the dynamic range of SL perception.

The catalytic triad is required for attenuation of SL signaling by PjKAI2d2 and PjKAI2d3.2

The serine residue of the Ser-His-Asp catalytic triad is required for the enzymatic and signaling functions of D14 and KAI2 proteins (Hamiaux et al., 2012; Seto et al., 2019; Waters et al., 2015a, 2015b; Yao et al., 2018). Therefore we replaced the catalytic serine

with alanine of PjKAI2d2 and PjKAI2d3.2 and tested whether PjKAI2d2^{S94A} and PjKAI2d3.2^{S94A} mutant proteins can inhibit the SL-induced degradation of PjSMAX1.1 by PjKAI2d1 or PjKAI2d4. Co-transformation of *PjKAI2d1* and *PjKAI2d2* (1:9) blocked the degradation of the PjSMAX1.1 reporter by 1 nM or 100 nM *rac*-strigol treatments (Figure 4A). In contrast, co-transformation of *PjKAI2d2^{S94A}* with *PjKAI2d1* had no effect on SL-induced degradation of PjSMAX1.1 reporter compared to *PjKAI2d1* alone. This result indicates that PjKAI2d2 requires hydrolytic activity to inhibit PjSMAX1.1 degradation. Co-transformation of *PjKAI2d1* and *PjKAI2d3.2* (1:9) had a different effect than *PjKAI2d2*. *PjKAI2d3.2* caused a significant increase in the PjSMAX1.1 reporter ratio in mock-treated leaf discs, implying that it inhibited PjSMAX1.1 degradation caused by endogenous SLs. As noted above, *PjKAI2d3.2* appeared to shift the dynamic range of the PjSMAX1.1 degradation response to SL (Figure 3B, 4A). In contrast, this effect was not observed from co-expression of *PjKAI2d3.2^{S94A}*. Similar trends were obtained when *PjKAI2d2* and *PjKAI2d3.2* were co-transformed with *PjKAI2d4* (Figure 4B). Both *PjKAI2d2* and *PjKAI2d3.2* caused an increase in the baseline PjSMAX1.1 reporter ratio, and their effects on the dynamic range of SL-induced PjSMAX1.1 degradation were dependent on the catalytic serine. These phenomena suggest that *PjKAI2d2* and *PjKAI2d3.2* are not pseudogenes; instead, these paralogs appear to have dominant-negative effects.

Discussion:

The prevailing model for host detection in parasitic plants is that KAI2d proteins sensitively perceive SLs in the rhizosphere and initiate responses such as seed germination or chemotropic root growth that improve the likelihood of successful attachment to a host root (Kee et al., 2023; Nelson, 2021). We found examples of three

KAI2d genes in *P. japonicum* that appear to be inactive in plant-based functional assays, similar to *ShKAI2d2*, *ShHTL10*, and *ShHTL11* from *S. hermonthica* (Conn et al., 2015; Toh et al., 2015). Interestingly, phylogenetic analysis separates *KAI2d* genes from *P. japonicum* and *S. hermonthica* into subclades of "inactive" and SL-responsive paralogs (Figure 5). We hypothesize that the "inactive" *KAI2d* are not actually pseudogenes, but instead have adaptive value as antagonists of SL signaling. This is based upon the observations that *PjKAI2d2* and *PjKAI2d3.2* are highly expressed in *P. japonicum* seedlings, show expression patterns that are consistent with feedback regulation (i.e. expression positively correlates with activation of SL signaling), and inhibit SL-induced degradation of PjSMAX1.1 protein in a manner that requires an active catalytic triad (Ogawa et al., 2022) (Figures 3, 4).

We do not yet know how PjKAI2d2 and PjKAI2d3.2 proteins may attenuate SL signaling, but at least two mechanisms seem plausible. One possibility is that these proteins have mutations that allow them to interact with only one signaling partner, SCF^{MAX2} or SMAX1, but not both. This could competitively sequester key components of KAI2-dependent signaling, reducing the ability of proteins like PjKAI2d1 and PjKAI2d4 to trigger polyubiquitination and degradation of SMAX1 in response to SL perception. Surface residues involved in interaction with MAX2 are normally well-conserved among KAI2 and D14 proteins (Bythell-Douglas et al., 2017). In PjKAI2d2 and PjKAI2d3.2 proteins, by contrast, these residues are not conserved, suggesting that interactions with MAX2 may be disrupted (Figure 6). It should be noted that amino acid substitutions at the KAI2 interface with MAX2 may sometimes strengthen, rather than weaken, KAI2–MAX2 protein-protein interactions (Guercio et al., 2023). An alternative possibility is that these proteins may be unable to interact with either SCF^{MAX2} or SMAX1, and instead function as

hydrolases that degrade SL. Indirectly supporting this idea, ShHTL10 and ShHTL11 bind and/or hydrolyze SLs *in vitro*, potentially with a greater affinity than ShHTL7, but do not interact with either MAX2 or SMAX1 in yeast two-hybrid assays in the presence of SLs (Tsuchiya et al., 2015; Wang et al., 2021). On the other hand, overexpression of PjKAI2d2^{R183H} in *P. japonicum* hairy roots blocks chemotropism (Ogawa et al., 2022). Arg183 is a surface residue that is well-conserved in KAI2 and D14 proteins. In *Arabidopsis* and rice D14, the R183H mutation (R233H equivalent in OsD14) putatively disrupts D14 interactions with SMXL7, but does not affect SL hydrolysis activity (Seto et al., 2019). If PjKAI2d2^{R183H} is affected similarly, it suggests that the attenuative activity of PjKAI2d2 occurs through protein-protein interactions rather than SL degradation.

KAI2d proteins that attenuate SL signaling could be advantageous to root parasitic plants. For example, inhibitory responses to SLs that are indicative of a non-host could prevent suicidal germination. Feedback inhibition of SL responses could also be important for chemotropic growth toward a host root by preventing SL signaling systems from becoming saturated and losing orientation.

So-called “perfectly adapted” chemotropic or chemotactic systems are able to sense a concentration gradient of a signal rather than an absolute concentration (Arkowitz, 2009; Insall et al., 2022; Levchenko and Iglesias, 2002). However, this is challenging to achieve; because of their small sizes, the different sides of cells or tissues typically experience very shallow gradients of a diffusible signal. Several strategies have evolved to increase the steepness of a signal gradient. First, the organism or cells may destroy the signal locally. This “self-guiding” or “self-generating” approach to chemotropism or chemotaxis reduces the amount of the signal in the immediate environment to prevent saturation of the receptors and create a local gradient. Second, the amount of available

receptor may be adjusted through transport to or from the site of perception, or changes in the rates of receptor synthesis or degradation. Third, asymmetric spatial distribution of the receptor or signaling machinery may be used to improve perception of a shallow gradient.

Regardless of how *PjKAI2d2* and *PjKAI2d3.2* work, their expression patterns suggest how and when the SL signaling attenuation mechanism is used. These genes are highly expressed in seedlings compared to other *PjKAI2d* paralogs, suggesting that they are more important for seedling growth than germination (Ogawa et al., 2022). In addition, these genes are induced by *rac*-strigol. This change in expression may indicate a negative feedback mechanism: as PjSMAX1 is degraded, putatively in response to *rac*-strigol perception by PjKAI2d1, PjKAI2d4, and PjKAI2d5, the expression of *PjKAI2d2* and *PjKAI2d3.2* increases. PjKAI2d2 and PjKAI2d3.2 activity could then reduce SL signaling locally to make it easier for the root to detect a SL gradient (Figure 7). This model may explain why overexpression of *PjKAI2d2* in *P. japonicum* led to an increase in the frequency of chemotropic root growth toward SL (Ogawa et al., 2022). Finally, expression of these genes is downregulated by nutrients (or upregulated by nutrient deprivation) (Ogawa et al., 2022). This could keep chemotropic growth from occurring when there is no benefit to seeking a host root and engaging in parasitism.

References:

Arellano-Saab, A., Bunsick, M., Al Galib, H., Zhao, W., Schuetz, S., Bradley, J.M., et al. (2021) Three mutations repurpose a plant karrikin receptor to a strigolactone receptor. Proc Natl Acad Sci U S A. 118.
Arkowitz, R.A. (2009) Chemical gradients and chemotropism in yeast. Cold Spring Harb Perspect Biol. 1: a001958.

Blázquez, M.A., Nelson, D.C., and Weijers, D. (2020) Evolution of Plant Hormone Response Pathways. Annu Rev Plant Biol. 71: 327–353.

Bombarely, A., Rosli, H.G., Vrebalov, J., Moffett, P., Mueller, L.A., and Martin, G.B. (2012) A draft genome sequence of Nicotiana benthamiana to enhance molecular plant-microbe biology research. Mol Plant Microbe Interact. 25: 1523–1530.

Bouwmeester, H., Li, C., Thiombiano, B., Rahimi, M., and Dong, L. (2021) Adaptation of the parasitic plant lifecycle: germination is controlled by essential host signaling molecules. Plant Physiol. 185: 1292–1308.

Bunsick, M., Xu, Z., Pescetto, G., Ly, G., Hountalas, J., Boyer, F.-D., et al. (2022) . bioRxiv.
Bythell-Douglas, R., Rothfels, C.J., Stevenson, D.W.D., Graham, S.W., Wong, G.K.-S., Nelson, D.C., et al. (2017) Evolution of strigolactone receptors by gradual neo-functionalization of KAI2 paralogues. BMC Biol. 15: 52.

Carbonnel, S., Torabi, S., Griesmann, M., Bleek, E., Tang, Y., Buchka, S., et al. (2020) Lotus japonicus karrikin receptors display divergent ligand-binding specificities and organ-dependent redundancy. PLoS Genet. 16: e1009249.

Clark, J., and Bennett, T. (2024) Cracking the enigma: understanding strigolactone signalling in the rhizosphere. J Exp Bot. 75: 1159–1173.

Conn, C.E., Bythell-Douglas, R., Neumann, D., Yoshida, S., Whittington, B., Westwood, J.H., et al. (2015) PLANT EVOLUTION. Convergent evolution of strigolactone perception enabled host detection in parasitic plants. Science. 349: 540–543.

Conn, C.E., and Nelson, D.C. (2015) Evidence that KARRIKIN-INSENSITIVE2 (KAI2) Receptors may Perceive an Unknown Signal that is not Karrikin or Strigolactone. Front Plant Sci. 6: 1219.

Cook, C.E., Whichard, L.P., Turner, B., Wall, M.E., and Egley, G.H. (1966) Germination of Witchweed (Striga lutea Lour.): Isolation and Properties of a Potent Stimulant. Science. 154: 1189–1190.

Dor, E., Plakhine, D., Joel, D.M., Larose, H., Westwood, J.H., Smirnov, E., et al. (2020) . Weed Science.
Fernández-Aparicio, M., Flores, F., and Rubiales, D. (2009) Recognition of root exudates by seeds of broomrape (Orobanche and Phelipanche) species. Ann Bot. 103: 423–431.

Fernández-Aparicio, M., Yoneyama, K., and Rubiales, D. (2011) The role of strigolactones in host specificity of Orobanche and Phelipanche seed germination. Seed Sci Res. 21: 55–61.

Flematti, G.R., Ghisalberti, E.L., Dixon, K.W., and Trengove, R.D. (2004) A compound from smoke that promotes seed germination. Science. 305: 977.

Guercio, A.M., Gilio, A.K., Pawlak, J., and Shabek, N. (2023) . bioRxiv.
Hamiaux, C., Drummond, R.S.M., Janssen, B.J., Ledger, S.E., Cooney, J.M., Newcomb, R.D., et al. (2012) DAD2 is an α/β hydrolase likely to be involved in the perception of the plant branching hormone, strigolactone. Curr Biol. 22: 2032–2036.

Insall, R.H., Paschke, P., and Tweedy, L. (2022) Steering yourself by the bootstraps: how cells create their own gradients for chemotaxis. Trends Cell Biol. 32: 585–596.
Jiang, L., Liu, X., Xiong, G., Liu, H., Chen, F., Wang, L., et al. (2013) DWARF 53 acts as a repressor of strigolactone signalling in rice. Nature. 504: 401–405.

Kee, Y.J., Ogawa, S., Ichihashi, Y., Shirasu, K., and Yoshida, S. (2023) Strigolactones in Rhizosphere Communication: Multiple Molecules With Diverse Functions. Plant Cell Physiol. 64: 955–966.

Khosla, A., Morffy, N., Li, Q., Faure, L., Chang, S.H., Yao, J., et al. (2020a) Structure-Function Analysis of SMAX1 Reveals Domains That Mediate Its Karrikin-Induced Proteolysis and Interaction with the Receptor KAI2. Plant Cell. 32: 2639–2659.

Khosla, A., and Nelson, D.C. (2020) Ratiometric Measurement of Protein Abundance after Transient Expression of a Transgene in Nicotiana benthamiana. Bio Protoc. 10: e3747.

Khosla, A., Rodriguez-Furlan, C., Kapoor, S., Van Norman, J.M., and Nelson, D.C. (2020b) A series of dual-reporter vectors for ratiometric analysis of protein abundance in plants. Plant Direct. 4: e00231.

Krupp, A., Bertsch, B., and Spring, O. (2021) Costunolide Influences Germ Tube Orientation in Sunflower Broomrape - A First Step Toward Understanding Chemotropism. Front Plant Sci. 12: 699068.

Larose, H., Plakhine, D., Wycoff, N., Zhang, N., Conn, C., Nelson, D.C., et al. (2022) . bioRxiv.
Levchenko, A., and Iglesias, P.A. (2002) Models of eukaryotic gradient sensing: application to chemotaxis of amoebae and neutrophils. Biophys J. 82: 50–63.

Li, Q., Martín-Fontecha, E.S., Khosla, A., White, A.R.F., Chang, S., Cubas, P., et al. (2022) The strigolactone receptor D14 targets SMAX1 for degradation in response to GR24 treatment and osmotic stress. Plant Communications. 100303.

Martinez, S.E., Conn, C.E., Guercio, A.M., Sepulveda, C., Fiscus, C.J., Koenig, D., et al. (2022) A KARRIKIN INSENSITIVE2 paralog in lettuce mediates highly sensitive germination responses to karrikinolide. Plant Physiol. 190: 1440–1456.

Mutuku, J.M., Cui, S., Yoshida, S., and Shirasu, K. (2021) Orobanchaceae parasite-host interactions. New Phytol. 230: 46–59.

Nakagawa, T., Kurose, T., Hino, T., Tanaka, K., Kawamukai, M., Niwa, Y., et al. (2007) Development of series of gateway binary vectors, pGWBs, for realizing efficient construction of fusion genes for plant transformation. J Biosci Bioeng. 104: 34–41.

Nelson, D.C. (2021) The mechanism of host-induced germination in root parasitic plants. Plant Physiol. 185: 1353–1373.

Nelson, D.C., Flematti, G.R., Ghisalberti, E.L., Dixon, K.W., and Smith, S.M. (2012) Regulation of seed germination and seedling growth by chemical signals from burning vegetation. Annu Rev Plant Biol. 63: 107–130.

Nomura, S., Nakashima, H., Mizutani, M., Takikawa, H., and Sugimoto, Y. (2013) Structural requirements of strigolactones for germination induction and inhibition of Striga gesnerioides seeds. Plant Cell Rep. 32: 829–838.

Ogawa, S., Cui, S., White, A.R.F., Nelson, D.C., Yoshida, S., and Shirasu, K. (2022) Strigolactones are chemoattractants for host tropism in Orobanchaceae parasitic plants. Nat Commun. 13: 4653.

Ogawa, S., and Shirasu, K. (2022) Strigol induces germination of the facultative parasitic plant in the absence of nitrate ions. Plant Signal Behav. 17: 2114647.

de Saint Germain, A., Jacobs, A., Brun, G., Pouvreau, J.-B., Braem, L., Cornu, D., et al. (2021) A Phelipanche ramosa KAI2 protein perceives strigolactones and isothiocyanates enzymatically. Plant Communications. 2: 100166.

Seto, Y., Yasui, R., Kameoka, H., Tamiru, M., Cao, M., Terauchi, R., et al. (2019) Strigolactone perception and deactivation by a hydrolase receptor DWARF14. Nat Commun. 10: 191.

Soundappan, I., Bennett, T., Morffy, N., Liang, Y., Stanga, J.P., Abbas, A., et al. (2015) SMAX1-LIKE/D53 Family Members Enable Distinct MAX2-Dependent Responses to Strigolactones and Karrikins in Arabidopsis. Plant Cell. 27: 3143–3159.

Stanga, J.P., Morffy, N., and Nelson, D.C. (2016) Functional redundancy in the control of seedling growth by the karrikin signaling pathway. Planta. 243: 1397–1406.

Stanga, J.P., Smith, S.M., Briggs, W.R., and Nelson, D.C. (2013) SUPPRESSOR OF MORE AXILLARY GROWTH2 1 controls seed germination and seedling development in Arabidopsis. Plant Physiol. 163: 318–330.

Steenwyk, J.L., Buida, T.J., 3rd, Li, Y., Shen, X.-X., and Rokas, A. (2020) ClipKIT: A multiple sequence alignment trimming software for accurate phylogenomic inference. PLoS Biol. 18: e3001007.

Stirling, S.A., Guercio, A.M., Patrick, R.M., Huang, X.-Q., Bergman, M.E., Dwivedi, V., et al. (2024) Volatile communication in plants relies on a KAI2-mediated signaling pathway. Science. 383: 1318–1325.
Stirnberg, P., Furner, I.J., and Ottoline Leyser, H.M. (2007) MAX2 participates in an SCF complex which acts locally at the node to suppress shoot branching. Plant J. 50: 80–94.

Sun, X.-D., and Ni, M. (2011) HYPOSENSITIVE TO LIGHT, an alpha/beta fold protein, acts downstream of ELONGATED HYPOCOTYL 5 to regulate seedling de-etiolation. Mol Plant. 4: 116–126.

Sun, Y.K., Yao, J., Scaffidi, A., Melville, K.T., Davies, S.F., Bond, C.S., et al. (2020) Divergent receptor proteins confer responses to different karrikins in two ephemeral weeds. Nat Commun. 11: 1264.

Takei, S., Uchiyama, Y., Bürger, M., Suzuki, T., Okabe, S., Chory, J., et al. (2023) A Divergent Clade KAI2 Protein in the Root Parasitic Plant Orobanche minor Is a Highly Sensitive Strigolactone Receptor and Is Involved in the Perception of Sesquiterpene Lactones. Plant Cell Physiol. 64: 996–1007.

Tamura, K., Stecher, G., and Kumar, S. (2021a) MEGA11: Molecular Evolutionary Genetics Analysis Version 11. Mol Biol Evol. 38: 3022–3027.

Toh, S., Holbrook-Smith, D., Stogios, P.J., Onopriyenko, O., Lumba, S., Tsuchiya, Y., et al. (2015) Structure-function analysis identifies highly sensitive strigolactone receptors in Striga. Science. 350: 203–207.

Trifinopoulos, J., Nguyen, L.-T., von Haeseler, A., and Minh, B.Q. (2016) W-IQ-TREE: a fast online phylogenetic tool for maximum likelihood analysis. Nucleic Acids Res. 44: W232–5.

Tsuchiya, Y., Yoshimura, M., Sato, Y., Kuwata, K., Toh, S., Holbrook-Smith, D., et al. (2015) PARASITIC PLANTS. Probing strigolactone receptors in Striga hermonthica with fluorescence. Science. 349: 864–868.

Uraguchi, D., Kuwata, K., Hijikata, Y., Yamaguchi, R., Imaizumi, H., Am, S., et al. (2018) A femtomolar-range suicide germination stimulant for the parasitic plant Striga hermonthica. Science. 362: 1301–1305.

Wang, L., Wang, B., Jiang, L., Liu, X., Li, X., Lu, Z., et al. (2015) Strigolactone Signaling in Arabidopsis Regulates Shoot Development by Targeting D53-Like SMXL Repressor Proteins for Ubiquitination and Degradation. Plant Cell. 27: 3128–3142.

Wang, L., Xu, Q., Yu, H., Ma, H., Li, X., Yang, J., et al. (2020) Strigolactone and Karrikin Signaling Pathways Elicit Ubiquitination and Proteolysis of SMXL2 to Regulate Hypocotyl Elongation in Arabidopsis. Plant Cell. 32: 2251–2270.

Wang, Y., Yao, R., Du, X., Guo, L., Chen, L., Xie, D., et al. (2021) Molecular basis for high ligand sensitivity and selectivity of strigolactone receptors in Striga. Plant Physiol. 185: 1411–1428.

Wang, Z.-P., Xing, H.-L., Dong, L., Zhang, H.-Y., Han, C.-Y., Wang, X.-C., et al. (2015) Egg cell-specific promoter-controlled CRISPR/Cas9 efficiently generates homozygous mutants for multiple target genes in Arabidopsis in a single generation. Genome Biol. 16: 144.

Waters, M.T., Gutjahr, C., Bennett, T., and Nelson, D.C. (2017) Strigolactone Signaling and Evolution. Annu Rev Plant Biol. 68: 291–322.

Waters, M.T., and Nelson, D.C. (2022) Karrikin perception and signalling. New Phytol.
Waters, M.T., Nelson, D.C., Scaffidi, A., Flematti, G.R., Sun, Y.K., Dixon, K.W., et al. (2012) Specialisation within the DWARF14 protein family confers distinct responses to karrikins and strigolactones in Arabidopsis. Development. 139: 1285–1295.

Waters, M.T., Scaffidi, A., Flematti, G., and Smith, S.M. (2015a) Substrate-Induced Degradation of the α/β-Fold Hydrolase KARRIKIN INSENSITIVE2 Requires a Functional Catalytic Triad but Is Independent of MAX2. Mol Plant. 8: 814–817.

Waters, M.T., Scaffidi, A., Moulin, S.L.Y., Sun, Y.K., Flematti, G.R., and Smith, S.M. (2015b) A Selaginella moellendorffii Ortholog of KARRIKIN INSENSITIVE2 Functions in Arabidopsis Development but Cannot Mediate Responses to Karrikins or Strigolactones. Plant Cell. 27: 1925–1944.

White, A.R.F., Mendez, J.A., Khosla, A., and Nelson, D.C. (2022) Rapid analysis of strigolactone receptor activity in a Nicotiana benthamiana dwarf14 mutant. Plant Direct. 6: e389.

Whitney, P.J., and Carsten, C. (1981) Chemotropic Response of Broomrape Radicles to Host Root Exudates. Ann Bot. 48: 919–921.

Williams, C.N. (1961) Tropism and morphogenesis of Striga seedlings in the host rhizosphere. Ann Bot. 25: 407–415.

Xing, H.-L., Dong, L., Wang, Z.-P., Zhang, H.-Y., Han, C.-Y., Liu, B., et al. (2014) A CRISPR/Cas9 toolkit for multiplex genome editing in plants. BMC Plant Biol. 14: 327.

Xu, Y., Zhang, J., Ma, C., Lei, Y., Shen, G., Jin, J., et al. (2022) Comparative genomics of orobanchaceous species with different parasitic lifestyles reveals the origin and stepwise evolution of plant parasitism. Mol Plant. 15: 1384–1399.

Yao, J., Mashiguchi, K., Scaffidi, A., Akatsu, T., Melville, K.T., Morita, R., et al. (2018) An allelic series at the KARRIKIN INSENSITIVE 2 locus of Arabidopsis thaliana decouples ligand hydrolysis and receptor degradation from downstream signalling. Plant J. 96: 75–89.

Yao, R., Ming, Z., Yan, L., Li, S., Wang, F., Ma, S., et al. (2016) DWARF14 is a non-canonical hormone receptor for strigolactone. Nature. 536: 469–473.

Yao, R., Wang, F., Ming, Z., Du, X., Chen, L., Wang, Y., et al. (2017) ShHTL7 is a non-canonical receptor for strigolactones in root parasitic weeds. Cell Res. 27: 838–841.

Yoshida, S., Kim, S., Wafula, E.K., Tanskanen, J., Kim, Y.-M., Honaas, L., et al. (2019) Genome Sequence of Striga asiatica Provides Insight into the Evolution of Plant Parasitism. Curr Biol. 29: 3041–3052.e4.

Zheng, J., Hong, K., Zeng, L., Wang, L., Kang, S., Qu, M., et al. (2020) Karrikin Signaling Acts Parallel to and Additively with Strigolactone Signaling to Regulate Rice Mesocotyl Elongation in Darkness. Plant Cell. 32: 2780–2805.

Zhou, F., Lin, Q., Zhu, L., Ren, Y., Zhou, K., Shabek, N., et al. (2013) D14-SCF(D3)-dependent degradation of D53 regulates strigolactone signalling. Nature. 504: 406–410.

Figures:

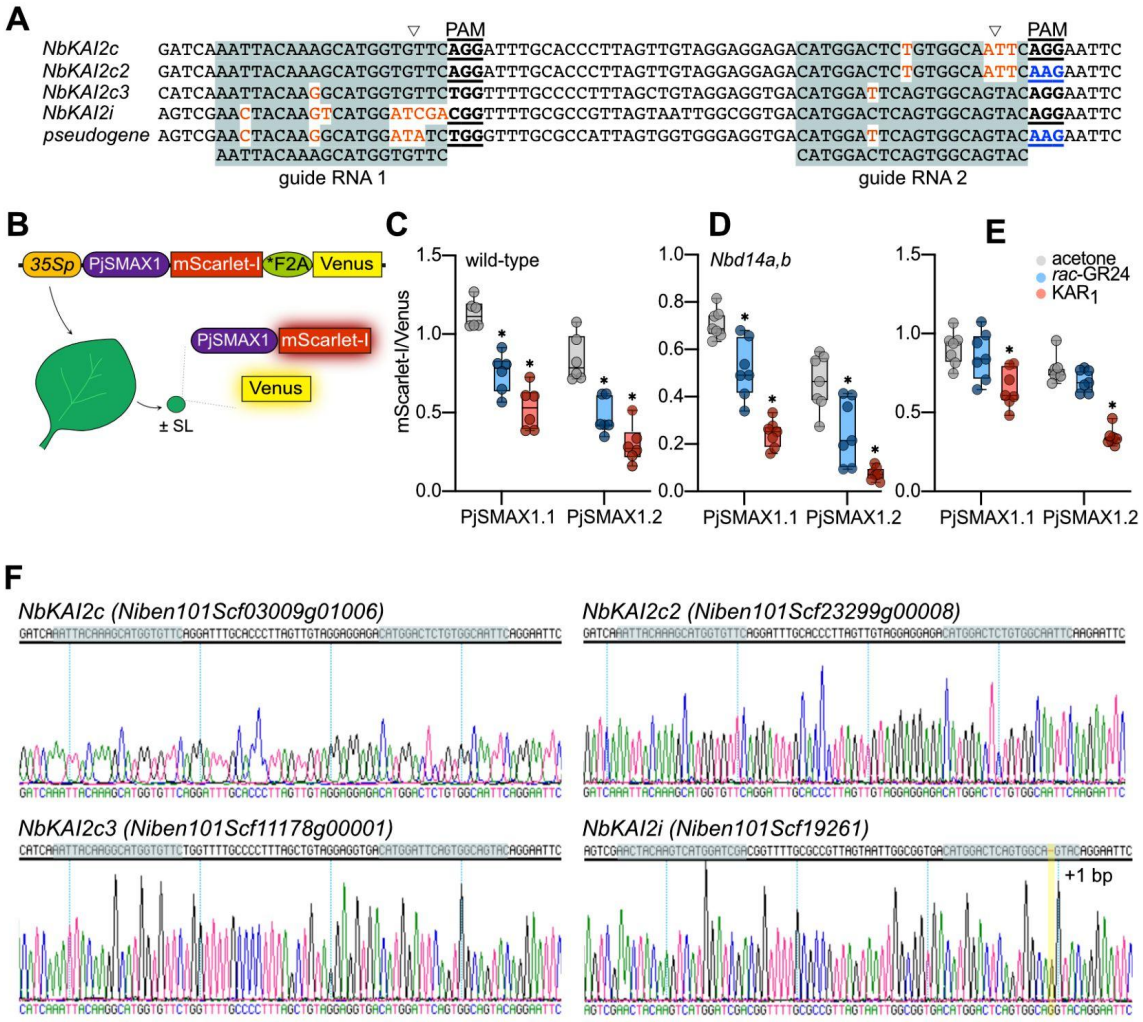


Figure 3.1. Generation of a SL-insensitive *N. benthamiana* mutant

(A) Two guide RNA (gRNA) target sites in *N. benthamiana KAI2* genes. Sequence excerpts from the second exon of the four *NbKAI2d* genes and one pseudogene are shown. Triangle, Cas9 cleavage site. Light-blue shading, gRNA recognition site. Blue text, non-preferred PAM 'NAG' for SpCas9. Red text, mismatch to gRNA. Protospacer adjacent motif (PAM) is underlined and in bold. **(B)** Schematic representation of the PjSMAX1 ratiometric reporter assay. pRATIO1212 construct (top, nuclear localization sequence at N-terminal end of PjSMAX1 is not shown) is transformed into *N. benthamiana* leaves. Excised leaf discs are treated and measured for mScarlet-I and Venus fluorescence by a plate reader. **(B)-(E)** Ratio of PjSMAX1-mScarlet-I fluorescence to Venus fluorescence in wild-type **(B)**, *Nbd14a,b* **(C)**, and a SL-insensitive mutant isolated from a Nbd14a,b transgenic CRISPR-Cas9 transgenic line using gRNAs described in **(A)**. Excised leaf discs were treated with either 0.02% (v/v) acetone, 10 µM *rac*-GR24, or 10 µM KAR_1 and fluorescence was

read ~16h post treatment. Each data point represents the average ratio of mScarlet-I to Venus fluorescence of 4-8 leaf discs from a single transformed leaf. n = 4-7 leaves. *$P < 0.05$, paired two-way ANOVA, comparison of treatments to acetone control with Bonferroni correction for multiple comparisons. Note that the range of mScarlet-I/Venus ratios varies between experiments due to experiment-specific optimization of gain for each fluorophore during fluorescence measurements. **(F)** Sanger sequence of the CRISPR-Cas9-targeted regions in the SL-insensitive mutant line identified in **(E)**. Top sequence is reference, bottom sequence is from the mutant. The mutant has a 1 bp insertion, which causes a frameshift, at the second gRNA site.

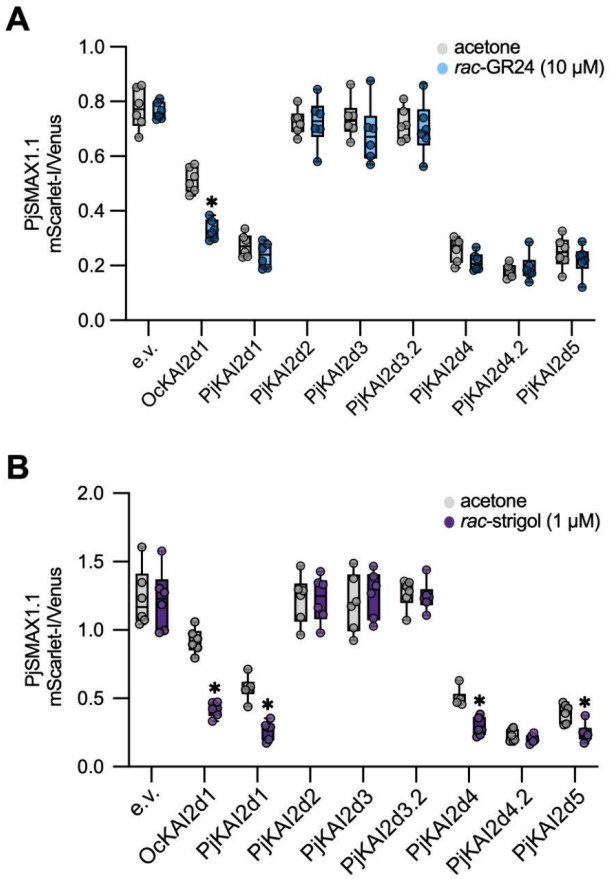


Figure 3.2 Analysis of PjKAI2d activity

Analysis of PjSMAX1.1 ratiometric reporter co-transformed with pGWB402-PjKAI2d constructs in *Nbd14a,b kai2i* leaves. **(A)** Co-transformed leaf discs treated with 0.02% (v/v) acetone or 10 µM *rac*-GR24 treatment. **(B)** Co-transformed leaf discs treated with 0.01% (v/v) acetone or 1 µM *rac*-strigol treatment. n = 6 leaves per construct, mean ratio of 4-6 discs per leaf. **P* < 0.05, paired two-way ANOVA, comparison of treatments to acetone control with Bonferroni correction for multiple comparisons. Box plot whiskers indicate minimum and maximum values.

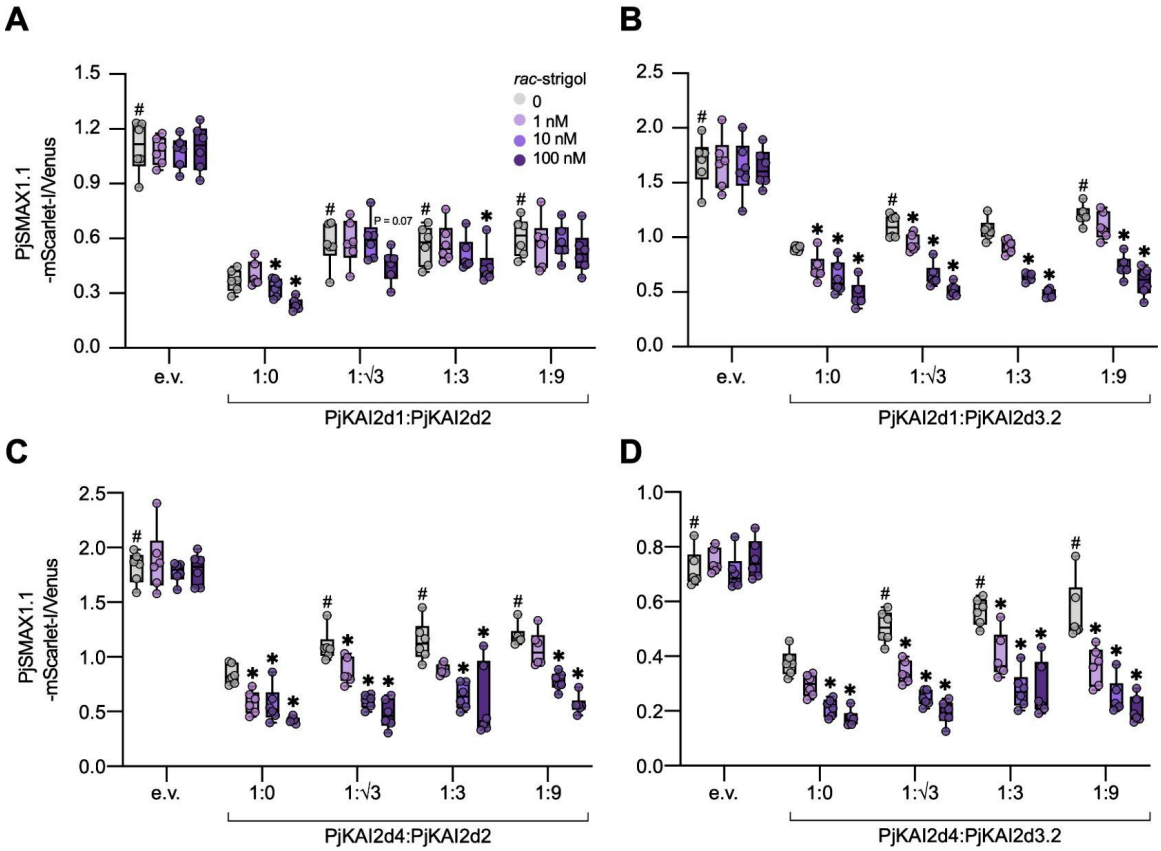


Figure 3.3 Attenuation of PjSMAX1.1 degradation by PjKAI2d2 and PjKAI2d3.2

pRATIO1212-PjSMAX1.1 was co-transformed with varying ratios of *A. tumefaciens* cells carrying **(A)** *PjKAI2d1* and *PjKAI2d2*, **(B)** *PjKAI2d1* and *PjKAI2d3.2*, **(C)** *PjKAI2d4* and *PjKAI2d2*, or **(D)** *PjKAI2d4* and *PjKAI2d3.2*. Final OD_{600} was brought to 1.2 with *A. tumefaciens* cells carrying an empty pGWB402 vector. Leaf discs were treated with 0.01% (v/v) acetone, 1 nM, 10 nM, or 100 nM *rac*-strigol. e.v., pGWB402. n = 6 leaves per construct, mean ratio of 4-6 discs per leaf. $^{*}P < 0.05$, paired two-way ANOVA, comparison of treatments to acetone control with Bonferroni correction for multiple comparisons. $^{\#}P < 0.05$, one-way ANOVA with Bonferroni correction, comparison of acetone-treated controls to 1:0 ratio transformations. Box plot whiskers indicate minimum and maximum values.

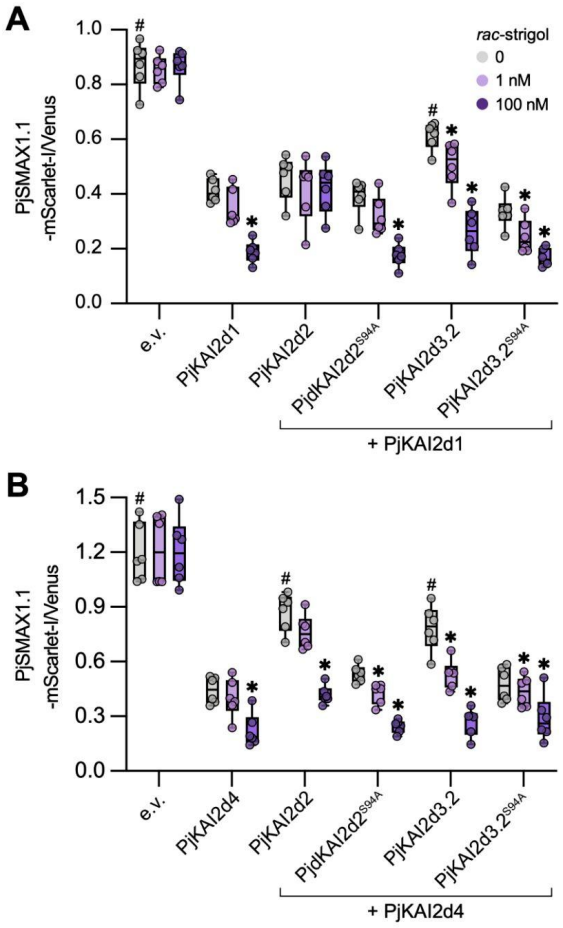


Figure 3.4 Catalytic serine is required for PjKAI2d2 and PjKAI2d3.2 attenuation effects

PjSMAX1.1 was co-transformed with mixtures (1:9) of *A. tumefaciens* cells carrying **(A)** PjKAI2d1 or **(B)** PjKAI2d4 with PjKAI2d2 or PjKAI2d3.2 and the S94A catalytic mutant for each.. Final OD_{600} was brought to 1.2 with *A. tumefaciens* cells carrying an empty pGWB402 vector. Leaf discs were treated with 0.01% (v/v) acetone, 1 nM, or 100 nM *rac*-strigol. e.v., pGWB402. n = 6 leaves per construct, mean ratio of 4-6 discs per leaf. $^{*}P < 0.05$, paired two-way ANOVA, comparison of treatments to acetone control with Bonferroni correction for multiple comparisons. $^{\#}P < 0.05$, one-way ANOVA with Bonferroni correction, comparison of acetone-treated controls to PjKAI2d2 or PjKAI2d4 1:0 ratio transformations. Box plot whiskers indicate minimum and maximum values.

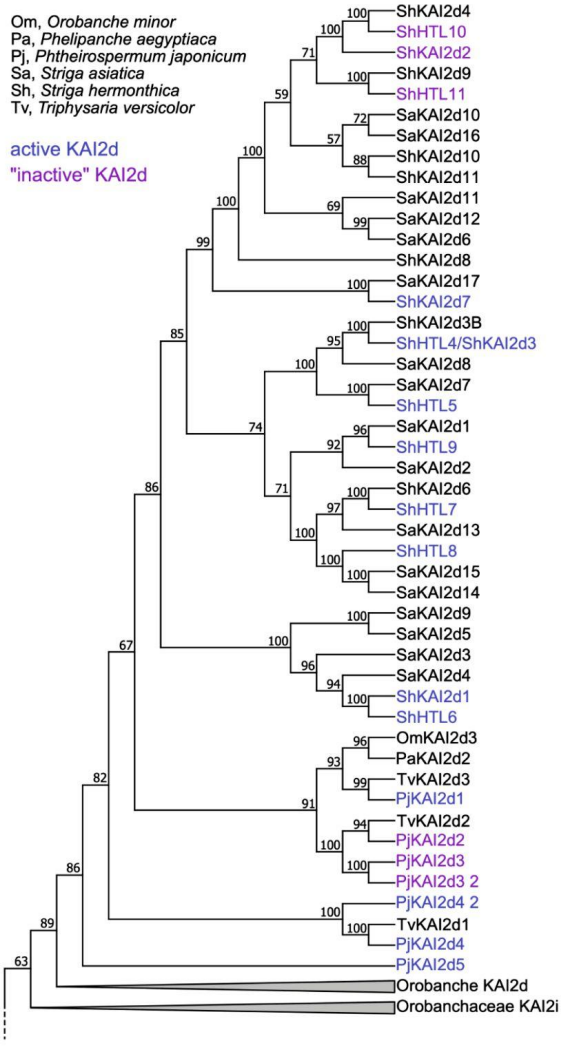


Figure 3.5 Phylogenetic analysis of KAI2 proteins in parasitic plants

Cladogram of KAI2d proteins in parasitic Orobanchaceae. Full cladogram of KAI2 proteins shown in Figure S1. Parasitic KAI2d proteins that have shown SL signaling activity in heterologous plant assays (e.g. cross-species complementation of *A. thaliana* or SMAX1 reporter degradation in *N. benthamiana*) are considered active (blue); those that have not shown SL signaling activity are termed “inactive” (purple) but may have alternative activities such as SL signaling attenuation. Activities were reported in (Conn et al., 2015; Toh et al., 2015) (Figure 2). Bootstrap values, shown, were calculated using UltraFast (10,000 iterations). Branches are not scaled.

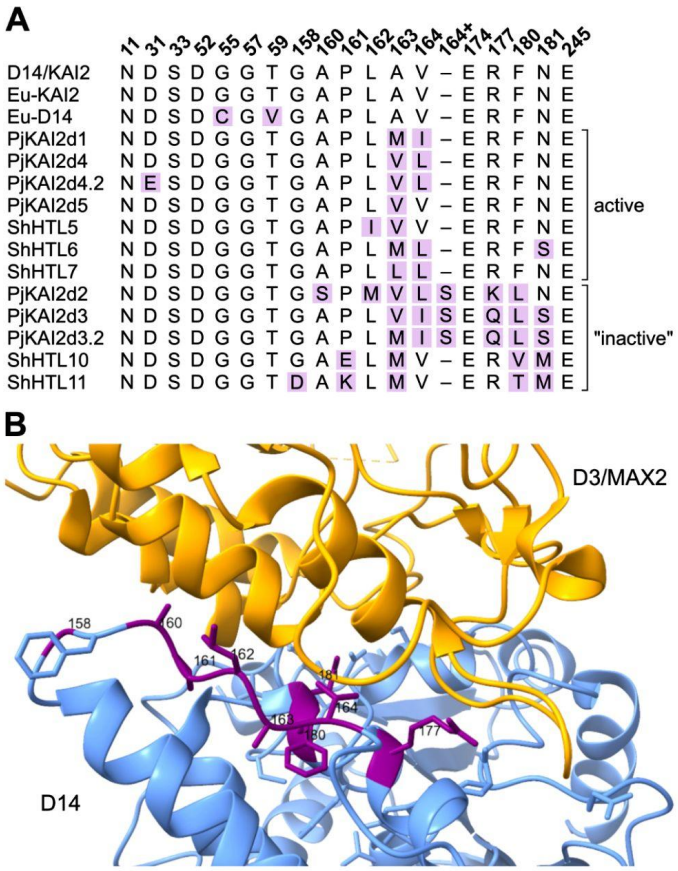


Figure 3.6 PjKAI2d amino acid identities at the MAX2 interface

(A) Amino acid identities of parasite KAI2d proteins at residues important for D14–D3/MAX2 interaction as determined by (Yao et al., 2016). Residues highlighted in purple indicate differences from the highly conserved consensus residues of D14/KAI2, Eu-KAI2, and Eu-D14 protein classes (Bythell-Douglas et al., 2017). Residue numbers are based on *Arabidopsis thaliana* D14 (Yao et al., 2016). Residue 164+ is an extra residue found in PjKAI2d2, PjKAI2d3, and PjKAI2d3.2 with no corresponding residue in AtD14. Parasitic KAI2d proteins that have shown SL signaling activity in heterologous plant assays (e.g. cross-species complementation of *A. thaliana* or SMAX1 reporter degradation in *N. benthamiana*) are considered active; those that have not shown SL signaling activity are termed “inactive” but may actually have alternative activities such as SL signaling attenuation. **(B)** Three-dimensional protein structure of AtD14–D3-ASK1 complex from PDB model 5HZG (Yao et al., 2016). Non-consensus residues from **(A)** in at least one “inactive” PjKAI2d or ShHTL protein are marked in purple. AtD14 structure, blue; D3/MAX2 structure, orange.

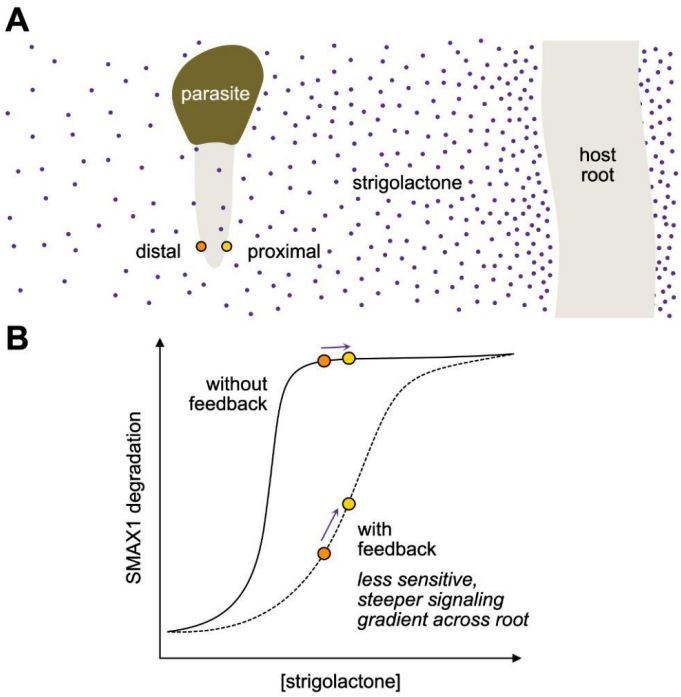


Figure 3.7 Model for strigolactone signaling attenuation during parasite chemotropism

(A) Strigolactones (purple) exuded from a host root putatively decrease in concentration at increasing distances from the root. Chemotropic growth toward the host root may require a nascent parasitic seedling to differentiate between very similar strigolactone concentrations at the host-proximal (yellow) and host-distal (orange) sides of its root. **(B)** Strigolactone perception in parasitic seeds and seedlings putatively causes degradation of SMAX1. Feedback inhibition or attenuation of strigolactone signaling by proteins such as PjKAI2d2 and PjKAI2d3.2 reduces responses to low concentrations of strigolactone (dashed line). This could allow the parasitic seedling to experience a steeper strigolactone signaling gradient across the proximal and distal sides of the root, allowing orientation toward the host based on differential SMAX1 degradation, at the expense of strigolactone sensitivity

Supplemental figures and tables:

Table S1. Primer sequences

Primer name	Sequence	Use
NbKAI2-F0	5'-TGCATGGACTCAGTGGCAGTACGTTTTAGAGCTAGAAATAGC-3'	gRNA cloning
NbKAI2-R0	5'-AACGAACACCATGCTTTGTAATTCAATCTCTTAGTCGACTCTAC-3'	
NbKAI2-BsR	5'-ATTATTGGTCTCGAAACGAACACCATGCTTTGTAATTCAA-3'	
NbKAI2-BsF	5'-ATATATGGTCTCGATTGCATGGACTCAGTGGCAGTACGTT-3'	
U6-26p-F	5'-TGTCCCAGGATTAGAATGATTAGGC-3'	colony PCR & sequencing of CRISPR-Cas9 construct
U6-29p-R	5'-AGCCCTCTTCTTTCGATCCATCAAC-3'	
U6-29p-F	5'-TTAATCCAAACTACTGCAGCCTGAC-3'	
pHEE401EhygB-F	5'-CGTGCTTTCAGCTTCGATGTAG-3'	transgene detection
pHEE401EhygB-R	5'-CAGTCAATGACCGCTGTTATGC-3'	
NbKAI2c1_int_F	5'-GGCTTAGGGATAGTTCCTTG-3'	NbKAI2 genotyping
NbKAI2c1_3utr_R	5'-CAACTTCCAAGTAATTGCGTAC-3'	
NbKAI2c2a_int_F	5'-GAGGAGGGGGTAATAGTGTAG-3'	
NbKAI2c2a_int_F	5'-CCCGGGTCTGCAGCTGCACTTTCT-3'	
NbKAI2c2b_int_F	5'-CCCGGGTCTGCACTTTCT-3'	
NbKAI2c2b_R	5'-CGAGGTGCTGGTTGAGGTACTCGGAC-3'	
NbKAI2i_int_F	5'-GGTAATTTTGGATCGTAGCATCAGTC-3'	

NbKAI2i_R	5’-CACAGGGACGGCCAAATCCTTGGAG-3’	
M13puc_F	5’-CCCAGTCACGACGTTGTAAAACG-3’	pENTR/pDONR221 a PjKAI2 and PjSMAX1 colony PCR and genotyping
M13_R	5’-GGAAACAGCTATGACCATG-3’	
35s_F	5’-CTATCCTTCGCAAGACCCTTC-3’	pGWB402 PjKAI2 colony PCR and genotyping
M13puc_R	5’-AGCGGATAACAATTTCACACAGG-3’	
35s_F	5’-CTATCCTTCGCAAGACCCTTC-3’	pRATIO1212 PjSMAX1 colony PCR and genotyping
MScarlet-I_R	5’-TAATCACAGCTTCGCCCTTG-3’	
PjSMAX1.1_F1	5’-GGAACCCAGTCTTAGTCGGTG-3’	
PjSMAX1.1_F2	5’-CAAGAAATGGACAGATACGTG-3’	
PjSMAX1.2_F1	5’-GGATTATGTAAATTTGAAGA-3’	
PjSMAX1.2_F2	5’-ATCAGAGCACTCGTCTTGAT-3’	
PjKAI2d2^{S94A}_F	5’- CATCGGCCACGCGTTGTCCTCCA-3’	PjKAI2^{S94A} site directed mutagenesis cloning
PjKAI2d2^{S94A}_R	5’- AATATACATTTTCCGACTTTAAATTCCTCTAG-3’	
PjKAI2d3.2^{S94A}_F	5’-CATCGGCCACGCGTTGTCCCCCT-3’	
PjKAI2d3.2^{S94A}_R	5’- AATATACATTTTCGGACGTTGAATTCATCG-3’	

Table S2. *NbKAI2* coding sequences

Gene Name	Gene Identifier	Sequence
NbKAI2c1	Niben101Scf11178:58570..58937	ATGGGAATAGTTGAAGAAGCACACAACGTCAAGGTTTTAGGGAC AGGGGAAGGAACCATAGTCCTAGCTCATGGGTTTGGGACAGAC CAATCGGTGTGGAAACATCTGGTTCCTCATCTAGTTGACGATTA CAAGGTTGTCTTGTTTGACAACATGGGTGCTGGAACTACCAACC CAGACTACTTTGACTTTGAAAGGTATTCAACCTTAGAAGGCTATG CCTATGATGTGATCGCTATTTTGGAAGAACTCCAAATTACTAGTT GCATTTATGTTGGACACTCTGTTTCTGCTATGGTTGGTGCCATC GCTTCTGTTGCTCGTCCCGATCTCTTCACCAAACTTGTTACTGTC TCCGCTTCTCCCAGGTATTTGAATGACGTGGACTATTACGGAGG ATTCGAGCAAGAAGATCTGGATCAACTGTTTGAAGCAATGACAT CAAATTACAAGGCATGGTGTTCTGGTTTTGCCCCTTTAGCTGTA GGAGGTGACATGGATTCAGTGGCAGTACAGGAATTCAGCAGGA CATTGTTCAACATGAGACCTGACATTGCATTAAGCGTATTACAAA TTATATTCCAAAGTGATTTAAGGCATTTGTTGCCTCATGTGACTG TTCCCTGTCATATAATTCAAAGCATGAAGGATTTGGCTGTACCAG TGGTGGTTTCTGAATATCTTCACCAGAACCTCGGCGGCGGATCT ATCGTCGAGGTAATGTCGACGGATGGCCATCTGCCGCAATTGA GTTCACCTGATGTTGTTATTCCGGTGTTGCTTAGGCATATTCGTT ATGATATTGCCGTTGACTAA
NbKAI2c2a	Niben101Scf03009:139775..140142	ATGGGTATTGTTGAAGAAGCACACAACGTGAAGATCTTAGGGTC AGGAGAGCAAACCGTAGTGTTAGCCCATGGGTTCGGAACAGAC CAGTCTGTGTGGAAACACTTGGTTCCTCACTTGGTTGATGATTAT AAGATCATATTGTTTGACAATATGGGTGCTGGAACAACTAATCCT GACTACTTTGACTTCGACAGATATTCTAGCCTACAAGGCTATGCT TATGATGTGATTGCGATTTTAGAGGACCTCAAAATTCCTAATTGC ATTTACGTCGGTCACTCTGTTTCTGCCATGATTGGCGTCATTGCT TCCATCGCTCGTCCTGATCTATTCACCAAACTTGTCACTGTCTCT

		GCCTCTCCAAGGTATCTGAACGACTCGGACTACTATGGAGGATT TGAACAGGAAGATCTGGATCAATTGTTCGAAGCAATGAGATCAA ATTACAAAGCATGGTGTTCAGGATTTGCACCCTTAGTTGTAGGA GGAGACATGGACTCTGTGGCAATTCAGGAATTCAGCAGGACATT ATTCAACATGAGGCCAGATATAGCACTAAGTGTGTTACAAATCAT ATTCCTAAGTGATTTAAGGCATTTGTTGGCTCATGTAACTGTCCC ATGTCACTTAATTCAGAGCATGAAGGACCTGGCCGTGCCTGTGG TGGTGTCTGAGTACCTCCATCAGCACCTCGGTGGCGAGTCTATC GTGGAGGTGATGTCCACGGAAGGCCATCTGCCGCAACTCAGCT CACCGGATGTTGTTATTCCGGTGCTGCTTCGCCATATTCGTCAT GATATTGTCGTTTGA
NbKAI2c2b	Niben101Scf23299:17977..18344	ATGGGTATAGTTGAAGAAGCACACAACGTGAAGATTCTAGGGTC AGGTGAGCAAACCGTAGTGTTAGCCCATGGGTTCGGAACAGAC CAGTCTGTGTGGAAACACTTGGTTCCTCACTTGGTTGATGATTA CAAGATCATATTGTTTGACAATATGGGTGCTGGAACAACTAATCC TGACTACTTTGACTTCGACAGATATTCTAGCCTAGAAGGCTATG CTTATGATGTGATCGCGATTTTGGAGGACCTCAAAATTCCTGGT TGCATTTACGTCGGCCACTCTGTTTCTGCCATGATTGGCGTCAT TGCTTCCGTCGCTCGTCCTGATCTTTTCACCAAACTTGTCACTGT CTCTGCCTCTCCAAGGTATCTGAACGACTCGGACTACTATGGAG GATTTGAACAGGAAGACCTGGATCAATTATTTGAAGCAATGAGA TCAAATTACAAAGCATGGTGTTCAGGATTTGCACCCTTAGTTGTA GGAGGAGACATGGACTCTGTGGCAATTCAAGAATTCAGCAGGA CATTATTCAACATGAGGCCAGACATTGCACTAAGTGTGTTACAAA TCATATTCCTAAGTGATTTAAGGCATTTGTTGGCTCATGTAACTG TCCCATGTCACATAATTCAGAGCATGAAGGATCTGGCCGTGCCT GTGGTGGTGTCCGAGTACCTCAACCAGCACCTCGGTGGTGAGT CTATCGTAGAGGTGATGTCCACGGAAGGCCATCTGCCGCAACT CAGCTCACCGGATGTTGTTATTCCGGTGCTGCTTCGCCATATTC GTCATGATATTGTCGTTTGA

NbKAI2i	Niben101Scf19261:35020..35387	ATGGGAGTAGTTGAAGAAGCTCACAACGTTAAAGTGGTTGGCTCAGGCGAGAAGACGGTGGTACTTGGCCATGGCTTTGGCACTGATCAATCTGTTTGGAAACACCTCATACCTTACCTAGTTGATGACTATAGAGTAGTTGTATATGACAACATGGGTGCTGGACCGACAAATCCTGATTACTTTGATTTTGAACGATATGCTTCTCTAGAAGGTTATGCCTATGATTTACTTGCCATTTTGGAGGAGCTTCAGATTGATTCTTGCATTTATTTAGGCCATTCCTTATCGTCTATGACTGGTGTTATTGCTTCCATATTTCGTCCTGATCTCTTCTCCAAAATCATCTTGCTTTCTGCTTCTCCAAGGTTTATAAATACAGATGACTATTACGGAGGATTTGAAAAGGAAGATATTGACCAACTAAGCCAAGCGATGGAGTCGAACTACAAGTCATGGATCGACGGTTTTGCGCCGTTAGTAATTGGCGGTGACATGGACTCAGTGGCAGTACAGGAATTCAGCAGAACCTTATTCAACATGAGACCAGACATAGCACTTAGTGTCTTTCGTACAATTTTCACATTTGATTTAAGGCATTTTCTATCTCGTGTCACAGTGCCTTGTCACATAATTCAGAGCTCCAAGGATTTGGCCGTCCCTGTGGCTGTCTCAGAATATATTCACCAAAATTTGGGAGGAAAGTCAATTGTGGAAGTCATCTCAACTGAAGGTCATCTTCCTCAGTTGAGTGCACCAGAAGTCACTGTTCCTGTGCTGCTTCGCCATATTTCTCATGATATTTCCAGTGATACTGTTTAG

Conclusion and future directions:

The work presented in this dissertation provides a novel method for testing SL and KAR receptors' functionality. This method uses a transient tobacco system to target downstream protein partners for degradation, thereby providing a unique approach to studying strigolactone signaling. By establishing strigolactone signaling mutants in *Nicotiana benthamiana,* we can test various aspects of strigolactone signaling. In this dissertation, I have demonstrated the effectiveness of this transient system by testing D14 variants and strigolactone signaling systems from a hemiparasite. This system offers a more feasible alternative to creating stable *Arabidopsis* lines or labor-intensive biochemical work that often accompanies the studies of SL and KAR signaling pathways. Therefore, there are many new directions in which this transient system can be used.

The evolutionary relationship between SL and KL signaling contains many unresolved questions. Non-seed plants typically contain KAI2-like orthologs and orthologs of the DDk lineage, the lineage from which D14 emerged; however, there has been limited research on the exact function of these receptors(Bythell-Douglas et al., 2017; Machin et al., 2020; Moturu et al., 2018). These receptors have yet to be tested, and the transient tobacco system could be used to understand what signaling partners interact with each other. For example, extensive research has investigated the roles of the 13 KAI2/D14 homologs found in the moss *Physcomitrium patens*(Lopez-Obando et al., 2021). However, when expressing these receptors into *Arabidopsis*, they did not rescue the *d14* and *kai2* mutant phenotypes was not achieved, likely due to poor interaction with *Arabidopsis* signaling components(Lopez-Obando et al., 2021). I recommend re-capitulating the *P.*

patens signaling pathway in *N. benthamiana* to determine how these receptors interact with PpSMXL proteins under various treatments.

It is worth noting that while gymnosperms contain D14 and KAI2 orthologs, they do not have an ortholog of SMXL7/D53 type SMXLs. This suggests that D14 may target the SMAX1 ortholog found in gymnosperms instead(Bythell-Douglas et al., 2017; Kodama et al., 2023; Machin et al., 2020; Moturu et al., 2018). If this is true, it could mean that the signaling specificity in gymnosperm D14s is more promiscuous than in angiosperm D14 proteins. While Arabidopsis D14 can interact with SMAX1, it is a weaker interaction than with SMXL7. I would propose gymnosperm D14 proteins could interact with gymnosperm SMAX1 proteins, potentially having a mix of specificity-determining residues KAI2-like and D14-like(Li et al., 2022; Wang et al., 2020). The transient system in this dissertation could offer a valuable platform for testing SL and KAR receptors and potential protein partners from different lineages.

This transient system could be used to test different parasitic SL receptors found in Orobanchaceae, as was done in Chapter Three. Most species in this family have multiple homologs of *KAI2* genes belonging to the divergent *KAI2* clade; however, it is unclear how each of these receptors functions(Conn et al., 2015). We could determine which parasitic receptors can transduce host-derived SL signals by transiently co-expressing each of these receptors with the SMAX1 reporter in *N. benthamiana*. Moreover, as demonstrated in Chapter Three, this system could be utilized to identify the function of SL receptors, previously considered non biologically functional or pseudogenes. Lastly, host-derived strigolactones can be used with each receptor to determine the specificity of KAI2d receptors. Parasitic weeds in Orobanchaceae cause devastating losses on economically important crops, such as maize, sorghum, and

cowpea (Clarke et al., 2019; Mutuku et al., 2021). Understanding which parasitic receptors transduce the host-derived signals can provide valuable information on which receptors to target for inhibitor design that can be used for mitigation strategies. This study thus forms a crucial foundation for future research in the field of plant signaling and receptor specificity.

References:

Bythell-Douglas, R., Rothfels, C. J., Stevenson, D. W. D., Graham, S. W., Wong, G. K.-S., Nelson, D. C., & Bennett, T. (2017). Evolution of strigolactone receptors by gradual neo-functionalization of KAI2 paralogues. BMC Biology, 15(1), 52.

Clarke, C. R., Timko, M. P., Yoder, J. I., Axtell, M. J., & Westwood, J. H. (2019). Molecular Dialog Between Parasitic Plants and Their Hosts. Annual Review of Phytopathology, 57, 279–299.

Conn, C. E., Bythell-Douglas, R., Neumann, D., Yoshida, S., Whittington, B., Westwood, J. H., Shirasu, K., Bond, C. S., Dyer, K. A., & Nelson, D. C. (2015). PLANT EVOLUTION. Convergent evolution of strigolactone perception enabled host detection in parasitic plants. Science, 349(6247), 540–543.

Kodama, K., Xie, X., & Kyozuka, J. (2023). The D14 and KAI2 Orthologs of Gymnosperms Sense Strigolactones and KL Mimics, Respectively, and the Signals Are Transduced to Control Downstream Genes. Plant & Cell Physiology. https://doi.org/10.1093/pcp/pcad072

Li, Q., Martín-Fontecha, E. S., Khosla, A., White, A. R. F., Chang, S., Cubas, P., & Nelson, D. C. (2022). The strigolactone receptor D14 targets SMAX1 for degradation in response to GR24 treatment and osmotic stress. Plant Communications, 3(2), 100303.

Lopez-Obando, M., Guillory, A., Boyer, F.-D., Cornu, D., Hoffmann, B., Le Bris, P., Pouvreau, J.-B., Delavault, P., Rameau, C., de Saint Germain, A., & Bonhomme, S. (2021). The Physcomitrium (Physcomitrella) patens PpKAI2L receptors for strigolactones and related compounds function via MAX2-dependent and -independent pathways. The Plant Cell, 33(11), 3487–3512.

Machin, D. C., Hamon-Josse, M., & Bennett, T. (2020). Fellowship of the rings: a saga of strigolactones and other small signals. The New Phytologist, 225(2), 621–636.

Moturu, T. R., Thula, S., Singh, R. K., Nodzyński, T., Vařeková, R. S., Friml, J., & Simon, S. (2018). Molecular evolution and diversification of the SMXL gene family. Journal of Experimental Botany, 69(9), 2367–2378.

Mutuku, J. M., Cui, S., Yoshida, S., & Shirasu, K. (2021). Orobanchaceae parasite-host interactions. The New Phytologist, 230(1), 46–59.

Wang, L., Xu, Q., Yu, H., Ma, H., Li, X., Yang, J., Chu, J., Xie, Q., Wang, Y., Smith, S. M., Li, J., Xiong, G., & Wang, B. (2020). Strigolactone and Karrikin Signaling Pathways Elicit Ubiquitination

and Proteolysis of SMXL2 to Regulate Hypocotyl Elongation in Arabidopsis. The Plant Cell, 32(7), 2251–2270.